Modelling diesel-ammonia two-stroke engines

J.S van Duijn

SDPO.21.011.m

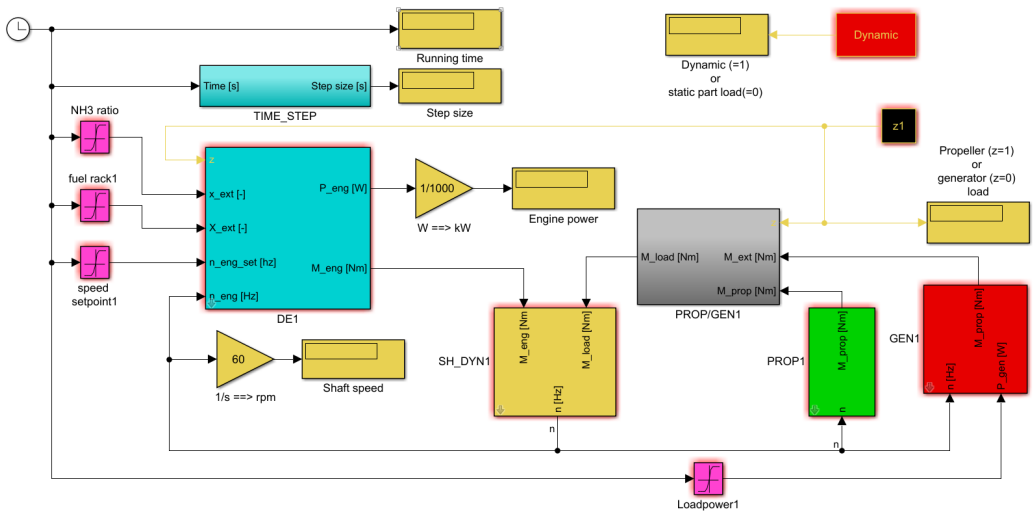

TU Delft Delft University of Technology

Challenge the future

Thesis for the degree of MSc in Marine Technology in the specialisation of Marine Engineering.

Modelling diesel-ammonia two-stroke engines

By

J.S. van Duijn

Performed at

TU Delft

This thesis (SDPO.21.011.m) is classified as confidential in accordance with the general conditions for projects performed by the TU Delft.

To be defended publicly on Wednesday 26 May 2021

Thesis exam committee

Chair/Responsible Professor:	ir. Klaas Visser,	TU Delft
Staff Member:	dr. ir. Peter de Vos,	TU Delft, Supervisor
Staff Member:	ir. Congbiao Sui,	TU Delft
Company Member:	ir. Niels de Vries,	C-Job Naval Architects, Supervisor

Author details

Student number:	4209273
Author contact e-mail	joelvanduijn@hotmail.com

An electronic version of this thesis is available at `http://repository.tudelft.nl/`.

Summary

Previous research on the safe and effective application of ammonia as a marine fuel, has found that ammonia with diesel as pilot would be a good first step to realise a wide implementation of ammonia as a marine fuel [67]. The pilot fuel is used to promote the combustion of ammonia. Ammonia with diesel as pilot has several benefits, it will reduce the harmful emissions significantly. Furthermore, it provides the same certainty and reliability as regular diesel engines because the system can run fully on diesel when the ammonia supply fails, or circumstances dictate diesel operation.

However, ammonia-diesel is a relatively new combustion concept, for which no engine model is available to the authors knowledge at the time of writing. To get a better understanding of diesel-ammonia engines, and to contribute to the application of diesel-ammonia engines in the maritime sector, a computer model could be helpful to predict the behaviour of diesel-ammonia engines.

Therefore, the goal of this project is to characterise diesel-ammonia combustion using a mean value first principle approach, based on available literature and to implement this characterisation of diesel-ammonia combustion in a time domain two-stroke engine model. This model will be used to indicate the technical feasibility of diesel-ammonia as a marine fuel. The main research question of this project is: How does the performance of the main engine of a deep-sea cargo vessel fuelled with diesel-ammonia compare to one fuelled by diesel only?

The TU Delft engine B model is chosen to model the behaviour of an engine of an ocean going cargo vessel. The model characterises the combustion with three combustion parameters: a, b and c. These parameters are mostly dependent on the ignition delay and the combustion efficiency. The combustion process of a dual fuel engine differs from a regular diesel engine due to two fuels being injected which both have different combustion rates. Additionally the gaseous fuels effect the ignition process and ignition delay. Therefore, the original TU Delft engine B model has to be adapted.

A second fuel supply is added to the model so it can be run in dual fuel mode. A new variable is introduced: the ammonia energy share ratio. This new variable indicates how much of the injected fuel energy is provided by ammonia. The maximum fuel flow is scaled to the same amount of energy flow into the engine as with diesel fuel.

To make the combustion shape of the model dependent on the ammonia energy share ratio two new terms are added to the equation for X_a and X_b, these parameters impact the initial pressure rise and diffusive combustion respectively. Based upon literature research, values are chosen for the new ammonia energy share ratio dependent parameters to replicate the impact of ammonia on the combustion shape. The main changes are a decrease in maximum pressure and a shift of energy release to the diffusive combustion phase.

The combustion efficiency of the engine is still dependent on the air excess ratio and was not changed because large marine reciprocating engines running on an ammonia-diesel mixture do not yet exist, so representative data is missing. The combustion efficiency remains 100% at nominal engine speed and load. It remains to be seen how realistic this assumption is.

The gas mixture in the engine was defined by the air mass fraction, this has been changed to the stoichiometric diesel gas fraction and the stoichiometric ammonia gas fraction. The same assumption as before has been used, no other reactions take place besides the combustion of the fuels itself. The properties of the stoichiometric ammonia gas are added to the model, and the model blocks used for calculating the thermodynamic properties of the gas mixture are updated to use the new definition of the gas mixture. Furthermore, the gas exchange model has been altered to consider the new definition for the gas mixture. This change introduces a limitation to the gas exchange model since it no longer supports negative scavenging.

The adapted TU Delft engine B model has been validated, and the impact of diesel-ammonia operation is tested. The following engine performance parameters are considered: engine efficiency, specific fuel consumption, power density, and the impact of diesel-ammonia operation on the operational limits of the engine.

In diesel only operation the adapted model behaves the same as the original TU Delft engine B model. Therefore, the changes have not caused any unexpected problems. Furthermore, the gas exchange model and the added thermodynamic properties of stoichiometric ammonia gas behave as expected. However, the ammonia energy share ratio dependent changes to the Seiliger parameters behave unexpected. When the ammonia energy share ratio is decreased, the late combustion phase and the combustion duration are decreased. This behaviour is not expected in reality.

The sfc and efficiencies of the TU delft engine B model and the adapted model are compared. The adapted model predicts an increase in both the thermodynamic and mechanical efficiency, the decrease in maximum cylinder pressure lowers the load on the mechanical components, and therefore reduces the mechanical losses. The increase in the thermodynamic efficiency is caused by the shorter late combustion phase. The decrease in the late combustion phase is caused by a modelling effect and not expected to happen in reality, therefore, the increase in thermodynamic efficiency is also not expected to happen in reality. The sfc for both the original model and the new model running on 100% diesel is 176.4 g/kWh. With an ammonia energy share ratio of 80% the sfc of ammonia is 302.4 g/kWh and the sfc of diesel is 32.9 g/kWh, which results in a total of 335.3 g/kWh. These changes to the sfc where expected because ammonia has a smaller LHV than diesel.

The power density in diesel only operation and diesel-ammonia operation are compared. The lower stoichiometric air-fuel ratio of ammonia implies that the power density of the engine could be increased, because more fuel can be burned in the same cylinder. However, the relatively bad combustive properties of ammonia could require a higher air excess ratio to achieve an acceptable combustion efficiency, reducing this effect. Furthermore, the lower pressure and temperatures in diesel-ammonia operation reduce the mechanical and thermal load on the engine, allowing more fuel to be injected without exceeding the maximum temperatures and pressures reached during diesel only operation. It should be considered however, that the model most likely exaggerates the decrease in maximum cylinder pressure. Lastly, it should be considered that when the power output of the engine is increased, and the engine design is not changed, the maximum load of the engine components such as the piston rods or crank shaft could be exceeded and they could fail.

The emissions in diesel only operation and diesel-ammonia operation are compared. Unfortunately the model does not simulate these emissions. However, some predictions regarding the emissions can be made. The CO_2 and SO_x emissions are dependent on the diesel fuel consumption. The diesel fuel consumption is greatly reduced in diesel-ammonia operation, and therefore, the CO_2 and SO_x emissions are also greatly reduced. This reduction in emissions and the sfc of diesel is also dependent on the ammonia energy share ratio, however, it is uncertain what the minimum amount of diesel fuel is to achieve acceptable combustion. Furthermore, it is expected that the nitrogen in ammonia increases the NO_x emissions, and that a lower combustion efficiency can cause ammonia emissions.

Lastly, the operational limits of the engine are reviewed. The maximum cylinder pressure decreases in the ammonia-diesel model and the temperature is slightly increased. The increase in maximum cylinder temperature however, is a model effect, and in reality, based on the properties of ammonia and experiments, it is expected that the maximum temperature decreases. Therefore, it is not expected that the maximum temperature and pressure exceed the mechanical and thermal capacity of the engine.

The turbocharger specifications have not been adapted to ammonia-diesel combustion, other alternative fuels have shown that it is highly likely that a different turbocharger is necessary. However, the model shows that the turbo charger operates at slightly lower power due to the higher thermodynamic efficiency, which leaves less energy in the exhaust gasses. However, the turbo charger still manages to supply the engine with enough air to operate at sufficient pressures and air excess ratios. The compressor operates within the stable region with and without the use of ammonia as fuel, therefore, no different turbocharger seems to be necessary.

Preface

In this report I present my graduation research about the modelling of diesel-ammonia two-stroke engines. The graduation research is the final step to conclude the master program Marine Technology at the Technical University Delft.

First, I would like to thank my TU Delft supervisor Peter de Vos, for providing the graduation assignment, and for his excellent guidance and advice during this project. I would like to extend my gratitude to Niels de Vries, for his guidance during this project and for the helpful advice he has given me. Furthermore, I would like to thank C-Job Naval Architects for providing a workplace during the COVID-19 pandemic. I also would like to thank Klaas Visser for being the chair of the graduation committee and for his feedback during the midterm meeting and later during the green light meeting.

Lastly, I would like to thank my friends for all the positive distractions and their support. I would also like to thank my family and girlfriend for supporting me during this period of my life. They have provided me with a lot of support and advice during the final chapter of my life as a student.

Joël van Duijn
Amsterdam, May 2021

Contents

List of Figures

List of Tables

Nomenclature

Abbreviations

BSFC	Brake Specific Fuel Consumption
CFD	Computational Fluid Dynamics
CI	Compression Ignition
CO	Carbon Oxide
CPU	Central Processing Unit
CR	Compression Ratio
DEM	Discrete Event Model
DMA	Marine Distillate Fuel
DME	Dimethyl Ether
EC	Exhaust Closes
EGR	Exhaust Gas Recirculation
EO	Exhaust Opens
FP	Fuel Pump
H-NG	Hydrogen-Natural Gas
HC	Hydro Carbon
HCCI	Homogeneous Charge Compression Ignition
HRR	Heat Release Rate
IC	Inlet Closes
IDT	Ignition Delay Time
IO	Inlet Opens
LHV	Lower Heating Value
MGO	Marine Gas Oil

MVM	Mean Value Model
NG	Natural Gas
NTC	Negative Temperature Coefficient
RPM	Rounds Per Minute
sfc	Specific Fuel Consumption
SI	Spark Ignition
TDC	Top Dead Centre
WHO	World Health Organisation

Roman variables

a	Iso-volumetric pressure ratio Seiliger process	$-$
b	Isobaric volume ratio in Seiliger process	$-$
bb	Seiliger parameter for first two combustion stages	$-$
c	Isothermal volume ratio in Seiliger process	$-$
c_v	Specific heat at constant volume	$kJ/kg \cdot K$
c_p	Specific heat at constant pressure	$kJ/kg \cdot K$
E_A	Activation energy	J/mol
E_A	Nominal propeller torque	kNm
i_{cyc}	Number of cylinders	$-$
k_cyc	Number of revolutions per cycle	$-$
k_{cyc}	Number of revolutions per cycle	$-$
LHV_{NH_3}	Lower heating value for ammonia	kJ/kg
LHV_p	Lower heating value for pilot fuel	kJ/kg
M_p	Propeller torque	kNm
M_{da}	Molecular weight dry air	$kg/kmol$
m_{da}	Mass dry air	kg
$m_{f,cyc}$	Injected fuel mass per cycle	kg
$m_{f,cyl,nom}$	Nominal injected fuel mass per cycle	kg
m_{NH_3}	Injected ammonia fuel mass per cycle	$-$
M_{ps}	Mean Piston speed	m/s
m_p	Injected pilot fuel mass per cycle	$-$
n_e	Engine speed	RPM
n_{comp}	Polytropic exponent during compression	$-$
$n_{e,nom}$	Nominal engine speed	RPM
n_{exp}	Polytropic exponent during expansion	$-$
n_f	Molecular quantity for number of kmol for fuel	$kmol$
n_{O_2}	Molecular quantity for number of kmol for oxygen	$kmol$
p	Pressure	bar

$q_{f,23}$	Heat per unit of mass in Seiliger stage 2-3	kJ/kg
R	Gas constant	$kJ/kg \cdot K$
R_u	Universal gas constant	$8.31446 J/mol \cdot K$
R_{45}	Gas constant during stage 4-5	$kJ/kg \cdot K$
s_m	Mixing entropy	$kJ/kg \cdot K$
s_p	Pressure dependent entropy	$kJ/kg \cdot K$
s_p	Pressure dependent entropy per unit of mass	$kJ/kg \cdot K$
s_t	Temperature dependent entropy	$kJ/kg \cdot K$
spe	Specific pollutant emission	g/kWh
T	Temperature	K
$t_{sc,r}$	Relative scavenge time	s
w_{45}	Work per unit mass in stage 4-5	kJ/kg
X_a	Engine speed and fuel injection dependent combustion fraction parameter stage 2-3	–
x_f	Ammonia energy share ratio	–
$X_{a,c}$	Constant parameter for a	–
$X_{a,c}$	Constant parameter for b	–
$X_{a,d}$	Ammonia energy share ratio dependent parameter for a	–
$X_{a,f}$	Fuel injection dependent parameter for a	–
$X_{a,f}$	Fuel injection dependent parameter for b	–
$X_{a,n}$	Engine speed dependent parameter for a	–
$X_{a,n}$	Engine speed dependent parameter for b	–
$X_{b,d}$	Ammonia energy share ratio dependent parameter for b	–
x_{sg}	mass fraction stoichiometric gas	$kmol$
y_{O_2}	Kmol fraction oxygen	–

Greek variables

η_{cb}	Combustion efficiency	–
η_{hl}	Heat loss efficiency	–
η_q	Heat input efficiency	–
η_{th}	Thermodynamic efficiency	–
κ	Ratio between the polytropic exponent at constant pressure and at constant volume	–
λ	Air excess ratio	–
ϕ_f	fuel flow	kg/s
ϕ_{BLD}	Mass flow	kg/s
σ_{da}	Stoichiometric air/fuel ratio with dry air	–
σ_{NH_3}	Stoichiometric air/ammonia ratio	$kmol$
τ_i	Ignition delay time	deg

Chapter 1

Introduction

1.1 Background

Previous research from Niels de Vries on the safe and effective application of ammonia as a marine fuel, has found that hydrogen-ammonia combustion engines are a good alternative for diesel engines in ammonia carriers [67]. To realise a wide implementation of ammonia as a marine fuel a stepwise implementation can be considered. The first stage would be ammonia with diesel as pilot fuel in a compression ignition internal combustion engine. The second stage is an internal combustion engine with ammonia and hydrogen as pilot fuel. The final stage would be a solid oxide fuel cell fuelled by ammonia.

The first step, using ammonia with diesel as a pilot fuel has several benefits. Using ammonia in combination with diesel fuel will significantly reduce the harmful emissions created by the engine. Furthermore, it provides the same certainty and reliability as a regular diesel engine since the system can be run on regular diesel if the ammonia fuel supply system fails. It also provides flexibility to cope with changing economic viability to comply with harmful emission reduction regulations since the operator can select the amount of ammonia used in the engine itself. On top of that, diesel ammonia systems will be less expensive because the ammonia fuel supply does not have to be redundant, since the operator can switch to diesel at any time. Therefore, it is recommended to further investigate marine internal combustion engines using ammonia and marine diesel [67].

1.2 Research objective

Ammonia-diesel is a relative new power plant concept with great potential to reduce harmful emissions. However, as far as the author knows, there is no diesel-ammonia engine model publicly available at the time of writing. To get a better understanding of diesel-ammonia engines, and to support further development of dual fuel diesel-ammonia engines, a computer model could be helpful to predict the behaviour of a diesel-ammonia engines. The model would allow the designer to simulate the behaviour of the engine during a voyage, to get a better understanding of the impact of such an engine on the performance of the design. The goal of this project is to characterise diesel-ammonia combustion using a mean value first principle approach, based on available literature and to implement this characterisation of diesel-ammonia in a time domain two-stroke engine model. This model will be used to indicate the technical feasibility of diesel-ammonia as a marine fuel. Furthermore, the accuracy of the developed model will be evaluated.

1.3 Research relevance

According to the World Health Organization (WHO), global warming poses a major challenge for humanity [70]. To stop global warming the emissions of CO_2 and other greenhouse gasses must be significantly reduced. Furthermore, in 2008 the International Maritime Organisation (IMO) has introduced a revised version of MARPOL Annex VI which introduces regulations on NO_x, SO_x, Particulate Matter (PM) and Emission Control Areas (ECA's) [29]. Due to the facing thread of global warming and stricter regulations, shipowners search for more sustainable ways of transportation. One way of doing so is replacing fossil fuels by more sustainable alternatives like hydrogen or ammonia. Ammonia is considered to be a good alternative for fossil fuels due to its relative low production cost and relative high volumetric energy density [67].

1.4 Research questions

To investigate the performance of marine engines using ammonia and marine diesel the main research question shown below, must be answered. The main research question is divided in multiple sub-questions. Sub-questions a and b argue why diesel ammonia is selected as an alternative fuel. Sub-questions c, d and e help selecting a model, characterising diesel-ammonia combustion and changing the model. The last sub-questions further clarify what parameters are selected to indicate the engine performance. The goal of the engine is to produce mechanical power, the performance parameters are quantities that relate the use full output power to the required input and the unwanted consequences. The performance of diesel engines has at least three aspects: power density, fuel economy and pollutant emissions [56]. Furthermore, since an excising engine is used, it is also important to see if the operational limits of the engine are exceeded in diesel-ammonia operation. Therefore, the following sub questions have been chosen:

1. How does the performance of the main engine of a deep-sea cargo vessel fuelled with diesel-ammonia compare to one fuelled by diesel only?
   (a) Why is ammonia an interesting fuel for deep-sea shipping according to literature?
   (b) Why is ammonia burned in combination with diesel fuel?
   (c) What model type is best suited for modelling the voyage of a deep sea cargo vessel?
   (d) How can diesel-ammonia combustion be characterised according to literature?
   (e) How to model the behaviour of a dual fuel diesel-ammonia engine on a deep-sea cargo vessel?
   (f) How do the specific fuel consumption and efficiency of a diesel only engine compare to a diesel-ammonia engine?
   (g) How does the power density of a diesel only engine compare to a diesel-ammonia engine?
   (h) How do the emissions of a diesel only engine compare to a diesel-ammonia engine?
   (i) What impact does diesel-ammonia operation have on the operational limits of a diesel only engine?

1.5 Research method

To get more familiar with the subject, the project starts with a literature study. The literature study will be presented in part I of this report. Subjects of interest for the literature study are: two-stroke diesel engine models, the diesel and diesel-ammonia combustion process, dual fuel, and emissions. The literature study will help to get a clear oversight of the in cylinder combustion process.

After the literature study the research phase starts. During the research phase the research questions will be answered. The research phase is divided in multiple parts. In the first part the two-stroke TU Delft engine B model [14] will be analysed to better understand how the model works and how to best convert the model to a diesel-ammonia engine.

The second part will be used to adapt the existing model, so it will simulate an engine running on a diesel-ammonia mixture. The information about two-stroke diesel engine models, the combustion process, dual fuel engines, ammonia, and emissions obtained during the literature study will be used to apply the changes to the model. The model is tested to verify if it behaves like expected.

In the last phase the adapted model is compared to the original TU Delft engine B model to determine the impact of diesel-ammonia operation on the engine performance in terms of: efficiency, specific fuel consumption, power density and emissions. Furthermore, it is verified if the engine still operates within the operational limits of a diesel only engine.

Part I

Literature study

Chapter 2

Renewable fuels

2.1 Introduction

There are multiple alternative fuels available for marine diesel. In this section the most promising alternatives are briefly compared, and it is explained why ammonia is such a good alternative for marine diesel.

The alternative fuel should be a fuel that can be produced in a sustainable way, a sustainable fuel is a fuel that meets the present energy demand without compromising the future generations in their energy needs [34]. Some fuels, like hydrogen, could be produced in a sustainable with electrolysis using water and electricity. However, hydrogen is mostly produced from steam reforming methane, which is a fossil fuel [43]. Only fuels which have the potential to be produced in a sustainable way are considered.

In marine engineering volume and weight are important factors, deep-sea cargo vessels are either limited in the amount of cargo they can carry by volume, or by weight [49]. The energy density and the volumetric energy density of the fuel have a big impact on the amount of cargo a vessel can carry. Other important fuel storage properties are under which pressure and temperature the fuel must be stored. High pressure tanks and low temperature storage are less cost effective as ambient storage methods [67].

The operational cost of a ship are heavily dependent on fuel consumption and fuel cost. When produced in a sustainable way, synthetic fuels will be produced using the overcapacity of renewable energy from wind and solar power for example. Therefore, the synthetic fuel costs are depended on how much energy is required to produce said fuel. Energy required to produce one Mega Joule of fuel will be used to compare the cost aspects of the fuels.

Furthermore, a fuel can only be considered if it is available in high enough quantities to supply cargo vessels. A reasonable sized infrastructure and production capacity should already exist.

2.2 Renewable fuel options

Table 2.1 shows the properties of MGO alternatives, MGO is also included in the table as a reference point. The energy density of hydrogen looks very promising and is almost three multitudes higher than the energy density of MGO however, due to the very low volumetric energy density of hydrogen and the unfavourable storage properties of hydrogen (700 bar or -253 °C), ammonia is considered to be a better alternative. Furthermore, the renewable production cost of both hydrogen and ammonia are equally low compared to other sustainable fuels. Lastly, ammonia is the second most commonly produced chemical in the world [15], therefore a good infrastructure is already available.

Fuel type	Energy density LHV [MJ/kg]	Volumetric energy density $[GJ/m^3]$**	Renewable synthetic production cost [MJ/MJ]	Storage pressure [bar]	Storage temperature [°C]
Marine Gas Oil	42.8 [19]	36.6	N/A	1	20
Liquid Methane	50.0 [19]	23.4	2.3	1	-162
Ethanol	26.7 [19]	21.1	3.6	1	20
Methanol	19.9	15.8	2.4*	1	20
Liquid Ammonia	18.6 [30]	12.7	1.8	1 or 10	-34 or 20
Liquid Hydrogen	120.0	8.5	1.8	1	-253[15]
Compressed Hydrogen	120.0	4.5*	1.7	700	20

Table 2.1: Renewable fuel options [67]

* corrected figure from source in agreement with author.
** volume is chemical only, consequences of tank not included.

2.3 Conclusion

Based on the renewable synthetic production cost, the already existing infrastructure, the gravitational energy density and the volumetric energy density, ammonia can be considered a balanced sustainable alternative for MGO. Currently ammonia is produced from natural gas, which is a fossil fuel. However, ammonia can be a sustainable fuel if produced from renewable sources instead of fossil fuels. The production of ammonia is not within the scope of this project and will not be further considered.

Chapter 3

Ammonia in reciprocating internal combustion engines

3.1 Introduction

The combustion of the air fuel mixture in internal combustion engines occurs either by providing an ignition source, mostly a spark as with spark ignition (SI) engines, or by compressing the mixture until the autoignition temperature is reached which is known as compression ignition (CI) engines. The auto ignition temperature of ammonia is 924K, diesel fuel has an autoignition temperature of 503K, natural gas 723K [15]. The relatively high autoignition temperature of ammonia makes it hard to ignite in internal combustion engines. Either extreme high pressures are required to reach the auto ignition temperature, or another ignition source has to be provided. In this chapter the most common options to overcome the high autoignition temperature of ammonia are discussed, and the most promising solution is selected.

3.2 Ammonia CI

Some of the first experiments regarding ammonia as an internal combustion fuel date back to the 1950's, after the Second World War the energy depot project funded by the US military was started to investigate alternative power generation methods [15]. During this project multiple experiments with ammonia as a fuel in internal combustion engines have been executed. In multiple publications under this project [24] [50] [13] Wagner T.O. commented on the importance of ammonia as a CI engine fuel and pointed out that he and Domke C.J. (American Oil Co.) investigated the performance of ammonia in internal combustion engines.

They were able to run the CI engine on pure ammonia and on ammonia with several additives. The engine had to be started on kerosene and could then be switched to ammonia, restarting the engine on ammonia with a compression ratio of 35:1,

normal coolant and inlet temperatures was not possible. However, increasing the coolant temperature to 188 degrees Celsius and the inlet air temperature to 132 degrees Celsius did enable regular combustion [13].

As a final part of the energy depo project, the compatibility of ammonia and existing CI engines was investigated [23]. It was tested if the materials used for the engine could resist ammonia. Additionally, the impact of ammonia on the lubricants was tested, no substantial problems were found. Combustion of ammonia could only be achieved with a compression ratio of 35:1 and an inlet temperature of 150 degrees Celsius.

More recently a simulation of a CI engine running on ammonia only was conducted. A two-stage injection strategy was simulated to determine if this would lower the required intake temperature and compression ratio for self-ignition. Compression ratios up to 30:1 resulted in less than 90% combustion efficiency for all tested injection timing conditions [37]. The two-stage injection strategy was able to reduce the NO emissions by 25% under certain conditions. However, the reduction in NO resulted in a considerable amount of ammonia slip. It was concluded that the pilot fuel injection time should be adjusted to minimise both ammonia slip and NO emissions [37]. The combustion of pure ammonia in CI engines required such a high compression ratio that the use of ammonia in CI engines was not technically feasible at that moment.

3.3 Ammonia SI

The first experiments of the energy depo project concluded that the compression ignition of pure ammonia requires very high compression ratios and intake temperatures. Thus multiple methods to decrease the ignition requirements where investigated, including multiple pilot fuels, additives, spark plugs and special high temperature glow coils.

Gray et al. [23] did research on the engine compatibility of ammonia under the Energy Depo Project and found that the engine could not be run on ammonia with conventional sparkplugs or glow coils. It was likely that the flame extinguished before it could properly propagate due to the high velocity of the gasses. However, with an experimental high temperature shielded glow coil successful combustion of ammonia at a compression ratio of 21:1 was achieved.

Starkman et al. [60] investigated the use of ammonia in internal combustion engines with multiple kinds of igniters. They found that internal combustion engines could run successfully using sparkplugs, ammonia and their conventional compression ratios. However, a reduction in power output of 70-77% was measured.

More recently Toyota has patented a engine running on ammonia which is combusted by several plasma jet igniters, or multiple spark plugs per cylinder [44]. Computational research on the ignition of ammonia by sparks concluded that the ammonia could be ignited with an 2kV arc [18]. However, ammonia as a SI fuel has never

been realized at a serious level. Research has suggested it is possible but ammonia in SI engines has not been developed into a feasible concept.

Moreover, the concept of SI ammonia has been tested in an experimental setup using a 814cc 4-stroke engine. The setup was run at multiple compression ratios to determine the best compression ratio in terms of NO_X emissions, ammonia slip and hydrogen slip (the ammonia gets partially cracked during the combustion). It was found that a compression ratio of 15:1 achieved the best trade-off between emissions [18].

The combustion of pure ammonia in SI engines using technically feasible compression ratios seems to be possible. However, the technology of SI ammonia engines is in a very early stage of development, and the interest and development of such technology comes mainly from the automotive industry and focuses on smaller automotive engines.

3.4 Ammonia hydrogen CI

Another method to overcome the high autoignition temperature of ammonia could be the addition of a fuel with a lower autoignition temperature. Hydrogen is often used because it does not contain CO_2 and has a lower autoignition temperature. Ammonia hydrogen mixtures can be created by partially cracking the ammonia onboard.

Recent research by Pochet et al. [45] with ammonia hydrogen blends in a homogeneous charge compression ignition (HCCI) engine has shown it can be operated with a 16:1 compression ratio and a 70% ammonia volume, 30% hydrogen volume mixture. However, to achieve combustion intake gas conditions of 1.5 bar and 428 to 473 K where required. Furthermore, when higher compression ratios were used ringing occurs; a rapid fuel burn creates excessive cylinder pressure, which in turn makes shock waves that can damage the engine. To prevent ringing the compression ratio must be reduced, which in turn lowers the engine efficiency. Although there are some undesirable side effect of ammonia hydrogen mixtures to overcome, the use of ammonia hydrogen CI mixtures seems technically feasible.

3.5 Ammonia hydrogen SI

In 2016 experiments with ammonia hydrogen mixtures in SI engines were done. SI engines that use hydrogen suffer from problems like backfiring due to its very high combustion velocity and wide flammability range. Ammonia has a low flame speed and temperature, a narrow flammability range and requires a very high ignition energy. It was hoped that by mixing hydrogen with ammonia an optimal compromise of the combustion properties of both fuels is achieved [9].

A 505cc twin engine with a compression ratio of 10.7:1 was used during the experi-

ments. The engine was operated between 2500 and 5000 RPM and produced 14kW around 5000 RPM. A direct injection system was developed to remain the same volumetric efficiency as with the original engine [9]. The tests confirmed that the addition of hydrogen increased the flame speed of the mixture and improved the combustive behaviour of the mixture [9].

Siemens has demonstrated the usage of ammonia hydrogen in their "Green Ammonia energy storage system demonstrator" test facility. They successfully ran a SI engine with a CR of 10.6:1 to power a generator [69] [10].

3.6 Ammonia diesel CI

During the Energy Depo project multiple methods to decrease the ignition requirements where investigated, diesel as a pilot fuel was one of those. When diesel was used as a pilot fuel the minimum compression ratio necessary for combustion was 15,2:1. This was within the limits of regular combustion engines, indicating that from a combustion standpoint this method can be used with almost any engine [23].

More recently in 2008 Reiter and Kong [47] have successfully demonstrated the operation of a dual fuel compression ignition engine running on ammonia with diesel as a pilot fuel. Ammonia was injected to partially replace the diesel fuel and reduce the carbon emissions of the engine. The engine was successfully operated at multiple loads, engine speeds and ammonia-diesel ratios. The engine could be operated up to a maximum energy share ratio of 95% ammonia and 5% diesel, however reasonable fuel economy could only be maintained between ammonia energy share ratios of 40 and 80%. An ammonia energy ratio of 40% means that NH_3 accounts for 40% of the total energy of the mixing fuel. When the engine was run on 60% or less ammonia energy share ratio, the NOx emissions were lower compared to 100% diesel operation despite the fuel bound nitrogen. The authors expect this to be caused by the lower combustion temperatures and the effect of ammonia in the aftertreatment system. An unwanted effect of the lower combustion temperatures is the relative high amount of hydrocarbon and ammonia emissions.

3.7 Conclusion

Although some researchers were able to run CI engines on ammonia only, the implementation of ammonia as a single fuel concept is challenging due to the high compression ratios required for ammonia combustion [15]. The use of sparkplugs in combination with ammonia or ammonia hydrogen showed promising results and is considered a valid option. Experiments from Gray [23], Reiter and Kong [47] have shown that the addition of a pilot fuel can lower the required compression ratio for self-ignition of the fuel mixture. This greatly improves the practical application of ammonia in CI engines. Both hydrogen and diesel are good pilot fuels. However, to store hydrogen special equipment is required which is not necessary for diesel.

Furthermore, diesel as a pilot fuel has the additional advantage that it can be used as a backup system when the ammonia fuel system fails or no ammonia is available, making it a very practical solution from a shipowners perspective. However, the use of diesel fuel is not a sustainable solution. Therefore, ammonia with diesel as a pilot fuel is seen as a good first step in the implementation of sustainable fuels and its implementation in deep sea cargo vessels will be further studied.

Chapter 4

Models of reciprocating internal combustion engine models

4.1 Introduction

The most common prime movers in ships are diesel engines because of their reliability and relatively high efficiency. The in-cylinder process, in which the fuel is combusted and work is delivered, is the most important part of diesel engine working principle. This process is extremely hard to describe due to changing mass, energy, and composition of working medium. The in-cylinder process has a direct impact on the power, fuel consumption and exhaust gasses, so it is crucial to describe the in-cylinder process properly [26, 4].

To predict the behaviour of a two-stroke diesel engine running on an ammonia diesel mixture, a model can be made. The model will be used to simulate the behaviour of such an engine and predict among other things the power output and fuel consumption. There is a big variety of engine models available, in this section the most common internal combustion engine models are listed. Their working principle is explained and the advantages and disadvantages of these models are reviewed. Lastly, the model best suitable for modelling the behaviour of the propulsion system of an ocean going cargo vessel using ammonia as fuel will be selected.

4.2 In-cylinder process model

Due to the popularity of the diesel engine many studies have been conducted in regard of the in-cylinder process. These studies have led to a great variety of different in-cylinder process models, all with different levels of detail and developed for different applications. In this paragraph the most common model types are categorized and the model best suited for the simulation of the voyage of a deep-sea cargo vessel is selected. These models can be categorized in multiple ways and models often fit in more than one category.

4.3 Step size based

As already mentioned, models can be categorized in multiple ways. A popular way is to group models into discrete event models (DEM) and mean value models (MVM). This categorization is based upon the step size and independent variable. Like most categorization methods the complexity or simplicity of a model can be linked with the different categories.

4.3.1 Discrete event models

Discrete event models use the crank angle as the independent variable instead of time as used by mean value models. Discrete event models or crank angle models are models who simulate an entire cycle of a combustion engine in small steps. These models can predict the behaviour of internal combustion engines quite precise. However, they require a lot of CPU resources and are very slow and expensive to use. Therefore, crank angle models are often used for the design of engines and are too slow to predict the behaviour of a propulsion system on board of a vessel. To be able to simulate the behaviour of a propulsion plant simpler models that can be run in real time are developed [26].

4.3.2 Mean value models

Mean Value Models (MVM) of the in-cylinder process are both accurate and simple. Due to their simplicity they are capable of simulating on a time scale of longer than one engine cycle and are suitable for simulating larger (propulsion) systems while limiting the calculation time [63].

MVM are control orientated models, that simplify the combustion characteristics as a static effect. MVM assume that, when the initial boundary conditions at the start of the cycle are fixed, the combustion will always be the same for a specific set of initial conditions. Due to these assumptions, MVM are not capable to reflect on all in-cylinder phenomena such as random combustion pressure variations [26]. MVM work with time as the independent variable. MVM for the modelling of marine diesel engines or systems are reported in great quantities. Vrijdag et al. [68] has applied a mean value diesel engine model to control the cavitation on a controllable pitch propeller in operational conditions. Theotokings et al. [66] have investigated the transient response of the propulsion plant of a ship using a MVM. Baldi et al. [6] have developed a MVM of a Handymax sized product carrier to investigate behaviour for constant and variable engine speed operation. Michele Martelli et al. [41] have developed a six degrees ship motion model and a corresponding ship propulsion plant model that uses a mean value diesel engine model. In these examples a system level model is sufficient to describe the engine's behaviour, a more complex model that describes the thermodynamics more extensively is not necessary [2, 63].

4.4 Dimension based

The number of dimensions considered in a model is another way to categorize models and tell something about the complexity of a model. These categories go from full blown CFD models (3-D) to arbitrary functions describing a relation between the input and output of a model.

4.4.1 Three-dimensional models

Three-dimensional models or CFD models are helpful to acquire detailed information about the in-cylinder process. These models are very complex and require a lot of computational power [51, 7, 20]. CFD models are used for designing and optimising the engine itself. Numerous studies using CFD models have been done to examine the engine performance of diesel engines and other fuels such as H-NG, DME and methanol [12, 38, 74].

4.4.2 One-dimensional models

One-dimensional and quasi dimensional models are less complex than CFD models but still require a significant amount of computational power. One- and quasi-dimensional models can be divided into single-, two- and multi-zone combustion models. In single-zone models the working fluid undergoing the combustion process is assumed to be lumped into one control volume, two-zone models split the control volume into two thermodynamic control volumes, an unburned control volume and a burned control volume. As the name suggests multi-zone models divide the thermodynamic control volume into multiple zones [51].

4.4.3 Zero-dimensional models

Zero-dimensional models are often used because they are simpler than one-dimensional models and require less computational power than one-dimensional models. Zero-dimensional models provide quick results on engine performs, however, the simplicity of the model can also reduce the accuracy and details of the results. As the name suggest, zero-dimensional models are characterised by their zero-dimensional special resolution. These models do not consider fluid dynamics and are not affected by specific engine geometries. Instead they take a few engine characteristics as input to model the engines behaviour [51].

4.5 Input-output relationship based

Internal combustion engine models can be divided in regression based models and thermodynamically based models. The models are grouped in different categories based on how their input-output relationship came into being, this does not necessary tell something about their complexity.

4.5.1 Regression based models

Regression based models predict the input-output relationship based upon experimental data, in this process the underlying physics are neglected. This makes them heavily dependent on experimental data [63]. The Wiebe function is probably best known regression based model used to model the in-cylinder process. Multiple variants of the Wiebe model are developed. Wiebe functions are defined by one or more Wiebe coefficients for combustion efficiency, shape factor and combustion duration [22, 1]. A single Wiebe function is not always able to precisely capture the combustion of the in-cylinder gas mixture if multiple fuel blends are used with different combustion rates. To better represent the combustion with multiple combustion phases a double Wiebe function can be used. According to Yildiz et al. [72] the double Wiebe function fitted the experimental data better. The experimental data was obtained with a 500cc SI engine running on methane and hydrogen methane blends. However, the capability of predicting the engine performance in varying engine loads was not discussed.

Lui et al. [39] demonstrated that a double Wiebe function was not able to predict the mass burn fraction in diesel engine converted to a SI NG engine. However, a modified double Wiebe function performed better. Furthermore, Lui et. al concluded that the effective use double Wiebe model is limited to the operating conditions used to determine the Wiebe parameters.

Most of the research concerning Wiebe and gaseous fuels are focused on smaller automotive four-stroke engines. Two-stroke engines work with much lower speeds, higher volumes and other cycles. The lower engine speeds allow for a longer combustion period. Furthermore, due to the larger cylinder volume there is relatively less surface area, which in term reduces the heat loss. The lower heat loss impacts the combustion heat, delivered work, cylinder pressures and temperatures. Since there is no experimental data available for large two-stroke marine engines fuelled with diesel ammonia blends and the scaling effects are unknown, regression based models are not suited for modelling large two-stroke marine engines.

4.5.2 Thermodynamically based models

Thermodynamically based models use thermodynamics and physics to predict the relation between input and output, rather than algebraic function derived from experimental data as with the Wiebe model [63]. Because no measurements are

available, a thermodynamic approach is preferred over a regression based approach.

An often used thermodynamic approach is the 5 or 6 stage Seiliger cycle, which is a mean value thermodynamic modelling approach. Sui et al. [63] compared the Seiliger model with experimental measurements. And Georgescu et al. [21] used the Seiliger cycle to study the dynamic behaviour of a dual-fuel natural gas engine. Skogtjarn [55] used the Seiliger cycle to estimate the temperature of exhaust gasses. Sapra H. et al. [51], compared the Seiliger cycle with the double Wiebe function for the characterisation of hydrogen natural gas combustion and recommend the use of the Seiliger cycle due to its ability to accurately capture the variations in combustion. In currently available literature the Seiliger model has mainly be used on a system level investigation. The Seiliger cycle requires only a low amount of computational power while providing enough details about the in cylinder process [51], making it a model well suited for studying system integration, smart maintenance, load variations, control strategies and voyage simulations.

4.6 Conclusion

The goal of this project is to simulate the behaviour during a voyage of a propulsion system running on ammonia, with diesel as a pilot fuel. The model should be able to simulate a longer time period (an entire voyage) and there is only a need to simulate on a system level. As described in the previous paragraph, zero-dimensional and Mean Value Models are widely used for system based design due to their simplicity and reasonable accuracy. Furthermore, due to the lack of experimental data of large two-stroke marine engines running on an ammonia diesel blend, regression based models are not considered to be suitable. Mean Value Seiliger models have previously been used for, among other things the simulation of voyages, proving it's capability. Therefore, a mean value zero-dimensional thermodynamic based model is most suited for our purpose.

Chapter 5

Ammonia diesel combustion characteristics

5.1 Introduction

In this chapter the combustion characteristics of ammonia diesel mixtures are investigated. Because the literature regarding the combustion of ammonia diesel mixtures in CI engines is scars, the characteristics of regular diesel engines and dual fuel diesel engines are also investigated. The findings of this chapter will be used to adjust the TU Delft Mean Value Model to simulate dual fuel ammonia diesel engines.

5.2 Diesel combustion characteristics

First the combustion process in a regular CI diesel engine is described. This process starts with the injection of the fuel, the fuel ignites when the auto ignition conditions are reached. The time between injection and ignition is called the Ignition Delay Time (IDT) and is a major parameter in the combustion characteristics of a CI engine. The process between injection and ignition can be described as follows.

The injector will inject a turbulent flow of diesel into the cylinder. This flow has a liquid core and becomes thinner as the fuel breaks up in its path. The fuel will break up in droplets, whom in turn will break up in smaller droplets. The smaller droplets will vaporize. At this point the fuel jet exists of a mix of fuel droplets, vaporized fuel and air. The distance the fuel travels through the cylinder before it is vaporized is dependent on the fuel jet speed, the temperature and the pressure. It is important that all fuel is vaporized before it hits the relative cold cylinder wall or piston bowl. When the fuel hits the cylinder wall or piston bowl it will condensate and most probably not burn.

Ignition occurs when a certain threshold determined by pressure and temperature is reached. This is often visualized using an explosion diagram, with temperature

on the vertical axis and pressure on the horizontal axis [58] as shown in figure 5.1.

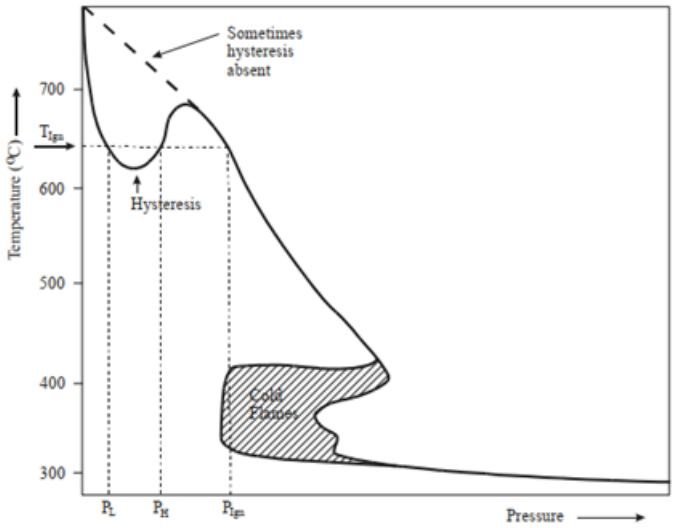

Figure 5.1: Example of explosion diagram [58]

The combustion process can be divided into three separate phases: rapid combustion, controlled combustion and final combustion.

The ignition delay time has a major impact in the engine characteristics because fuel must be burned within a few milliseconds, if the ignition delay is too long the engine will misfire [48, 47]. The ignition delay period can be divided into two parts: the physical delay and the chemical delay.

The physical delay is the time between injection and reaching the conditions required to start the chemical reaction. During this period the fuel is mixed with air, atomized and vaporized, and the temperature and pressure are raised to the self-combustion threshold. The physical delay is mostly affected by the viscosity of the fuel, a more viscus fuel takes more time to vaporize, a less viscus fuel has a smaller physical ignition delay [53].

In the chemical delay period the chemical reactions start slowly and speed up until ignition. Generally the chemical delay is longer than the physical delay, however, this process is temperature dependent and under higher temperature the chemical process speeds up, possibly resulting in a shorter chemical delay.

After the ignition delay the ignition starts. This process can be divided into two stages: the premixed, rapid or uncontrolled combustion phase and diffusive or controlled combustion phase.

The premixed combustion phase is characterised by a rapid rise in pressure, which is caused by the autoignition of the fuel injected during the ignition delay. A longer ignition delay allows more fuel to be injected which in turn causes a stronger pressure rise in the premixed combustion phase. If this pressure rise is too big it can cause vibrations and damage to the engine, this phenomenon is known as diesel knock.

During the diffusive combustion the rate of combustion is mostly affected by the rate

of fuel injected. The rate of chemical reactions drops due to the cylinder backing up, decreasing the pressure and temperature of the gas mixture [53].

5.3 Dual fuel combustion characteristics

The dual fuel process differs from the regular diesel combustion process due to both liquid and gaseous fuels being present. Gaseous fuels influence both the pre-ignition and post-ignition process in a complex manner, depending on which fuel is used, fuel concentrations and operating conditions [32]. When combustion models for dual fuel engines are developed, reliable details of the ignition delay are essential [46].

Multiple studies have reported that the ignition delay of the pilot fuel increases with an increasing presence of gaseous fuels up to a maximum value, above this value the ignition delay time decreases [32, 31, 35].

The increase of ignition delay with low percentages of gaseous fuels may be caused by the gaseous fuels reducing the air intake and thus the amount of oxygen in the cylinder. Another reason for the extended ignition delay might be the formation of intermediate compounds caused by the oxidation of the gaseous fuel mixture during the compression in the cylinder. This is caused by OH radicals reacting with the molecular hydrogen present in the cylinder, leaving less reactive species that cannot accelerate the reaction at the same speed as OH radicals. When more gaseous fuels are added, the amount of species able to accelerate the chemical reaction increase, which reduces the ignition delay at higher gas concentrations [35].

The combustion heat release rate of a dual fuel engine can be separated into three overlapping components. The first component (I) as shown in figure 5.2, represents the energy released due to the pilot fuel. The second component (II) is the energy released due to the gaseous mixture that is in the immediate vicinity of the ignition and combustion centres of the pilot fuel. The third component (III) consists of all the pre-combustion activity, the subsequent turbulent flame propagation and, when applicable, the autoignition of the gaseous mixture.

The fuel to air ratio affects the three different components of the energy released. With lean gaseous -air mixture most of the energy is released from the rapid combustion, the released heat comes from the pilot fuel and the gaseous mixture in the pilot zone and its direct surroundings. As shown in figure 5.3 under these conditions relatively small amount of the energy released comes from the gaseous mixture, because the very lean gaseous mixtures will not allow for a consistent flame propagation. Increasing the pilot zone will greatly increase the total released energy because more of the gaseous mixture will be within proximity of the pilot combustion. When the concentration of gaseous fuel is increased a proper flame propagation through the charge will be allowed, resulting in an increase in the contribution of the gaseous fuel to the total heat release. If the concentration of gaseous fuel is increased even further, component II and III will have a greater overlap effectively merging them together. This results in an increase of energy released directly after the auto-ignition of the pilot fuel [31].

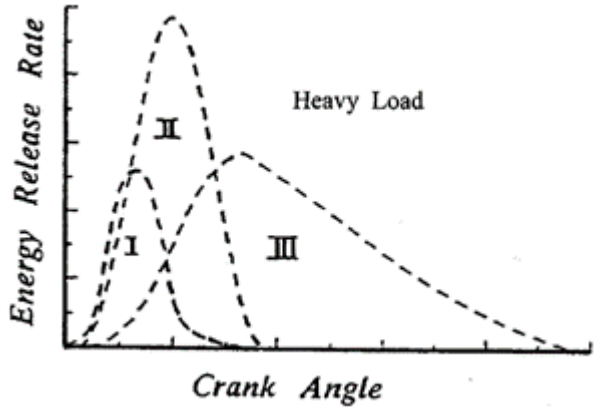

Figure 5.2: Schematic representation of the different components of the combustion energy release rate in a dual fuel engine for a heavy load condition [31]

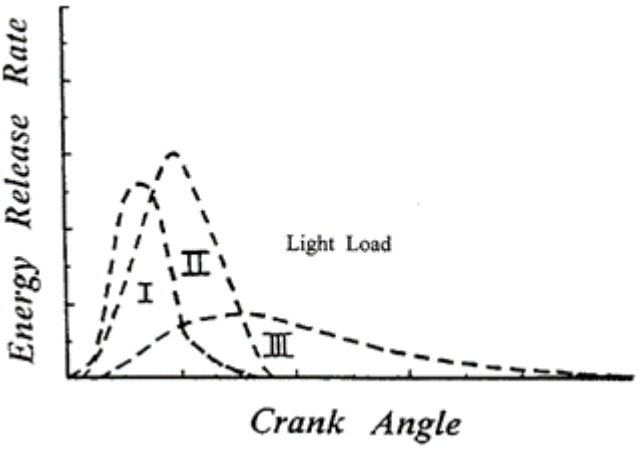

Figure 5.3: Schematic representation of the different components of combustion energy release rate in a dual fuel engine for a light load condition [31]

5.4 Ammonia diesel combustion characteristics

Unfortunately, studies with ammonia diesel fuel mixtures and their combustive characteristics are scarce. However, Liang Yu et. al [73] investigated the autoignition of ammonia n-heptane mixtures both experimental and numerical. N-heptane is used as a surrogate for diesel, since diesel is a mixture of hundreds of hydrocarbons, all with different properties [75]. The experimental tests were conducted using a rapid compression machine, this device has a bore of 215mm and is capable to control the temperature and pressure inside the combustion chamber.

During the tests, the compression temperature was systematically raised by changing the compression ratio and initial temperature. This is done with different fuel blends of 0%, 20% and 40% ammonia. with different starting temperatures, different compression ratios and different fuel blends. Additionally, numerical experiments regarding the ignition delay of n-heptane ammonia blends are done using the CHEMKIN PRO software. CHEMKIN PRO is a chemistry effects predicting simulation software developed by ANSYS and allows the user to simulate complex

chemical reactions within a system.

Results show that as expected the IDTs get longer when the ammonia fraction gets bigger. Similar behaviour is seen with other duel fuel tests. However, tests with other gaseous fuels saw a decrease in ignition delay with higher gaseous fuel fraction which is not seen in these experiments.

The three blends show similar Negative Temperature Coefficient (NTC) behaviour whose temperature range and intensity seem unaffected by the change in ammonia fraction.

Reiter and Kong [47] also investigated the combustion of ammonia diesel mixtures, both numerical and experimental. For the numerical research diesel was again simulated by the use of n-heptane, the experimental research made use of a John Deere 4045 turbocharged 4-stroke engine with a modified air intake manifold. Reiter and Kong concluded that up to 95% of the power could be replaced by ammonia, which also did increase the ignition delay. Reiter and Kong did use higher ammonia diesel ratio's but no signs of a shorter ignition delay with higher gaseous concentrations was noted. It seems that this effect does not take place with gaseous ammonia air mixtures.

Furthermore, Reiter and Kong also observed the negative temperature coefficient seen with typical hydrocarbon fuels, which is caused by the dominance of the diesel fuel in the ignition process.

The engine tests showed good overall fuel efficiency between 20% and 60% diesel load. Below 20% diesel load the fuel efficiency was poor due to poor part-load efficiency as with regular diesel engines. Above 60% diesel load only a small amount of ammonia is supplied, creating relatively lean gas mixtures, which did not burn effectively.

Reiter and Kong [48] conducted a second research project to further investigate the combustion characteristics of ammonia diesel blends. They used the same 4-stroke engine as with the previous tests. During these tests multiple ammonia energy share ratios were used to see the effects of ammonia on emissions, BSFC, combustion efficiency and the cylinder pressure. The different energy ratios are obtained by first increasing the diesel flow to reach for example 20% power, next the ammonia supply is increased until the engine runs on full power, resulting in an 20% diesel, 80% ammonia energy share ratio.

The BSFC, defined as the mass flow rate divided by the power output from the corresponding fuel only, and not the total power output. The BSFC results show opposite trends for diesel and ammonia as shown in figure 5.4. When the diesel load goes under 15% the BSFC of diesel increases due to the typical low efficiency of diesel engines in low loads. Furthermore, the low diesel power goes together with high ammonia power, because the engine runs at 100% load. The combustion of ammonia produces lower temperatures, which in turn results in a less complete combustion. In figure 5.5 is shown that incomplete combustion leads to higher HC emissions. On the other hand the ammonia BSFC is about 400g/KW-hr, when

compared to a BSFC of 200g/KW-hr for 100% diesel operation the combustion efficiency is almost equal (the LHV of ammonia is about half of the LHV of diesel, so the BSFC of ammonia should be twice as high as diesel fuel).

When the diesel energy contribution passes 60% the engine may be approaching its flammability limit, and the ammonia air mixture can be to lean for effective combustion. Therefore, the ammonia BSFC is high. Overall, when either a very high or low ammonia diesel ratio is used the BSFC is poor.

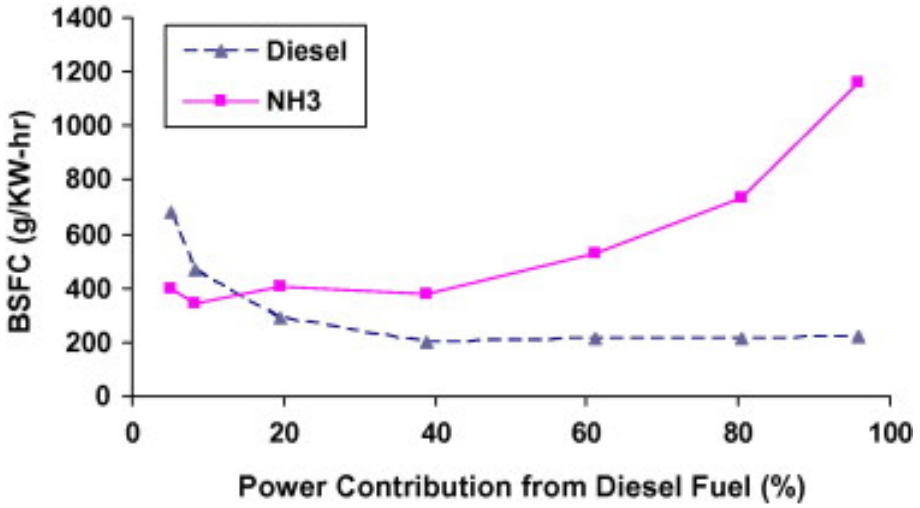

Figure 5.4: Measured engine BSFC data for respective fuels under constant power output operation using various combinations of ammonia/diesel fuel [48].

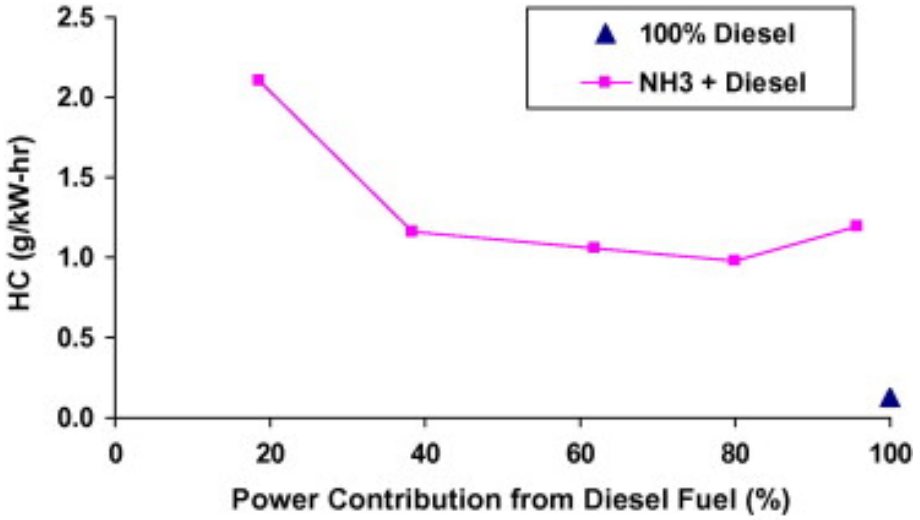

Figure 5.5: Exhaust HC emissions under constant power output operation using various combinations of ammonia/diesel fuel, compared to emissions using 100% diesel fuel [48].

Figure 5.6 shows a combustion efficiency ranging from 91 to 97%. Both the volumetric and mass based methods to determine the combustion efficiency show similar results, although the volumetric method is about 1% higher. The figure shows that most of the ammonia is consumed during combustion. Interestingly the combustion

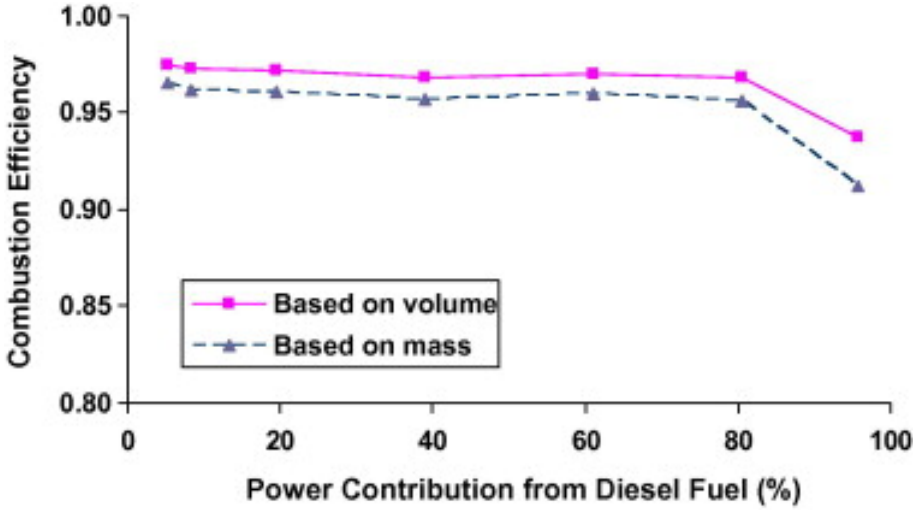

Figure 5.6: Combustion efficiency of ammonia under constant power output operation using various combinations of ammonia/diesel fuel [48].

efficiency in this study is similar to that of a typical CI engine at near stoichiometric conditions an even better than a SI engine operated at slightly rich conditions.

According to Reiter and Kong ammonia diesel operations shows some similarities with natural gas diesel operation, the amount of unburned hydrocarbon increases when more natural gas displaces diesel fuel due to the incomplete combustion of premixed gas-air mixture in the cylinder.

Figure 5.7 shows the cylinder pressure and Heat Release Rate for multiple diesel energy contributions. All the dual fuel cases are compared to the 100% diesel operation, shown with the blue dotted line. The engine uses a system that automatically changes the start of injection according to the fuelling rate, the start of injection corresponding to specific scenario is shown in figure 5.7.

Although some figures show a lower peak pressure, all figures produce the same output power. For instance, the 60% diesel case shows a lower peak pressure, the expansion work is less, but this is compensated by the compression work, which is also lower. As a result the net work output of the engine is in all scenarios the same.

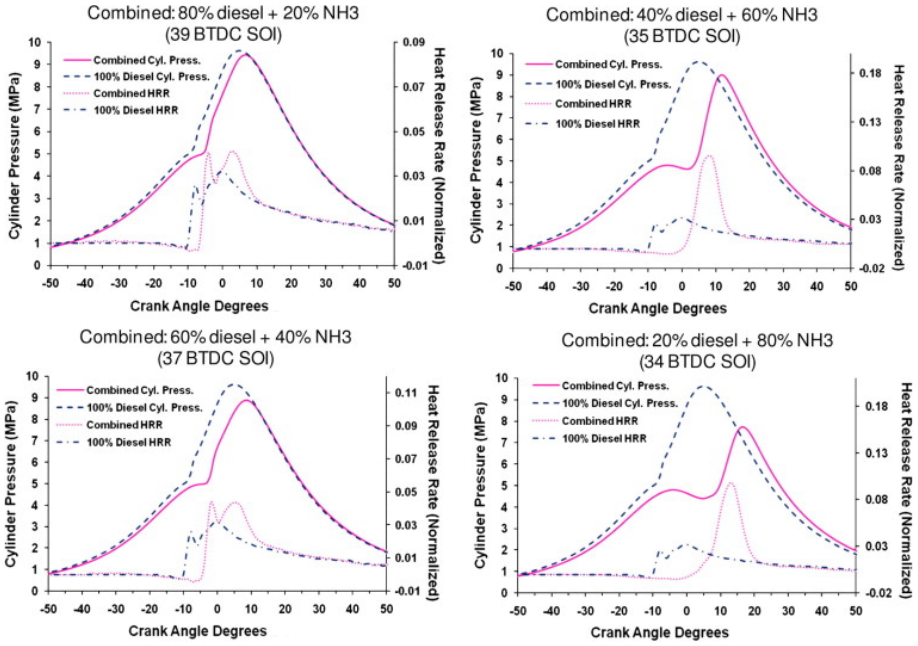

Figure 5.7: Cylinder pressure histories and heat release rate data of constant power output operations at various ammonia and diesel fuel combinations, compared to data using 100% diesel [48].

The figures clearly show an increase in IDT when more ammonia is used, the peak pressure also decreases when more ammonia is used. Reiter and Kong believe that the decrease in IDT is caused by two main reasons. First, less diesel fuel is injected, which decreases the fuel momentum for effective atomization and mixing of the fuel. Secondly, due to ammonia's high resistance to autoignition it is harder to ignite the mixture when it contains more ammonia. At high ammonia energy share ratios (80% ammonia, 20% diesel), the in-cylinder pressure is relatively low, but the expansion pressure is relatively high, resulting in the same net engine torque.

The HRR of the 100% diesel fuel case shows typical features of diesel combustion, which are distinct premixed and diffusion phases. These features are also present in the 80% and 60% diesel cases, but when the diesel contribution further decreases to 40% these features disappear as shown in the combined HRR curves in figure 5.7.

The longer IDT causes a large premixed combustion and a relatively high peak in the heat release rate. It is not known how ammonia is exactly burned, which could be by premixed flame propagation in the ammonia-air mixture or volumetric auto-ignition in the cylinder. It is assumed that the diesel fuel causes a high temperature which initiates the ammonia combustion. The author thinks that the smooth heat release rate from the measurements with high ammonia ratios indicates that ammonia is consumed with a mechanism similar to flame propagation. A modelling study on dual fuel natural gas combustion found a similar flame propagation mechanism [54].

The lower cylinder pressure also implies a lower cylinder temperature when ammonia is used, lower combustion temperatures can lead to higher CO and HC emissions caused by incomplete combustion as shown in figures 5.5 and 5.8, this also leads to lower fuel efficiency.

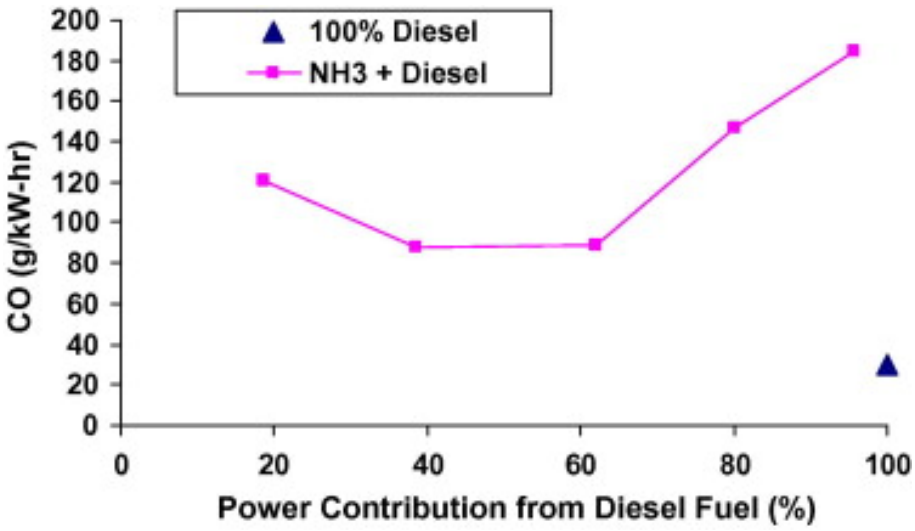

Figure 5.8: Exhaust CO emissions under constant power output operation using various combinations of ammonia/diesel fuel, compared to emissions using 100% diesel fuel [48]

Lately Kun Lin Tay et al. [65] investigated the influence of injection timing and pilot fuel on the combustion of ammonia using a numerical approach. Their results also showed an increase in IDT when more ammonia was used.

5.5 Conclusion

The combustion process in a diesel or dual fuel engine is very complex but can to some extend be described with simple parameters. The ignition delay is a crucial part of this process and has great impact on the engine behaviour. Therefore the ignition delay is considered an important parameter.

Much is known about the combustion in dual fuel engines, and this process is well documented. The dual fuel process differs from the regular diesel process due to the gaseous fuels causing complex reactions during the compression stroke and due to their impact on the ignition. The ignition delay time in dual fuel engines is dependent on the ratio between gaseous fuels and diesel, and on the properties of the fuels.

Ammonia also effects the combustion process, when higher ammonia ratios are used the distinctive pre-combustion and diffusive combustion phases seem to be less distinctive. The HRR shows a more distinctive peak and becomes smoother. The cylinder pressures appear to be lower, which also indicates lower temperatures, the lower temperatures could cause bad combustion efficiency and therefore HC and CO emissions.

The effects of the different combustion characteristics on the partial efficiency's, fuel consumption, power characteristic and turbo charging concept for large two-stroke

dual-fuel ammonia engines has not yet been investigated. Implementing the combustion characteristics found in this chapter into a large two-stroke model will help to give an good estimation of the effects of the different combustion characteristics on the engine performance.

Chapter 6

Ignition delay

6.1 Introduction

Previous chapters have shown the importance of the ignition delay in CI engines, and a fast amount of research has been done regarding the ignition delay time. Multiple simple formals have been made to predict the ignition delay of diesel engines. However, as discussed in previous chapters dual fuel engines behave different compared to regular diesel engines due to the use of gaseous fuels and the chemical properties of those fuels.

6.2 Empirical formulas

M. Bednarski et al. [75] evaluated multiple approaches to determine the ignition delay of CI engines. The most common approaches where considered, which where the correlation introduced by Wolfer, Watson and Hardenberg, and Hase are compared. Hardenberg and Hase [27] created an empirical formula to predict the ignition delay of CI engines. This expression is used in the TU Delft engine model. The expression is of empirical nature and based upon a large amount of tests with different sized diesel engines However, the range of sizes, for example bore diameters or nominal engine speeds, are not listed. Making it hard to determine of the empirical expression applies for large marine diesel engines. The formula to predict the ignition delay in degrees crank angle is shown below.

$$\tau_{i(CA)} = C_f(0.36{+}0.22M_{ps})exp\left[E_A\left(\frac{1}{RT_m(r_c)^{n-1}} - \frac{1}{17190}\right) + \left(\frac{21.2}{P_m(r_c)^n - 12.4}\right)^{0.63}\right] \tag{6.1}$$

The ignition delay $\tau_i[deg]$ is expressed using the following input; mean piston speed $M_{ps}[m/s]$, the universal gas constant R, the mean pressure and temperature in

the inlet manifold, $P_m[bar]$ and $T_m[K]$, the compression ratio r_c, the polytropic compression constant n, and the activation energy $E_A[J/mole]$. The activation energy can be calculated using formula 6.2 and the cetane number CN.

$$E_A = \frac{618840}{CN + 25} \tag{6.2}$$

Wolfer proposed the following approach:

$$t_s = Fp^{-n} exp\left(\frac{E_A}{RT}\right) \tag{6.3}$$

Wherein p and T are the pressure and temperature in the cylinder respectively, E_A is the activation energy, R is the universal gas constant and F and n are empirical chosen constants. Wolfer proposes $F = 0.44$ and $n = 1.19$ for the constants.

Watson improved Wolfs equations by determine the constants F and n in a more accurate way, which results in the following formula:

$$t_s = 3.45p^{-1.02} exp\left(\frac{E_A}{RT}\right) \tag{6.4}$$

All three approaches were compared to experimental test with a 4-stroke turbo charged 4 cylinder engine. The results show that the Hardenberg Hase method is most accurate, the author suspects this is due to the bigger number of empirically chosen coefficients. It should be noted that although the Hardenberg and Hase method was most accurate, it was not able to give an accurate prediction of IDTs over the full range of engine speeds. Figure 6.1 shows the results.

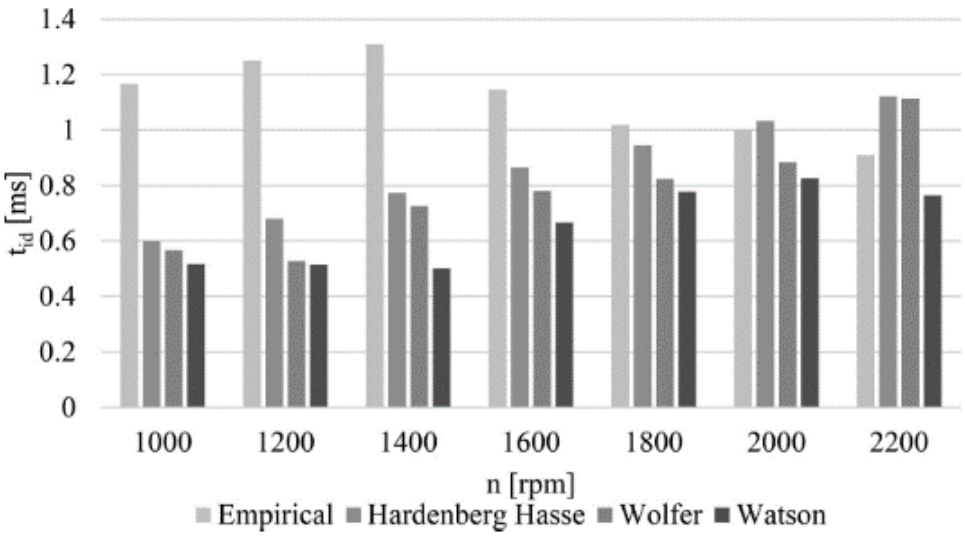

Figure 6.1: Results of experimental and empirical tests

Prakash et al. [46] developed an expression to determine the ignition delay of a dual fuel engine operated with biogas and diesel as pilot fuel. The formula from Hardenberg and Hase [27] to estimate the ignition delay of a regular diesel engine was modified using experimental data and considering the change in oxygen concentration due to the gaseous fuel [36].

$$\tau_{i(CA)} = C_f(O_{df})^k(0.36{+}0.22M_{ps})exp\left[E_A\left(\frac{1}{RT_m(r_c)^{n-1}} - \frac{1}{17190}\right) + \left(\frac{21.2}{P_m(r_c)^n - 12.4}\right)^{0.63}\right] \tag{6.5}$$

C_f, k and O_{df} are the modified coefficient, exponent for oxygen concentration, and oxygen concentration ratio, respectively. The oxygen concentration ratio is defined as the ratio between the oxygen concentration in the charge and the oxygen concentration in in the atmosphere. The oxygen concentration exponent k was obtained with the method of least squares by comparing the results of the predicted and experimental ignition delay data at multiple engine loads.

The modified coefficient C_f was added by Prakash and Ramesh to match the formula with the experimental data, this was also done with the method of least squares.

Multiple parameters are determined using experimental data obtained with a dual fuel 4-stroke engine using diesel and biogas, these parameters are both depended on the engine and the fuel mixture. To use Prakash his formula with large two-stroke ammonia diesel engines new parameters have to be determined with experimental data, using ammonia diesel mixtures and preferably a large two-stroke engine, since scaling effects are not considered in Prakash his formula.

6.3 Chemical simulation

Another approach to predict the ignition delay is the use of chemical simulation software, CHEMKIN PRO is often used for this purpose. CHEMKIN PRO has the advantage of being independent of engine specific measurements, and therefore is not affected by engine size.

Reiter and Kong [47] used CHEMKIN PRO to demonstrate the potential of ammonia diesel mixtures in CI engines. However, they used the software to determine if the fuel mixture would ignite in their test setup, and did not try to determine the ignition delay.

Liang Yu et al. [73] determined the IDT of ammonia n-heptane mixtures using both CHEMKIN PRO and a rapid compression machine (RCM). A RCM allows the user to precisely control the pressures and temperatures inside the machine to replicate the compression stoke of an engine. Three different types of ammonia energy share ratio mixtures were used: 0% (mixture 1), 20% (mixture 2) and 40% (mixture 3). The results are shown in figure 6.2, the experimental results are dots and the simulation results are lines.

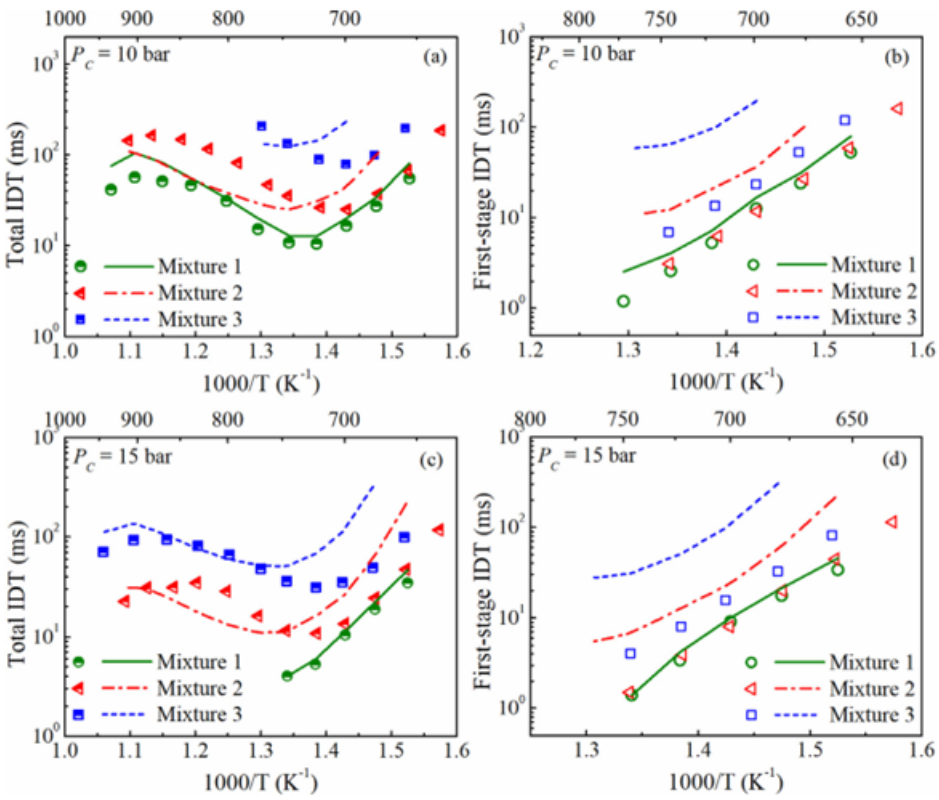

Figure 6.2: Comparison of the IDTs of multiple ammonia n-heptane mixtures.

The results show that the simulation is capable of predicting the IDT of mixture 1 which is 100% n-heptane. The effect of ammonia on the auto ignition of n-heptane is greatly over predicted resulting in an overestimation in IDT with higher ammonia energy share ratios. At temperatures below 720K the simulated IDTs are much longer than the experimental results.

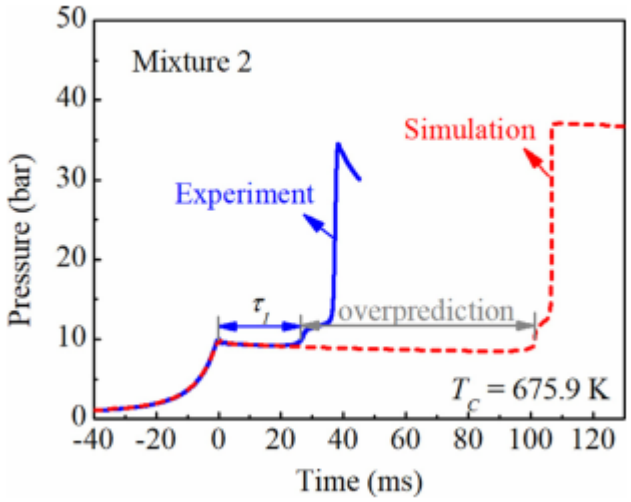

Figure 6.3: Comparison of auto ignition curves of mixture 2: 20% ammonia energy share ratio.

Figure 6.3 compares the ignition delay of a 20% ammonia energy share ratio determined using experiments and simulations. The figure clearly shows an overestimation of simulated first stage ignition delay. The authors expect that the difference in delay time is caused by the relatively unknown reactions between the nitrogen and carbon.

6.4 Conclusion

The ignition delay can be estimated using multiple approaches. The approach from Hardenberg and Hase has proven to be the most accurate empirical approach. Furthermore, this approach has been converted to be used for dual fuel engines and proven to be accurate. However, no test were done big two-stroke engines, and the accuracy of this empirical approach for larger engines is unknow.

The CHEMKIN PRO software provides an alternative approach in determining the combustion delay by only considering chemical reactions, this makes the approach independent of the engine size. However, tests have shown the accuracy of the CHEMKIN PRO software for predicting the ignition delay of ammonia n-heptane mixtures is low due to the relatively unknown chemical interactions between nitrogen and carbon.

The formula from Hardenberg and Hase modified by Prakash et al. [46] is expected to give the most reliable estimation of the ignition delay of the engine of an ocean going freight vessel due to its proven accuracy in determine the ignition delay time of dual fuel diesel engines.

Chapter 7

Conclusion literature study

Ammonia can be considered as an interesting alternative fuel for deep sea shipping due to its relative high energy density and easy storage at practical temperatures and pressures when compared to hydrogen. Ammonia can be produced in a sustainable way and the energy required to produce ammonia is low when compared to carbon based hydrogen carriers. Furthermore, infrastructure to produce, transport and store ammonia is already in place because ammonia is one of the most produced chemicals in the world.

Ammonia itself has poor combustion characteristics and requires very high temperatures to self-ignite. To stimulate the ignition of ammonia multiple solutions are tried. Spark ignition is a feasible solution, so is using hydrogen or diesel as a pilot to ignite the ammonia. Ammonia with diesel as pilot fuel in CI engines is considered the most practical and promising short term solution. A dual fuel ammonia diesel engine would allow the engine to run on 100% diesel in case no ammonia is available or the ammonia fuel system fails, making ammonia with diesel as pilot the most practical solution from a shipowners perspective.

The simulation of the voyage of an ocean going cargo vessel requires a model capable of simulating on a very long time scale. Complex 3D models are not capable of modelling on such a long time scale, whereas mean value models require less computational power and can operate on a longer time scale. Additionally previous research has confirmed mean value accurate enough for system level simulations and the simulation of cargo vessel voyages.

The TU Delft mean value Seiliger model is chosen to model the voyage of an ocean going cargo vessel. The model characterises the combustion with three combustion parameters, a, b and c. These parameters are mostly dependent on the ignition delay and the combustion efficiency.

The combustion process of a dual fuel engine differs from a regular diesel engine due to the gaseous fuels reacting during compression. Additionally the gaseous fuels effect the ignition process and ignition delay.

The ignition delay of an engine can be predicted with empirical formulas or chemical simulations. Although empirical formulas are dependent on measurements with engines, they are preferred over chemical simulations because CHEMKIN PRO greatly overestimates the ignition delay of ammonia n-heptane mixtures. The formula from Prakash et al. [46] is expected to give the most reliable estimation of the ignition delay of the engine of a deep-sea cargo vessel due to its proven accuracy in determine the ignition delay time of dual fuel diesel engines.

Part II

Modelling

Chapter 8

The dual fuel model

8.1 Introduction

This chapter will go over the separate elements in the original TU Delft engine B model to see if they have to be changed to accommodate a dual fuel ammonia mode. The original model will be explained and its assumptions and limitations will be discussed, the necessary changes will be explained and the new assumptions introduced with those changes will be discussed as well.

8.2 The benchmark engine

The TU Delft engine B model is capable of simulating the performance of two engines: the MAN 6S35ME ZJ3 and the MAN 6S35ME ZJ5. In this thesis only the MAN 6S35ME ZJ3 engine is used. The selected engine is a two-stroke marine diesel engine with a nominal engine speed of 167 RPM and a nominal engine power of 4170 kW, the general engine information is shown in table 8.1.

Type	MAN 6S35ME
Rated Power [kW]	4170
Rated Speed [rpm]	167
Stroke [m]	1.55
Bore [m]	0.35
p_{max} at MCR [Mpa]	18.5

Table 8.1: General engine data [61]

This type of engine can typically be found in an ocean going chemical tanker, an example of a ship wherein such engine is used is the Castillo de Tebra, which is a 13000 DWT chemical tanker with a length of 113.8 meter. The ship uses a direct drive configuration with a shaft generator and a controllable pitch propeller [61] [62].

The regular diesel engine is converted to an ammonia-diesel engine, multiple changes have to be made to covert the engine for diesel-ammonia use. First of all the ammonia has to be injected into the system, two methods are possible: ammonia gas can be injected into the inlet manifold or ammonia can be directly injected into the cylinder. The second option means that separate injectors have to be build into the cylinder heads of the engine [40].

MAN has used the direct injection solution for their methanol engines and have shown that they intend to use the same method for ammonia. Since the engine in the model is a MAN engine their intended method for injecting ammonia is selected [40].

Since the term pilot fuel is used in multiple ways within the industry, the meaning within this thesis is clarified. Hereafter, the term pilot fuel is used to refer to the fuel injected to promote the combustion of ammonia as a fuel.

Furthermore, as discussed in chapter 6 ammonia will most likely cause an increase in ignition delay, the injection timing and strategy will have to be adapted when ammonia is injected into the engine.

8.3 Fuel supply

The fuel supply to the engine is used to control the power output of the engine. Together with the load on the engine this results in the engine speed, the engine speed can indirectly be controlled with the fuel supply.

8.3.1 Original model

The original model can be operated in multiple ways and with multiple load cases. The engine can be used in generator mode, at constant speed with a varying load which can be set in the 2_stroke_driver.m file. Or with a propeller load, in which the propeller curve as shown in formula 8.1 is used and an engine speed can be set which it will try to maintain. The third control option is setting a manual fuel rack, in which the user determines the fuel flow into the engine by hand.

$$M_{prop} = 1000 \cdot M_{nom} \cdot \left(\frac{n_e}{n_{e,nom}} \right)^e \tag{8.1}$$

When the fuel rack is set by hand the user can set a value from zero to one as the fuel rack, which is defined as the fraction of the nominal fuel mass used per engine cycle. When the engine is controlled by setting an engine speed the governor is used to determine the fuel rack, the governor uses a PID controller to compare the current engine speed with the desired engine speed and sets the fuel rack accordingly.

The fuel flow and the fuel mass per cycle are determined in the fuel pump block (FP), in which the fuel rack provided either by the user or the governor and the engine speed are used to calculate the fuel mass per cycle and the fuel flow as shown in formulas 8.2 and 8.3.

$$m_{f,cyc} = X_f * m_{f,cyc,nom} \tag{8.2}$$

$$\phi_f = m_{f,cyc} * i_{cyc} * \frac{n_{eng}}{k_{cyc}} \tag{8.3}$$

8.3.2 Model changes

The original model is quite simple however, it uses the nominal fuel flow into the engine determined by the manufacturer, a value not known for ammonia. Furthermore, the addition of a second fuel creates an extra variable besides the fuel rack: the ratio between ammonia and diesel fuel.

To determine the ratio between ammonia and diesel fuel a new variable is introduces into the model: the ammonia energy share ratio, which is a value from zero to one and indicates the fraction of energy delivered by ammonia. Note that this ratio is based on the energy of the fuel and not the fuel mass. The ammonia energy share ratio is set by the user and can be changed over time during the simulation.

To determine an appropriate ammonia supply the nominal fuel mass per cycle is converted to the nominal fuel energy per cycle using the lower heating value of the selected diesel fuel and ammonia. The newly introduced ammonia energy share ratio together with the lower heating values of the two fuels are used to determine the mass per cycle and flow of both fuels into the engine. The therm fuel rack is not valid anymore, the operator or governor determines the fuel flow by setting a fraction of the nominal chemical fuel flow to the engine, which is still a value from zero to one with 1 nominal chemical energy flow to the engine.

In Simulink the Fuel Pump (FP) block is altered to determine the fuel flow of both ammonia an diesel fuel into the engine. The FP block takes the ammonia share ratio and the chemical energy flow as input and gives the ammonia fuel flow, diesel duel flow, ammonia mass per cycle and diesel mass per cycle as output. A new constant is necessary to do these calculations, the LHV of ammonia.

A new Matlab file called "gas_specification.m" is added to the properties folder, in this file the properties of ammonia are described. Which are the stoichiometric air fuel ratio $\sigma_{NH_3} = 6.0466[kg/kg]$, the density at 15 degree Celsius $\rho_{NH_3} = 0.712[kg/m^3]$ and the lower heating value $H_0 = 18600[kJ/kg]$. Furthermore, the control vector "energyshareratio1" is added to the Matlab file "DE_B_2stroke_driver.m" to be able to control the energy share ratio between ammonia and diesel fuel.

Note that the maximum amount of fuel that can be effectively injected into the engine depends on ratio between fuel and oxygen in the cylinder. If there is not enough oxygen present the fuel will not completely combust. Ammonia has a low LHV with respect to diesel fuels so more fuel mass is required to deliver the same amount of energy. However, ammonia has a lower stoichiometric air fuel ratio which compensates for the LHV. It is expected that the engine running on ammonia can operate at approximately the same air excess ratio as with diesel fuel. In the original model the combustion efficiency is dependent on the air access ratio, if the addition of ammonia decreases the air excess ratio significantly the combustion efficiency should decrease.

The LHV of ammonia is less than half of Marine Gas Oil (MGO), so more than double the amount of ammonia has to be injected to deliver the same amount of power. In practice this will affect the fuel system, a second fuel pump for ammonia is necessary which will most likely require more power due to the increase in fuel flow. In the current model the energy consumption of the pumps is only dependent on engine speed and not on fuel mass flow, this effect is not considered in the model. Furthermore, the increase in injected mass into the cylinder will most likely effect the mass flow through the engine, the model does consider the increase in injected mass and the effects will be studied in chapter 10.

8.3.3 Conclusion fuel supply

The fuel supply model has been successfully changed to accommodate ammonia, to do so a new variable has been added, the ammonia energy share ratio. The fuel rack is changed to a percentage of the chemical energy flow into the engine. Ammonia will increase the total mass flow into the engine, this is not considered for the energy consumption of the fuel pump, the changes in mass flow through the engine do consider these changes.

8.4 The Seiliger stages

In this section the combustion process is described, during this process the fuel is combusted and the heat released is converted to mechanical energy. The combustion process is an essential part of the model and greatly impacts the engine performance.

The Seiliger model describes the combustion process using six points and six trajectories in between as shown in figure 8.1. Values of pressure and temperature are only known in these six points, heat input and delivered power are calculated per trajectory. The use of only six points significantly reduces the computational time required to run the model [33].

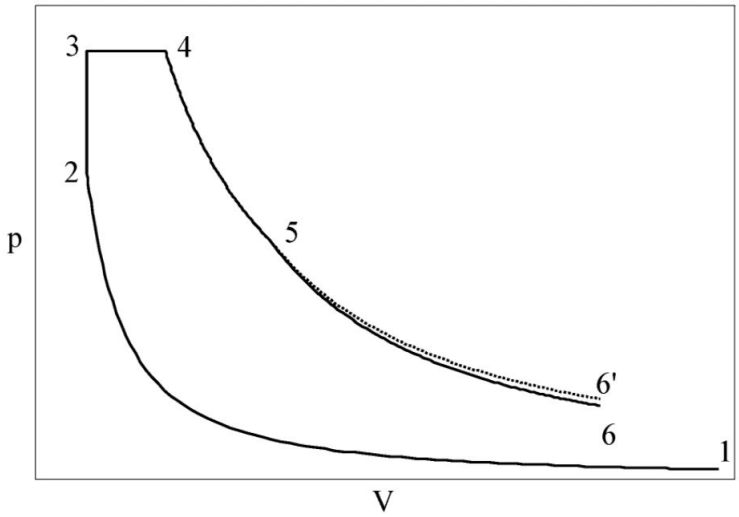

Figure 8.1: Seiliger cycle p-V diagram [17]

8.4.1 Stage 1-2

The temperature and pressure in the first point are determined by the gas exchange process. From point one the air inside the cylinder is compressed, this trajectory is assumed to be a polytropic process. The first stage is dependent on the geometric compression ratio ϵ, the moment when the exhaust closes (EC) and the polytropic compression exponent.

8.4.2 Stage 2-3

The second stage from point 2 to 3 is assumed isochoric. This trajectory starts when the piston is at TDC, in this stage isochoric combustion takes place, heat is fed into the cylinder until the peak pressure is reached. The combustion parameter a is used to determine the size of the iso-volumetric pressure rise and is defined as the ratio between the compression pressure and the peak pressure. The parameter a also has a great impact on the thermodynamic efficiency of the engine. Schulten derived a formula to determine the isochoric pressure ratio a, dependent on the ignition delay and the engine load [52].

8.4.3 Stage 3-4

During the isobaric stage, from point 3 to 4, the pressure remains constant. The temperature increase is determined by the combustion parameter b. Baan introduced a new parameter bb, which is a multiplication of the combustion parameters a and b, making parameter b dependent on a and bb. Parameter bb is mostly dependent on the injected fuel during this period [5].

8.4.4 Stage 4-5

The trajectory of stage four is assumed to be a isothermal process and defined by the combustion parameter c, which is the ratio between the pressures in point four and five. Parameter c is determined by using the heat input between point four and five. The heat released in the three combustion stages from point two to five are equal to the total heat input.

The total heat input can be calculated via the injected amount of fuel, not all fuel is burned. The unburned fraction is represented by the combustion efficiency η_{cb}. Furthermore, during combustion heat is transferred via the cylinder walls and piston head. The loss of this heat is considered using the heat release efficiency η_q. The heat release efficiency is calculated with the Woschni heat exchange model.

The heat input between point four and five and Seiliger parameter c can be determined by subtracting the heat input in stages two and three from the net heat input.

8.4.5 Stage 5-6

The last trajectory from point five to six is modelled to be a polytropic process. The expansion ratio during this process is related to the volume in point five and the volume when the exhaust opens (EO).

The result of the Seiliger stages is shown in figure 8.2.

8.4.6 Model changes

The definition of the stages is not changed and remain the same. However, stages 2-3, 3-4 and 4-5 take the injected fuel as an input, a second fuel supply for ammonia is added to the model. The distribution of the fuel remains the same, which automatically makes it so that the distribution of the injected and combusted mass over the Seiliger stages is equal for both fuels. This distribution of the injected fuels is not changed because the available information on ammonia-diesel combustion provides graphs with the cylinder pressure or released heat as function of the crank angle or time. These graphs do not differentiate between which fuel causes the increase in pressure on the released heat. Therefore, it is assumed that per combustion stage, the percentage of released heat from ammonia is equal to the percentage of released heat from diesel. In reality it is not certain that both fuels are burned at the same rate. Even more so, ammonia has a relatively slow flame propagation speed, making it likely that it will burn slower than the diesel fuel which will lead to an uneven distribution. Furthermore, due to the low LHV of ammonia, a relatively big amount of ammonia mass has to be injected, which makes is plausible that the ammonia is injected slower than diesel which will also cause a shift of ammonia to the later stages. Lastly, the manufacturer uses separate injectors for the fuel, the manufac-

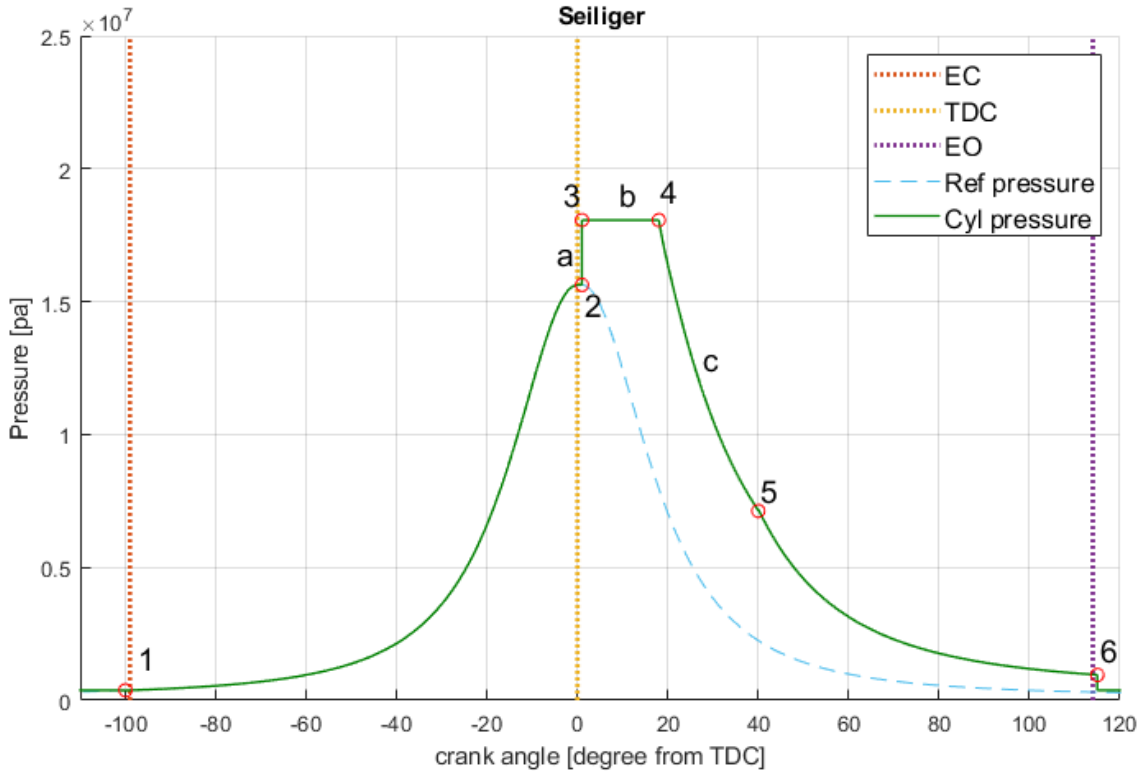

Figure 8.2: Seiliger stages pressure as function of crank angle.

turer can choose to injected the two fuels at different times and rates, which would also make the assumption that both fuels are equally distributed over the Seiliger stages invalid.

Although, the two fuels are not considered separately, the changes in the trapped mass mixture can be considered for the whole mixture by changing the parameters describing the Seiliger cycle. These parameters and changes will be discussed in section 8.5. Furthermore, research comparing the capability of the Seiliger and Vibe model to capture the combustion characteristics of hydrogen-natural gas combustion has confirmed that both models are reasonably accurate [51], so it is certainly not impossible to capture the properties of dual fuel combustion with the Seiliger cycle.

8.4.7 Conclusion Seiliger stages

The Seiliger stages have been changed so both ammonia and diesel fuel can supply energy into the system. The available information on ammonia-diesel combustion provides graphs with the cylinder pressure or released heat as function of the crank angle or time. These graphs do not differentiate between which fuel causes the increase in pressure on the released heat. Therefore, it is assumed that per combustion stage, the percentage of released heat from ammonia is equal to the percentage of released heat from diesel.

The distribution of the fuels over the Seiliger stages is equal for both fuels, in reality it is possible that for example more diesel fuel is combusted in the first stage.

Although the combustion of both fuels is equally distributed, the effect of ammonia can be considered by changing parameters shaping the Seiliger cycle, these changes are discussed in the next section.

8.5 The Seiliger parameters

The previous sections has defined the Seiliger stages and mentioned that they are dependent on the Seiliger parameters a, b and c. This section will explain how these parameters are determined.

8.5.1 Parameter a

Seiliger parameter a is defined as the ratio between the compression pressure and the peak pressure as shown in formula 8.4.

$$p_3 = p_2 \cdot a \tag{8.4}$$

Schulten derived an empirical formula for the isochoric pressure ratio a, which is dependent of the injected fuel, and T_2. The heat released in stage 2-3 is described with $\tau_{cb} \cdot \eta_{cb} \cdot q_{f,23} \cdot X_a$ in formula 8.5. Wherein η_{cb} describes how much of the injected fuel is burned, τ_{cb} the ignition delay and X_a the fraction of heat released in stage 2-3.

$$a = 1 + \frac{\tau_{cb} \cdot \eta_{cb} \cdot q_{f,23} \cdot X_a}{C_v \cdot T_2} \tag{8.5}$$

$$X_a = X_{a,n} \cdot \frac{n_e}{n_{e,nom} - 1} + X_{a,f} \cdot \left(\frac{m_f}{m_{f,nom}} - 1 \right) + X_{a,c} \tag{8.6}$$

Previous research by Schulten has shown that with increasing fuel supply the pressure rise first increases and later decreases [52]. When a small amount of diesel fuel is injected there is enough time for all the fuel to be injected before the start of combustion, when the fuel supply decreases further the pressure ratio also decreases. This explains the effect of the fuel supply on the pressure rise. This effect is modelled with the factor X_a, the factor X_a is lower at high engine speeds and increases with lower engine speeds, this means that the incompleteness of the explosive combustion is bigger at higher engine speeds, less energy is released during stage 2-3. X_a is based upon experimental measurements. The original formula is fitted to measurements with a four-stroke engine. During the calibration of the model it was noticed that at part loads with the same engine speed X_a still changes, hence $X_{a,f}(m_f)$ is added to make X_a dependent on both engine speed and the fuel injection to accommodate the simulation of part load conditions.

8.5.2 Parameter bb

Baan introduced a new parameter bb, which is a multiplication of the combustion parameters a and b. As shown in the formula below, bb is dependent on the energy in the fuel, the temperature in point 2, the specific heat at constant pressure, and the fit function X_b. The parameter bb is used to determine b, which is the ratio between the temperature in point 4 and 3.

$$bb = a \cdot b = 1 + \frac{X_b \cdot q_f}{c_p \cdot T_2} \tag{8.7}$$

$$X_b = X_{b,n} \cdot \frac{n_e}{n_{e,nom} - 1} + X_{b,f} \cdot \left(\frac{m_f}{m_{f,nom}} - 1 \right) + X_{b,c} \tag{8.8}$$

$$b = \frac{bb}{a} \tag{8.9}$$

The fit function X_b is the same function as for a but with different constants, this function is also fitted to data obtained with tests.

8.5.3 Parameter c

Parameter c is used to find the ratio between volume 4 and 5, and pressure 4 and 5, during the isothermal combustion by definition the temperature is constant. The model assumes that the remainder of the injected energy is burned in this last stage. The formula to find c is shown below:

$$c = EXP\left(\frac{w_{45}}{T_4 \cdot R_{45}} \right) \tag{8.10}$$

8.5.4 Model changes

The use of ammonia does change the shape of the Seiliger cycle, for which the parameters a, b and c have to be changed. However, the relation of these parameters with the Seiliger cycle stay the same. The heat input q_f is changed to the sum of q_p (heat pilot fuel) and q_{NH_3} (heat ammonia). The fit functions X_a and X_b distribute the heat release over the Seiliger stages 2-3, 3-4 and 4-5. These functions are fitted to measurements which were done with a regular diesel engine. There is no data available to fit these functions to an ammonia diesel engine. However, some assumptions based on the properties of ammonia can be made. The lower flame speed and poor auto-ignition properties of ammonia will most likely cause more fuel to be burned in later stages because it will take longer for the fuel mixture to ignite and to burn. This shift to later stages will most likely increase when more ammonia

is used, when only diesel fuel is used the original distribution should be used. To account for the different properties of ammonia an extra therm, dependent on the ammonia energy share ratio is added to X_a and X_b. These therms can be tweaked with the constants $X_{a,d}$ and $X_{b,d}$, the size of these ammonia dependent constants are not known, during the analysis of the combustion model multiple values will be used and the results will be compared to the available experimental data in chapter 10.

Furthermore, some changes to the equation has to be made to allow for two different fuels to be used. The fuel dependent factor is changed to scale with energy to account for the different lower heating values of the two fuels. The same changes are made in the formula for X_b. These changes bring the same assumptions as discussed in section 8.4, ammonia an diesel will be equally distributed over the multiple Seiliger stages. The new formula's are shown in equation 8.11 and 8.12.

$$X_a = X_{a,n} \cdot \frac{n_e}{n_{e,nom} - 1} + X_{a,f} \cdot \left(\frac{m_p \cdot LHV_p + m_{NH_3} \cdot LHV_{NH_3}}{m_{f,nom} * LHV_f} - 1 \right) + X_{a,d} \cdot x_f + X_{a,c} \tag{8.11}$$

$$X_b = X_{b,n} \cdot \frac{n_e}{n_{e,nom} - 1} + X_{b,f} \cdot \left(\frac{m_p \cdot LHV_p + m_{NH_3} \cdot LHV_{NH_3}}{m_{f,nom} * LHV_f} - 1 \right) + X_{b,d} \cdot x_f + X_{b,c} \tag{8.12}$$

8.5.5 Conclusion Seiliger parameters

The Seiliger parameters are adapted to accommodate two fuels, these changes allow the model to run with diesel and ammonia as a fuel. New constants dependent on the ammonia energy ratio are added to X_a and X_b, multiple values for these constants will be tested in chapter 9.

8.6 Ignition delay

The ignition delay is defined as the time between the moment of fuel injection and a steep pressure rise. The ignition delay is used to determine parameter a, and therefore has a big influence on the initial pressure rise in the cylinder. A bigger ignition delay allows more fuel to be injected in the cylinder before the start of combustion, which will lead to a bigger pressure rise and a higher value for a.

8.6.1 Original model

Heywood [28] has developed a formula to determine the ignition delay which is dependent on the mean piston speed, activating energy, gas constant, temperature at injection, pressure at injection and compression ratio. The formula from Heywood is shown below. The origin and limitations of this formula are already discussed in chapter 6.

$$\tau_{i(CA)} = C_f(0.36{+}0.22M_{ps})exp\left[E_A\left(\frac{1}{RT_m(r_c)^{n-1}} - \frac{1}{17190}\right) + \left(\frac{21.2}{P_m(r_c)^n - 12.4}\right)^{0.63}\right] \tag{8.13}$$

8.6.2 Model changes

The alternative model selected in chapter 6 considers the oxygen concentration in the cylinder. The addition of a gaseous fuel would lower the oxygen concentration which would increase the ignition delay. Experiments with other gaseous fuels have confirmed this relation. The new formula has an empirical nature, the modified coefficient and the exponent for oxygen concentration are determined by matching the formula with measurements using the least squares method. However, no data is available to match the ignition delay with the oxygen concentration. But the research from Reiter and Kong [48] does show the pressure as function of crank angle for multiple ammonia diesel ratios. These graphs are imported into a Microsoft Excel file. Note that the injection time is automatically changed by the engine used in the experiments, the applicable injection time is shown in the graphs by the authors.

The IDT is defined as the time between start of injection and a steep pressure rise, the definition of a steep pressure rise is somewhat vague, therefore this is often defined in a mathematical way. According to Syrims et al. [64] and Ando et al. [3] the second derivative of the cylinder pressure always peaks at, or slightly after the start of ignition. Therefore, the start of ignition is determined by finding the peak in the second derivative of the cylinder pressure. The derivative is calculated numerically in excel, figure 8.4 shows the pressure, the first, and the second derivative of the pressure. The figure clearly shows a peak in the second derivative which indicates the start of combustion. The crank angle at the start of injection is subtracted from

the crank angle corresponding to the peak in the second derivative of the pressure, this results is the ignition delay in crank angle degrees.

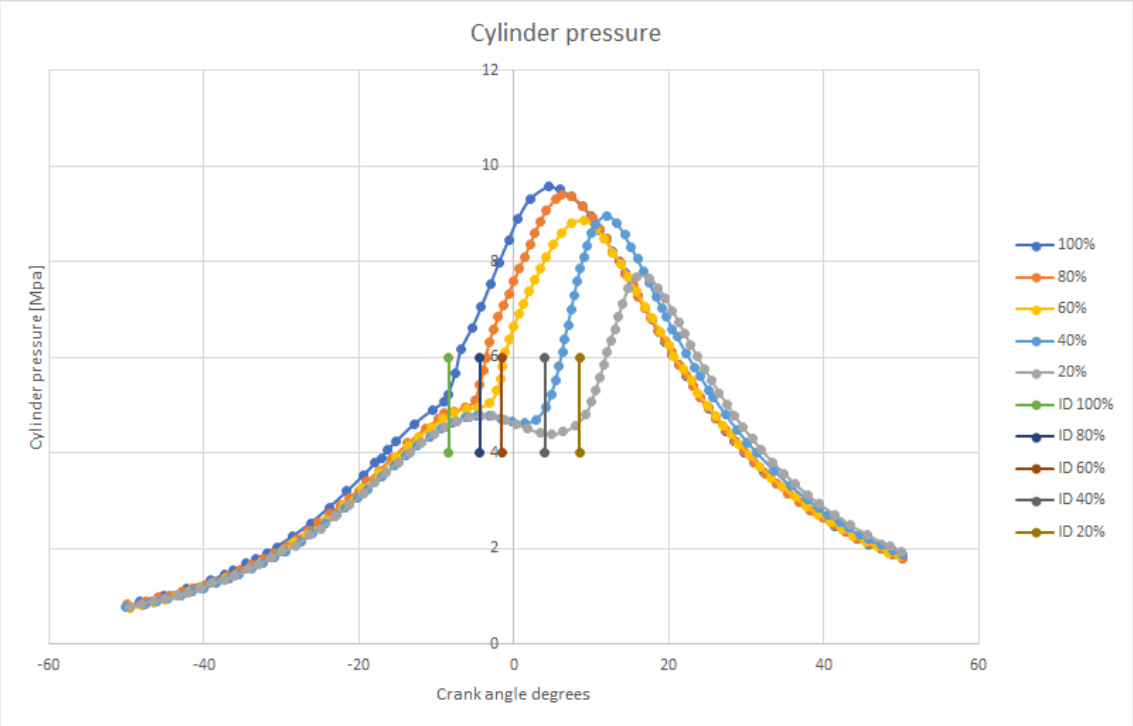

Figure 8.3: Cylinder pressure

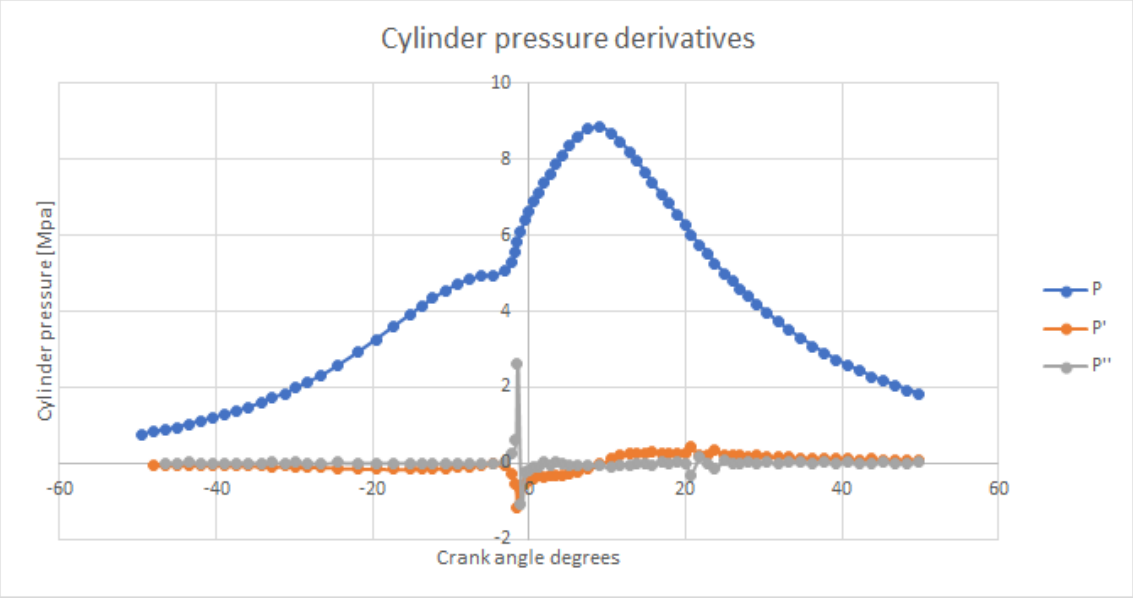

Figure 8.4: Cylinder pressure derivatives

The relative ignition delay is calculated by dividing the ignition delay at a certain ammonia diesel ratio by the ignition delay with 100% diesel operation. The relative ignition delay is plotted as a function of the ammonia energy share ratio in figure 8.5.

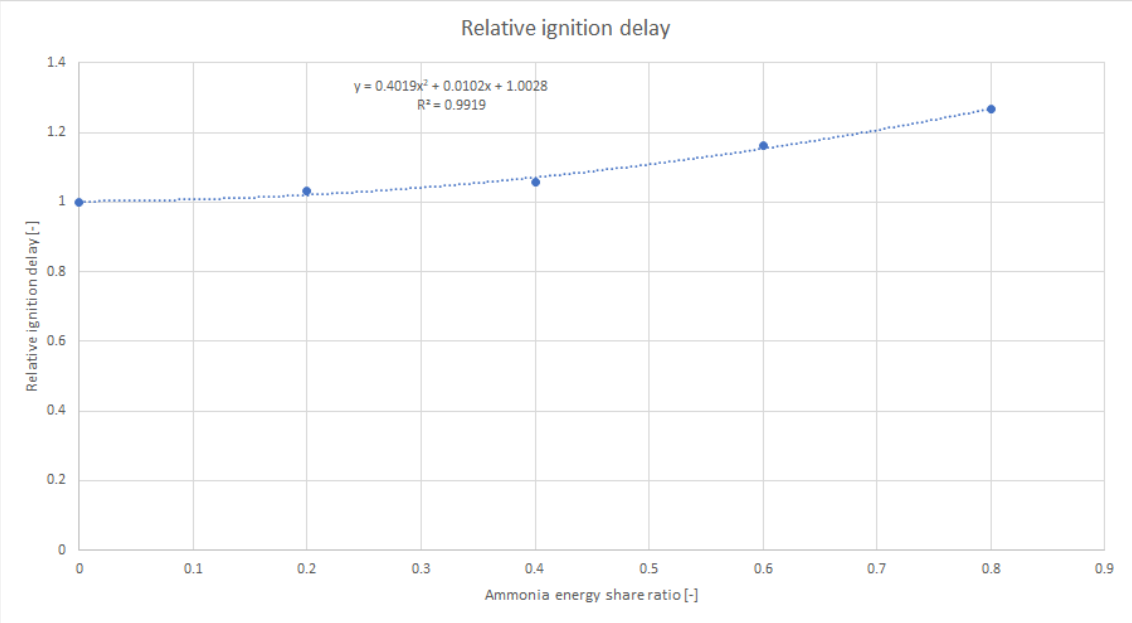

Figure 8.5: Relative ignition delay time

A trend line is used to find the relation between ignition delay and ammonia energy share ratio. The function created by this trend line is used in the model, the original formula for the ignition delay is multiplied with the trend line function to make it dependent on the ammonia energy share ratio as shown in figure 8.6. The most right rectangle in figure 8.6 shows the formula to correct for the use of ammonia.

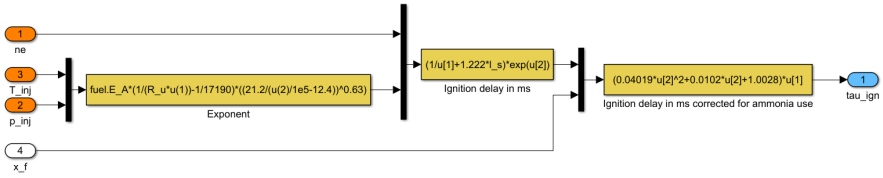

Figure 8.6: Ignition delay time model

The data used to create the trend line is generated at nominal load. The trend line is only dependent on the ammonia energy share ratio, and not the engine power and speed. The effect of part load conditions and engine speed on the increase in ignition delay due to ammonia are not considered in this function. The impact of engine speed, injection temperature and injection pressure are considered separately in the original model for the ignition delay.

Furthermore, the tests on which the correction for ammonia on IDT is based are done with a relatively small four-stroke engine. It is likely that the lower engine speed, higher pressures and bigger volumes in the two-stroke engine have an effect on the relation between the ammonia energy ratio and the IDT. These effects are not considered in the new model.

It should be noted that in reality a change in ignition delay time can, to some extend, be compensated by changing the injection timing or the injection strategy. However, in the TU Delft engine B model the injection timing is only used to

determine the pressure and temperature at the start of injection. The ignition delay time in dependent on these values. Furthermore, in the model the ignition delay time determines how much fuel can be injected before the fuel ignites, so in the model the IDT only impacts the Seiliger parameter a. The diesel-ammonia experiments discussed in chapter 5 show a different link between the initial pressure rise and the ammonia energy share ratio, when more ammonia is used, the ignition delay increases, but the initial pressure rise decreases. This effect could be explained by the lower combustion speed of ammonia being the limiting factor instead of the time to inject fuel. The TU Delft engine B model does not consider the combustion speed of the fuels directly, however, the impact of ammonia on the combustion process if further implemented in chapter 9.

8.6.3 Conclusion ignition delay

Although the modified formula from Hardenberg and Hase has been selected as a good alternative, it cannot be implemented because the necessary data is not available. However, a function to correct for the effect of ammonia on the ignition delay is implemented in the model. The function is derived from measurements on a small four-stroke engine at nominal loads, therefore, the effect of engine load and the scaling are not considered in the ammonia correction function. Furthermore, the injection timing of the engine can be changed to compensate for the increased ignition delay time of ammonia, in the model this only effects the pressure and temperature at the start of injection, no changes to the injection timing are made. Although, the effects of engine load and scaling are not considered in the model, it is expected that the new IDT model will give a reasonable representation of the effects of ammonia on the IDT and that the model will be usefully to predict the effect of ammonia on the overall engine performance.

8.7 Air excess ratio

The combustion of fuel requires oxygen, how much oxygen is required is an important factor because it is often the limit of how much fuel can be effectively injected in the engine. Injecting too much fuel will lead to incomplete combustion because there is no oxygen to burn it.

8.7.1 Original model

The reaction between diesel fuel and air is modelled with basic chemical reactions. The model assumes that the only reaction taking place is that between oxygen and diesel fuel, the other gasses present in the cylinder will not react according to this model, this however, is not true. In reality for example nitrogen often reacts with oxygen to form NO_x emissions. Assuming that diesel fuel consist of a combination of carbon, hydrogen and sulphur, the complete combustion of diesel fuel can be described with the chemical reaction shown below.

$$C_pH_qS_r + (p + \frac{q}{4} + r) \cdot O_2 \rightarrow p \cdot CO_2 + \frac{q}{2}H_2O + r \cdot SO_2 \tag{8.14}$$

From reaction 8.14 the kmol ratio of oxygen in the air to the amount of fuel can be derived which leads to equation 8.15

$$\frac{n^a_{O_2}}{n_f} = p + \frac{q}{4} + r \tag{8.15}$$

$$n^a_{O_2} = y^{da}_{O_2} \cdot \frac{m_{da,min}}{M_{da}} \tag{8.16}$$

Equations, 8.14, 8.15 and 8.21 combined express the stoichiometric air/fuel ratio as function of the fuel composition p,q and r.

$$\sigma_{da} = \frac{M_{da}}{Y^{da}_{O_2}} \cdot \frac{p + \frac{q}{4} + r}{p \cdot M_C + q \cdot M_H + r \cdot M_S} \tag{8.17}$$

The air excess ratio is defined as the mass of air divided by the minimum required amount of air by definition of the stoichiometric air/fuel ratio. The air excess ratio is calculated as shown in formula 8.18.

$$\lambda = \frac{m_{air}}{m_{fuel} \cdot \sigma_{fuel}} \tag{8.18}$$

8.7.2 Model changes

The definition of the air excess ratio remains the same. But due to the addition of a second fuel the minimum required air mass changes. First the stoichiometric air/fuel ratio of ammonia is calculated. The chemical reaction describing the combustion of ammonia is shown in 8.19.

$$NH_3 + \frac{3}{4}O_2 \rightarrow \frac{3}{2}H_2O + \frac{1}{2}N_2 \tag{8.19}$$

From reaction 8.19 the kmol ratio of oxygen in the air to the amount of fuel can be derived which leads to equation 8.20

$$\frac{n^a_{O_2}}{n_{NH_3}} = \frac{3}{4} \tag{8.20}$$

$$n^a_{O_2} = y^{da}_{O_2} \cdot \frac{m_{da,min}}{M_{da}} \tag{8.21}$$

Equations, 8.14, 8.15 and 8.21 combined express the stoichiometric air/fuel ratio of ammonia.

$$\sigma_{da,NH_3} = \frac{M_{da}}{y^{da}_{O_2}} \cdot \frac{\frac{3}{4}}{M_N + 3 \cdot M_H} = 6.1 \tag{8.22}$$

The air excess ratio is defined as the mass of air divided by the minimum required amount of air by definition of the stoichiometric air/fuel ratio. The minimum air requirement is now dependent on both the ammonia and the pilot fuel in the cylinder, formula 8.23 shows the air excess ratio dependent on both the fuels. No extra assumptions are added by this modifications, the model still assumes that the combustion of fuel is the only reaction taking place.

$$\lambda = \frac{m_{air}}{m_{pilot} \cdot \sigma_{fuel} + m_{NH_3} \cdot \sigma_{NH_3}} \tag{8.23}$$

8.7.3 Conclusion air excess ratio

To determine the air excess ratio of ammonia diesel blends the stoichiometric air/fuel ratio of ammonia is calculated. The air excess ratio is altered to be dependent on both injected ammonia and diesel mass as shown in formula 8.23. The model uses the same assumptions as it has before, it assumes no other reactions besides the combustion of the fuel take place.

8.8 Combustion efficiency

The combustion efficiency is defined as the fraction of the injected fuel that is burned during the combustion process. When not enough oxygen is present in the cylinder part of the injected fuel will not combust which leads to poor fuel efficiency and hydrocarbon emissions (un-burned fuel). Most engines are run with a lean mixture, which means more oxygen than the minimal requirement is used to guarantee complete combustion.

8.8.1 Original model

Betz and Woschni derived an empirical formula to derive the combustion efficiency of diesel engines, they found a relation between the air excess ratio and the combustion efficiency. The combustion efficiency increases linear with the air excess ratio until a certain maximum efficiency as shown in figure 8.7

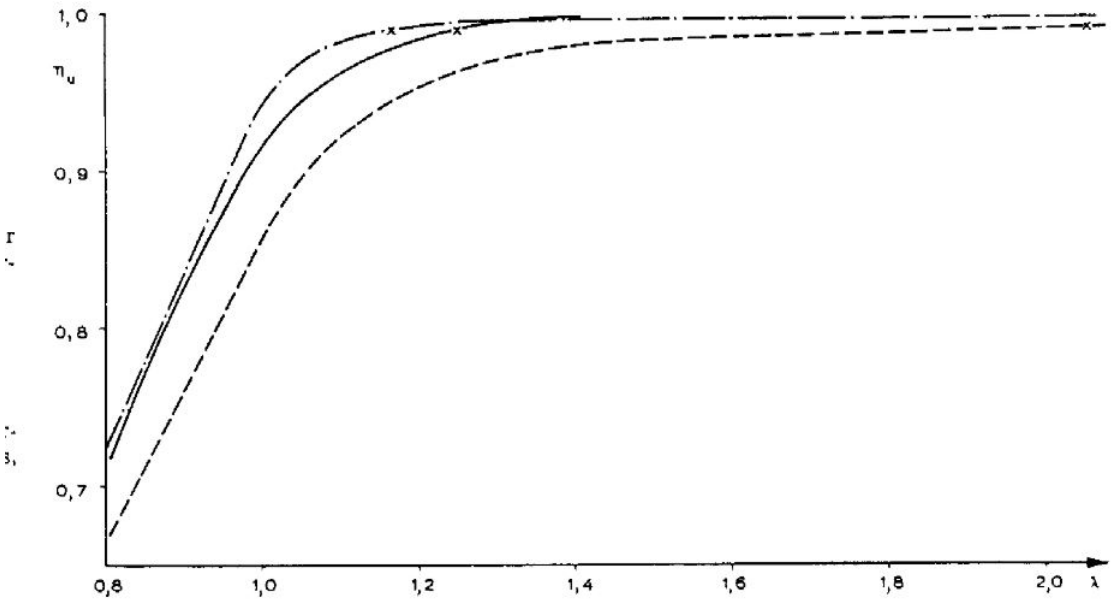

Figure 8.7: Combustion efficiency in diesel engines [8]

Betz and Woschni their empirical formula is dependent on the air excess ratio and the smoking point. Which is the air excess ratio at which the engine starts to smoke due to un-burnt fuel. The model uses a smoking point of $\lambda_{sm} = 1.7$. And assumes complete combustion if $\lambda \geq \lambda_{sm}$ the combustion efficiency is 1.

8.8.2 Model changes

The behaviour of an increase in combustion efficiency when the air excess ratio increases up to a certain value is still expected with mixtures of the two gasses. Unfortunately no data is available to fit a function made for ammonia diesel mixtures. However, some research has been done regarding the combustion of ammonia and the following concludes can give an indication of how well the original function resembles the behaviour of ammonia diesel blends.

Reiter has tested different ammonia diesel blends in smaller four-stroke engines. The combustion efficiency was determined by measuring the ammonia flow into the engine and the ammonia flow in the exhaust gasses. They noticed that the combustion efficiency was comparable to that of the engine running on diesel fuel near stoichiometric conditions [48]. However, the combustion efficiency was only determined for multiple ammonia diesel ratios at nominal engine load and speed, so no conclusion about part load combustion efficiency can be drawn.

The engine manufacturer MAN is currently working on ammonia powered two-stroke engines and have published some papers about their progress. In those papers MAN expects to accomplish complete combustion because the slower engines allow for more time for the fuel to combust. The high injection pressure allows for a near complete distribution of the fuel in the combustion chamber, which will also help with the complete combustion of the fuel [40].

Although Reiter suggested a combustion efficiency equal to that of near stoichiometric conditions, those test where done in smaller faster running engines. Therefore, the claim from MAN to be able to achieve complete combustion seems more likely. However, this statement is most likely only valid for nominal conditions, in which the air excess ratio is above the smoking point and the combustion efficiency is 100%. No measurements are available about the smoking point of diesel ammonia mixtures in marine two-stroke engines, so the smoking point is not changed. However, due to the poor combustion characteristics of ammonia a change in the smoking point is expected. The smoking point will most likely be dependent on the diesel ammonia ratio, with 100% diesel fuel the smoking point will remain at 1.7, when more ammonia is added it is expected to increase due to the poor combustion properties of ammonia. Therefore, it is expected that the model gives reliable results at lean conditions, but will decrease in accuracy in scenarios with lower air excess ratios.

8.8.3 Conclusion combustion efficiency

The same relation between air excess ratio and combustion efficiency is maintained because the same behaviour is expected and no data is available. Based on claims from engine manufactures working on ammonia engines similar efficiency's can be expected with lean mixtures, which makes the model plausible at nominal loads. However, at conditions with lower air excess ratios, the effects of ammonia are unknown.

8.9 Gas mixture

For the combustion of any fuel oxygen is required, engines use air, which is a mixture oxygen and multiple other gasses. During the combustion the fuel reacts with the oxygen in the air, this results in a mixture of air and the reaction products. The composition of the gas mixture after the combustion is important to determine the energy in the mixture during the multiple Seiliger stages and in multiple other parts of the engine.

8.9.1 Intake gasses

The composition of dry air has been standardised for the purpose of calculations. Table 8.2 shows the composition of air according to the DIN standard [58].

Chemical element	Mass fraction [-]	Mass [g/mol]
N_2	0.7809	28.013
O_2	0.2095	31.999
Ar	0.0093	39.948
CO_2	0.0003	44.010

Table 8.2: Mass fractions of chemical elements in air.

The molecular weight of the mixture can be calculated as shown in formula 8.24.

$$M_{da} = M_{N_2} \cdot y_{N_2}^{da} + M_{O_2} \cdot y_{O_2}^{da} + M_{Ar} \cdot y_{Ar}^{da} + M_{Ar} \cdot y_{Ar}^{da} = 28.9639 \tag{8.24}$$

Air also contains water, the amount of water in the air is expressed as the absolute humidity. Which is defines as the mass of water vapour relative to the mass of dry air.

$$X_{H_2O}^{da} = \frac{m_{H_2O}}{m_{da}} \tag{8.25}$$

The ambient relative humidity in the model is set to 0.5, which makes the relative humidity $x_{H_2O} = 0.0097$ kg water per kg dry air. The addition of water vapour to the gas mixture changes the mass fractions, the results are shown in table 8.3

Chemical element	Mass fraction [-]	Mass [g/mol]
N_2	0.7689	28.013
O_2	0.2063	31.999
Ar	0.0092	39.948
CO_2	$2.9539 \cdot 10^{-4}$	44.010
H_2O	$2.9539 \cdot 10^{-4}$	18.0151

Table 8.3: Mass fractions of chemical elements in wet air.

8.9.2 Exhaust gasses

Now the ambient gas mixture entering the engine is known, during combustion part of this mixture reacts with the diesel fuel which creates new gasses. The reaction products effect the thermodynamic properties of the exhaust gasses and the in cylinder gasses since some reaction products remain in the cylinder effecting compression and temperature ratios in the engine. It is important to know these properties and thus define the content of the exhaust gasses. Stoichiometry is the calculation of reactant products after a chemical reaction took place. Stoichiometry is based on the law of conservation of mass where the total mass of reactants equals the total mass of the products. The model assumes that the only reaction taking place is that of diesel fuel with oxygen, in reality multiple reactions can take place, most known is the reaction of oxygen with nitrogen to form NO_x emissions.

The amount of nitrogen in the exhaust gasses can be obtained with the nitrogen balance, as mentioned it is assumed no nitrogen reacts with oxygen which results in the following balance:

$$x_{sg,N_2} = x_{air,N_2} \cdot \frac{\sigma_{fuel}}{\sigma_{fuel} + 1} \tag{8.26}$$

Argon is a noble gas and does not react with any other gas, the mass balance is equal to that of nitrogen.

$$x_{sg,Ar} = x_{air,Ar} \cdot \frac{\sigma_{fuel}}{\sigma_{fuel} + 1} \tag{8.27}$$

The combustion of diesel fuel creates carbon-dioxide, water and sulphur oxide. The production of carbon dioxide is dependent on the mass fraction carbon in the fuel, and can be calculated as shown in formula 8.28. The same goes for sulphur oxide and water as shown in equations 8.30 and 8.29

$$x_{sg,CO_2} = \frac{M_{CO_2}}{M_C} \cdot \frac{x_C^{fuel}}{\sigma_{fuel} + 1} \tag{8.28}$$

$$x_{sg,H_2O} = \frac{M_{H_2O}}{2 \cdot M_H} \cdot \frac{x_H^{fuel}}{\sigma_{fuel} + 1} \tag{8.29}$$

$$x_{sg,SO_2} = \frac{M_{SO_2}}{M_S} \cdot \frac{x_S^{fuel}}{\sigma_{fuel} + 1} \tag{8.30}$$

Since the stoichiometric gas is defined as the reaction product of the complete combustion of the fuel no oxygen is left.

$$x_{sg,O_2} = 0 \tag{8.31}$$

When DMA is selected as the fuel, which has the following mass fractions: $x_C = 0.865, x_H = 0.133, x_S = 0.002$, the mass fractions of the stoichiometric gas are as shown in table 8.4.

Chemical element	Mass fraction [-]
N_2	0.7003
O_2	0
Ar	0.0119
CO_2	0.2023
H_2O	0.0759
SO_2	$2.5505 \cdot 10^{-4}$

Table 8.4: Mass fractions of chemical elements in stoichiometric gas produced by DMA.

8.9.3 Gas composition

The composition of the exhaust gasses can now be defined with the ratio between air and the stoichiometric gas produced by the combustion of diesel fuel. The stoichiometric gas produced by the complete combustion of the selected diesel fuel is used to define the properties of the gas mixture in the different parts of the engine. The model defines the mixture as the ratio of air and stoichiometric gas produced by the complete combustion of diesel. The variable "x" indicates the mass fraction of air, when x=1 the mixture consists of 100% air and no stoichiometric combustion gasses. The foul gas concentration can be determined as shown in formula 8.32.

$$x_{sg} = 1 - x_{air} \tag{8.32}$$

The amount of stoichiometric gas produced in the cylinder is defined by the amount of burned fuel and is determined using the conservation of mass as shown in formula 8.33. The model assumes that all injected fuel is converted to stoichiometric exhaust gas since the combustion efficiency is only considered with the heat release and not in the calculation of stoichiometric gasses produced by the combustion of the diesel fuel.

$$m_{sg,comb} = m_{fuel} \cdot (\sigma_{fuel} + 1) \tag{8.33}$$

The reactant gasses released due to the combustion of diesel are divided over the Seiliger stages 2-3, 3-4 and 4-5 using the q_{ratio}, which indicates the distribution of fuel combustion over the different stages.

8.9.4 Model changes

The addition of ammonia creates different reaction products during its combustion. These reaction products are not only dependent on the air excess ratio and the stoichiometric air/fuel ratio, but also on the ammonia diesel ratio. The mass fractions of the multiple gasses forming the stoichiometric gas produced by the combustion of ammonia are calculated with the formulas below.

$$x_{ag,SO_2} = \frac{M_{SO_2}}{M_S} \cdot \frac{x_S^{NH_3}}{\sigma_{NH_3} + 1} = 0 \tag{8.34}$$

$$x_{sg,CO_2} = \frac{M_{CO_2}}{M_C} \cdot \frac{x_C^{NH_3}}{\sigma_{NH_3} + 1} = 0 \tag{8.35}$$

$$x_{sg,Ar} = x_{air,Ar} \cdot \frac{\sigma_{NH_3}}{\sigma_{NH_3} + 1} \tag{8.36}$$

$$x_{sg,N_2} = (x_{air,N_2} \cdot \sigma_{NH_3}) + \left(\frac{M_{N_2}}{\frac{1}{2} \cdot M_N} \right) \cdot \frac{x_N^{NH_3}}{\sigma_{NH_3} + 1} \tag{8.37}$$

$$x_{sg,H_2O} = \frac{M_{H_2O}}{\frac{1}{2} \cdot M_H} \cdot \frac{x_H^{NH_3}}{\sigma_{NH_3} + 1} \tag{8.38}$$

The results are shown in table 8.5, when these results are compared to those of DMA in table 8.4 the advantages of ammonia are clear, it produces no CO_2 and SO_2 emissions. However, ammonia produces more N_2. Nitrogen itself is not a greenhouse gas, however, under high temperatures N_2 can react with O_2 and form NO_x which is a harmful emission. The higher nitrogen mass fractions can lead to bigger NO_x emissions. NO_x emissions are formed in local hot spots in the cylinder, this is a complicated process which can not be simulated with a mean value model. A workaround would be an empirical relation based om mean cylinder temperatures and nitrogen concentration to predict the NO_x emissions. Unfortunately no data is available to make such an empirical formula. Therefore, the NO_x production is not simulated.

Chemical element	Mass fraction [-]
N_2	0.7586
O_2	0
Ar	0.0109
CO_2	0
H_2O	0.2252
SO_2	0

Table 8.5: Mass fractions of chemical elements in stoichiometric gas produced by ammonia.

The composition of the gas mixture can no longer be described by the mass ratio of air because the mixture is made up of three known gas mixtures instead of two. Therefore, the definition of the description of the mixture is changed and two variables are used to describe the contents of the mixture: $x_{sg,pilot}$ and $x_{sg,ammonia}$ who describe the mass ratio of stoichiometric gas produced by the combustion of diesel fuel and ammonia respectively. The mass fraction air can be calculated as shown in formula 8.39.

$$x_{air} = 1 - (x_{pilot} + x_{ammonia}) \tag{8.39}$$

The production of stoichiometric gas is calculated with the same formula as with diesel fuel. However, the gas production is calculated separately for diesel fuel and ammonia, which creates three mass fractions, $m_{sg,pilot}, m_{sg,NH_3}$ and m_{air}. Here the same assumption as in the section 8.4; it is assumed that the combustion of ammonia is equally distributed over the Seiliger stages 2-5.

8.9.5 Conclusion gas mixture

The reaction products of the combustion of ammonia are determined using the stoichiometric mass balance. The additional fuel ammonia produces a different stoichiometric gas, therefore, the gas mixture in the model can no longer be defined with one variable. A new variable is introduced to define the mixture: x_{sg,NH_3}, the variable x_{air} is replaced by $x_{sg,pilot}$. The new definitions do not introduce extra assumptions to the model, however, because of the extra nitrogen introduced by ammonia the assumption that nitrogen does not react with oxygen gets less likely.

8.10 Thermodynamic properties of the mixture

The thermodynamic properties such as the isobaric and isochoric specific heats are used to determine the pressure and temperature ratios in multiple parts of the engine, and to calculate the energy in the mixture the enthalpy and entropy must be known. These can all be calculated using known thermodynamic properties of separate elemental compounds. The next section shows how the multiple thermodynamic properties used throughout the model are calculated. Furthermore, the changes made to the model for the use of ammonia in the engine are described in this section.

8.10.1 Gas constant

The gas constant R of the air and stoichiometric gas mixtures can be determined by multiplying the gas constant of a specific elemental gas with the corresponding mass fraction and adding them all together, the calculation for the gas constant of air is

shown in equation 8.40. The gas constants of the elemental gasses are determined by dividing the universal gas constant by the corresponding molar mass as shown in equation 8.41. The gas constants of air and stoichiometric diesel gas are constant and calculated in Matlab before the start of the simulation. During simulation the gas constant of a mix of the two gas mixtures can be determined by formula 8.42.

$$R_{air} = x_{N_2} \cdot R_{N_2} + x_{O_2} \cdot R_{O_2} + x_{Ar} \cdot R_{Ar} + x_{CO_2} \cdot R_{CO_2} + x_{H_2O} \cdot R_{H_2O} \tag{8.40}$$

$$R = 1000 \cdot \frac{R_u}{M} \tag{8.41}$$

$$R = (1 - x_{sg}) \cdot R_{air} + x_{sg} \cdot R_{sg} \tag{8.42}$$

8.10.2 Specific heats

The specific heat at constant pressure of the elemental gasses are temperature dependent. The fluid_properties.m file provides six coefficients of a polynominal function for each elemental gas, with the polynomial functions the specific heat at constant pressure of the elemental gasses can be calculated. The six coefficients of the polynomial functions for air and stoichiometric gas can be calculated by multiplying the coefficients of the elemental gasses present in the mixture with their mass ratio and summing them as shown in equation 8.43. Note that c_{p,N_2} is a vector containing the six coefficients of the polynomial function of nitrogen. The polynominal coefficients of air and stoichiometric gas are determined in a Matlab file before the start of the simulation.

$$c_{p,air} = x_{N_2} \cdot c_{p,N_2} + x_{O_2} \cdot c_{p,O_2} + x_{CO_2} \cdot c_{p,CO_2} + x_{H_2O} \cdot c_{p,H_2O} + x_{Ar} \cdot c_{Ar} \tag{8.43}$$

The c_p of an elemental gas at a specific temperature can be calculated as shown in equation 8.44 and 8.45

$$c_{p,air} = c_{p,air}(1) + c_{p,air}(2) \cdot \theta + c_{p,air}(3) \cdot \theta^2 + ... + c_{p,air}(6) \cdot \theta^5 \tag{8.44}$$

$$\theta = T - T_{shift}/T_{norm} \tag{8.45}$$

T_{shift} is the temperature around which the c_p data is developed, the temperature is $0K$. T_{norm} is the normalised temperature which is $1000K$. T is the temperature for which the c_p is calculated. When the c_p of a mixture of air and stoichiometric gas

has to be calculated formula 8.43 and 8.44 can be used. The mass fractions and c_p of the elemental gasses are substituted by those of the air and stoichiometric gas.

The specific heat at constant volume can be derived from the gas constant and the specific heat at constant pressure as shown in formula 8.46.

$$c_v = c_p - R \tag{8.46}$$

8.10.3 Enthalpy

The enthalpy h of the mixture is determined by adding the weighted enthalpy of stoichiometric gas and air in the mixture. First the enthalpy of the separate elemental gasses are determined using the polynominal function which develops their enthalpy around a set reference point of 25 degree Celsius and 1 bar. Next the enthalpy of air and stoichiometric gas for multiple points are determined by adding the weighted enthalpy of the separate elemental gasses in the mixture as shown in equation 8.47. This equation forms a vector with six elements, which can be used to determine the enthalpy of mixtures at various temperatures. These vectors are constant and determine before the start of the simulation with Matlab.

$$h_{air} = h_{N_2} \cdot x_{air,NO_2} + h_{O_2} \cdot x_{air,O_2} + h_{Ar} \cdot x_{air,Ar} + h_{CO_2} \cdot x_{air,CO_2} + h_{H_2O} \cdot x_{air,H_2O} \tag{8.47}$$

During the simulation the enthalpy at a certain temperature can be calculated as shown in equations 8.48 and 8.49. The enthalpy consists of a reference enthalpy which is a constant value stored in the Matlab files and change in enthalpy due to the temperature.

$$\Delta h_{air} = h_{air}(1) + h_{air}(2) \cdot \theta + h_{air}(3) \cdot \theta^2 + h_{air}(4) \cdot \theta^3 + h_{air}(5) \cdot \theta^4 + h_{air}(6) \cdot \theta^5 \tag{8.48}$$

With θ the normalised temperature as in previous equation 8.45.

$$h_{air} = h_{ref,air} + \delta h_{air} \tag{8.49}$$

The enthalpy of the mixture can be determined by adding the weighted enthalpy at the desired temperature of the separate gasses in the mixture as shown in in equation 8.50.

$$h = (1 - x_{sg}) \cdot h_{air} + x_{sg} \cdot h_{sg} \tag{8.50}$$

8.10.4 Entropy

The entropy is dependent on three factors, the temperature, the pressure and the mixing entropy. The entropy as a consequence of the temperature is named s_T and calculated in a similar way as the enthalpy with formula's 8.47, 8.48, 8.49 and 8.45 wherein h is substituted with s. The pressure dependent enthalpy s_p is calculated with formula 8.51 and 8.52.

$$s_p = -R \cdot ln(p^*) \tag{8.51}$$

$$p^* = \frac{p}{p_{ref}} \tag{8.52}$$

The mixing entropy s_x is dependent on the mole fractions of the elemental gasses in the mixture. The mole fractions are calculated as in formula 8.53. With the mole fractions known the mixing entropy can be calculated with formula 8.54.

$$y_{sg} = 1000 \cdot \frac{R_u}{R \cdot x_{sg} \cdot M_{sg}} \tag{8.53}$$

$$s_x = -R \cdot y \cdot ln\,(y) \tag{8.54}$$

When for example a component in the mixture is absent and the value for $y = 0$, $Ln(0)$ gives a math error. To prevent math errors $y \cdot ln\,(y)$ is written in an if else statement; if $(y == 0)$ out $= 0$, else out $= y \cdot ln\,(y)$. To determine the total entropy all the parts have to be added together 8.55.

$$s = s_{ref} + s_T + s_p + s_x \tag{8.55}$$

Because the mixing entropy is dependent on the mixture, formula 8.50 cannot be used to determine the entropy of mixtures, the entropy has to be calculated from the start.

8.10.5 Model changes

The addition of ammonia does not change the way in which the thermodynamic properties are determined. The same formulas can be used, only one extra mass fraction is added. The properties of the elemental gasses in the stoichiometric gas produced by the combustion of ammonia are already in the Matlab file. However, the calculation for the six coefficients of the polynomial functions for stoichiometric ammonia gas is added to the fluid_properties.m file. The same formula as for air is used, which is formula 8.43.

The TU Delft engine B model already contains a library file with all the blocks to calculate the thermodynamic properties, these blocks take the air mass fraction as input among other values like temperature and pressure. These blocks are adapted to take the stoichiometric diesel gas mass fraction and the stoichiometric ammonia gas mass fraction as input.

The addition of a second fuel does not introduce new assumptions or simplifications within the calculations of thermodynamic properties. However, the addition of a new stoichiometric gas has a big impact in the model. The thermodynamic properties of the gas mixture in the engine are used to determine the pressure and volume in a multitude of parts in the engine by using the ideal gas law. Furthermore, the enthalpy en entropy are used to determine how much energy is in the system, a change in these values due to different gasses could have a big impact on the turbo charging since this process is dependent on the energy in the exhaust gasses and the pass flow and pressure ratio over the cylinder. A further analysis of the impact of change in stoichiometric gasses will be done in chapter 10. Table 8.6 shows the differences in thermodynamic properties of air, stoichiometric diesel gas and stoichiometric ammonia gas. The values are calculated for a temperature of 691K which is a representative value for the temperature in the outlet receiver at nominal load and speed of the engine. The table clearly shows a difference between the three gasses. Stoichiometric diesel gas and air have quite similar properties, in contrast stoichiometric ammonia gas has a higher gas constant, which also increases the specific isochoric and isobaric heat of the gas. Due to these changes more heat is required to increase the temperature of stoichiometric ammonia gas, which is expected to decrease temperatures and pressure ratios in the model.

Property	Stoichiometric ammonia gas	Stoichiometric diesel gas	Air
R	331.3	283.6	288.7
c_v	976.8	878	798.3
c_p	1308	1162	1087

Table 8.6: Gas properties at 690K

8.10.6 Conclusion thermodynamic properties of the mixture

The model has been altered so that stoichiometric ammonia gas is considered in the calculation of the thermodynamic properties of the gas mixture. To do so the composition of stoichiometric ammonia gas is defined in the fluid_properties.m file. The model blocks to determine the thermodynamic properties of the gas mixtures are adapted so they can calculate the thermodynamic properties of a mixture of three gasses instead of two.

8.11 Gas exchange

During the gas exchange phase the combustion products are removed from the cylinder and fresh air is supplied. This process is not only important to provide oxygen for the combustion of fuel, but also plays a part in the cooling of the cylinder. The gas exchange process is divided into multiple mechanism whom all play a part in the disposal of foul gas and the cooling of the cylinder. The gas exchange process determines the conditions of the trapped mass at the start of compression.

8.11.1 Original model

After the combustion the exhaust opens (EO) and the gas exchange starts, the gasses in the cylinder flow into the exhaust receiver due to the higher pressure in the cylinder. The expansion of the gas into the exhaust receiver causes the cylinder temperature to drop. The temperature of the gasses leaving the cylinder also drop over time. The pressure difference between the cylinder and outlet receiver also drops until the pressure equalises and the mass flow stops.

The blow-down is simulated at the location de_b_2stroke/DE1/DEC/CYL/GEX/BLD, the blow-down temperature is calculated using the Zinner model, which is shown in formula 8.57 [58]. The composition is equal to the composition at the end of combustion. The blow-down mass flow is dependent of the engine speed and the trapped mass at Seiliger point 6, and is calculated with formula 8.58, wherein $k = 1$ for two-stroke engines and i the number of cylinders.

$$T_{BLD} = T_6 \cdot \left(\frac{1}{\kappa} + \frac{\kappa - 1}{\kappa} \cdot \frac{p_{BLD}}{P_6} \right) \tag{8.56}$$

$$\kappa = \frac{c_p}{c_v} \tag{8.57}$$

$$\phi_{BLD} = n_e \cdot m_6 \cdot \frac{i}{k} \tag{8.58}$$

The scavenging phase starts after the blow-down. When the pressure has decreased the inlet valve opens. The cylinder gasses expand to a pressure between the inlet receiver pressure and the outlet receiver pressure. For effective scavenging in the short time that is available it is important that the inlet receiver pressure is higher than the outlet receiver pressure, this will assure that there is a flow of fresh air through the cylinder. The turbo charger will help in creating a positive pressure difference over the cylinder and increase the scavenging effectiveness.

The residual gasses in the cylinder will mix with the fresh air supplied during scavenging of which a big part will be expelled into the exhaust receiver, removing the residual gasses from the cylinder. To ensure proper disposal of the exhaust gasses a sufficient crank angle with both inlet and exhaust valves open must be available.

The scavenging process stops when either the inlet closes (IC) or the exhaust closes (EC). When the exhaust closes first the cylinder can be further charged, allowing for more air in the cylinder. When the inlet is closed first the charge is lost into the exhaust receiver. However, closing the inlet first allows the engine to be reversed because in reverse the exhaust vale will open before the inlet valve which allows for a blow-down in reverse operation. Another advantage to closing the exhaust valve relatively late is that the compression will start later, which will decrease the required work for compression. The latter choice is used for the MAN engine in the model and is common practice with modern two-stroke engines [58].

The scavenging model is divided in multiple blocks, in the first block the relative scavenge time is calculated with formula 8.59, wherein ϕ_{sc} the scavenge flow is.

$$t_{sc,r} = k \cdot R_{sc} \cdot T_{sc,in} \cdot \frac{\phi_{sc}}{p_{sc} \cdot i \cdot n_e \cdot V_{sc}} \tag{8.59}$$

In the scavenge core block the temperature of the trapped mass after scavenging, the temperature of the gasses leaving the cylinder due to scavenging and the composition of the trapped mass after scavenging is determined. The model assumes perfect mixing and determines the trapped mass composition based upon the mass leaving and entering the cylinder during scavenging, this process is dependent on the relative scavenging time.

8.11.2 Model changes

To adapt the gas exchange model for dual fuel operation an important assumption is made, it is assumed that the fresh air supply into the cylinder consists of 100% fresh air and no stoichiometric gas. In the current model this is true because no Exhaust Gas Recirculation (EGR) is used and no negative scavenging takes place. However, when a EGR is used or negative scavenging takes place the gas exchange model will have to be further altered to comply for exhaust gasses in the fresh air supply. This assumption is made in the scavenging core model, here the model determines the temperature and composition of the in cylinder mass after savaging. Originally the air fraction x_{air} is used in the phase I and II mixing models. This is kept the same, the mass fraction of air is calculated using formula 8.60.

$$x_{air} = 1 - (x_{sg,a} + x_{sg,p}) \tag{8.60}$$

The model gives the ratio between trapped mass temperature before and after scavenging and the ratio between the scavenging mix going into the cylinder and the scavenging mix going out of the cylinder. Furthermore, the mass fraction of air after scavenging is determined. The change in mass fraction air is caused by the mixing of fresh air from the inlet receiver with gas from the cylinder and exhaust gas leaving the cylinder. As mentioned, the fresh air from the inlet receiver consists of 100% air, and the different properties of air and stoichiometric gas are not considered for the

calculation of the gas composition after scavenging. Which means that the amount of $m_{sg,p}$ leaving the cylinder is equal to the amount of $m_{sg,a}$ leaving the cylinder, and since no stoichiometric gas is entering the cylinder the ratio between $m_{sg,p}$ and $m_{sg,a}$ stays the same during scavenging. Before scavenging the mass ratio between stoichiometric gasses is calculated as shown in formula 8.61. After scavenging the output $x_{sc,tr}$ is converted to the stoichiometric mass ratio as follows: $x_{sg} = 1 - x_{air}$. This mass ratio is multiplied with mr_{sg} to determine the mass fraction stoichiometric ammonia and diesel gas as shown in formula 8.62.

$$mr_{sg,p} = \frac{x_{sg,p}}{x_{sg,a} + x_{sg,p}} \tag{8.61}$$

$$x_{sg,tr,p} = x_{sg,tr} \cdot mr_{sg,p} \tag{8.62}$$

8.11.3 Conclusion gas exchange

The model has been altered so that the stoichiometric gas of ammonia is considered in the gas exchange model. To do so a work around is used to determine the change in mass fractions as a consequence of savaging, the assumption is made that the gas mixture in inlet receiver consists of 100% air. This brings limitations to the model, when the gas mixture in the inlet receiver contains stoichiometric gas because a EGR system or negative scavenging the gas exchange model is not valid anymore.

8.12 Conclusion

The fuel supply has been changed to deliver both ammonia and diesel fuel, the fuel injection is scaled to the LHV of the fuels so that the same amount of energy is injected into the engine. An extra variable to determine the ratio between injected ammonia and diesel is created.

An extra fuel line is added to the Seiliger stages so that both diesel and ammonia can be supplied. In the model the distribution over the Seiliger stages is the same for of both fuels, in reality there is most likely a difference in the distribution.

The Seiliger parameters are also adapted to have both diesel fuel and ammonia as input fuels, in this section it is also assumed that the distribution of both fuels is equal. Parameters dependent on the ammonia energy share ratio are added to account for the impact of ammonia on the energy release distribution over the Seiliger stages.

To account for the longer ignition delay caused by the poor auto-ignition properties of ammonia the function for the ignition delay is multiplied with a correction function. This function is dependent on the ammonia energy ratio, increasing the IDT when more ammonia is used. The correction function is based on experiments

done with a small four-stroke engine, and the combined effect of ammonia and part load injection pressures and temperatures are not considered, it is expected that the function will give a reasonable representation of the effect of ammonia on the IDT.

The stoichiometric air/fuel ratio of ammonia is calculated and implemented in the model to calculate the air excess ratio of the mixture of both fuels and air. The combustion efficiency is related to the air excess ratio, this relation is not changed because no data is available for two-stroke marine engines. During nominal loads the combustion efficiency is 100%, this corresponds to predictions of marine engine suppliers. However, the behaviour of ammonia diesel mixtures at part load conditions is unknown.

To define the mixture that is produced by the combustion of both ammonia and diesel fuel the air mass ratio x_{air} is replaced by $x_{sg,p}$ and x_{sg,NH_3}. The model assumes that the only reactions taking place are those of the fuels with oxygen. In reality also other reactions take place, the extra nitrogen present in ammonia is expected to produce more NO_x emissions, this is neglected in the current model. Furthermore, the model blocks for calculating the thermodynamic properties of the gas mixture are changed so they can be used with the new gas mixture definition stated above.

The gas exchange model has also been adapted for the new gas mixture definition, this introduces a new assumption into the model. It is now assumed that the mixture entering the cylinder contains no stoichiometric gasses, in case of an EGR or negative scavenging this is not true.

To conclude, the model has been changed and is now capable in simulating a diesel-ammonia engine. The ammonia energy ratio can be changed during the simulation and and the thermodynamic properties of the gasses produced by the combustion are considered in the model, this has introduced a new limitation: the model is not valid if there are exhaust gasses in the inlet receiver. The effects of ammonia on the combustion shape can be modelled with the newly added variables, from which the values will be determined in chapter 9.

Chapter 9

The combustion parameters

9.1 Introduction

In this section the impact of ammonia on the Seiliger cycle will be compared to the known combustion characteristics of ammonia diesel blends. Furthermore, the effect of the constants $X_{a,d}$, $X_{b,d}$, n_{comp} and n_{exp} will be analysed and compared to the ammonia diesel characteristics whom are investigated in the literature review. Based on the comparison between the model and the literature research, suitable values will be picked for $X_{a,d}$, $X_{b,d}$, n_{comp} and n_{exp}. These values will be used in the further analysis of the model.

9.2 Dual fuel ammonia combustion characteristics

The combustion characteristics of ammonia diesel fuel are discussed in chapter 6, the most important characteristics relevant for the Seiliger parameters will be shortly summarised here. After the start of ignition the combustion can be divided in two phases, the premixed combustion and the diffusive combustion. The premixed combustion phase is characterised by a rapid rise in pressure. The controlled or diffusive combustion phase is mostly controlled by the fuel injection speed, the rate of chemical reactions drops because the expansion decreases the pressure and temperature in the cylinder.

The ignition delay, which is defined as the time between injection and the start of combustion mostly impacts the premixed combustion. A longer ignition delay allows for more fuel to be injected before the start of combustion, which increases the initial pressure rise.

Multiple studies have shown that ammonia increases the ignition delay in a CI engine, which is expected behaviour due to the poor auto ignition properties of ammonia.

Although ammonia increases the ignition delay, figure 9.1 from Reiter et al. shows a decrease in the initial pressure rise. This is counter intuitive, since an increase in IDT is known to increase the initial pressure rise in diesel engines. This relation is based on the assumption that when the IDT increases more fuel can be injected before the start of combustion. However, with ammonia the flame speed seems to be the limiting factor instead of the amount of injected fuel. Furthermore, figure 9.1 from Reiter et al. shows a relative high pressure during the expansion. Both the 100% diesel and 20% diesel cases deliver the same amount of power, a later start of ignition and a lower peak pressure means more heat has to be released in later stages to deliver the same amount of power. The HRR diagram clearly shows that the ammonia case has a higher peak which is shifted to a later part of the cycle.

Most of the reference material regarding ammonia-diesel combustion is based on smaller 4-stroke engine who run at much higher speeds and lower compression ratios. Furthermore, these engines are fed ammonia in a premixed state, while the MAN engine that is under development uses a separate injector injecting the ammonia directly into the cylinder, a similar method is used in the current model. The premixed gasses have can absorb more heat, and therefore lower the compression in stage 1-2, which lowers the work required to compress but also the cylinder pressure during injection. Since direct injection is used in the model, the lower compression ratio should not be considered.

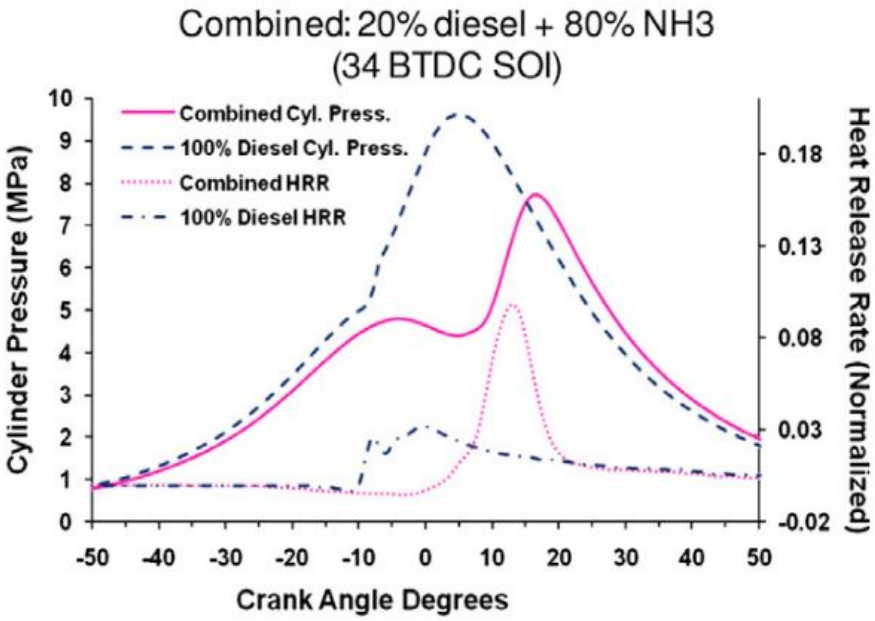

Figure 9.1: Pressure as function of the crank angle [48]

9.3 Impact of combustion parameters on combustion shape

Yu Ding investigated the Seiliger cycle and its parameters to better understand how these parameters change the cycle and how this relates to characteristics measured with real engines [16]. By exploring the interrelations between Vibe and Seiliger parameters he created a better understanding of the effect of combustion shapes on the basic engine thermodynamics, which in turn create a better understanding of the impact of the combustion shape on the partial engine efficiency's.

Yu Ding his research found a connection between the premix combustion and Seiliger parameter a. Furthermore, The parameters b, c and n_{exp} are associated with the diffusive combustion, n_{exp} mostly the very late combustion [16].

Yu Ding also looked into which properties of the curve are most important in determining the engine characteristics, according to Yu Ding the work and heat input are important factors as they do determine the engine efficiency, furthermore, the maximum pressure is seen as evenly important because the maximum cylinder pressure represents the mechanical load on the engine [16].

9.4 Impact of model parameters on combustion shape

To get a better understanding of the impact of the multiple variables defining the combustion shape tests are done with the modified model. Yu Ding already did investigate the impact of the different Seiliger parameters, however, since they are slightly differently implemented in the modified model new test have to be done to see how the parameters change the combustion shape.

The test are done at 80% ammonia energy share ratio, because that is the same amount of ammonia used in the tests from Aaron Reiter, which is currently the best available reference material. The parameters $X_{a,d}$ and $X_{a,d}$ are tested by using multiple values for them. Furthermore the impact of the compression and expansion coefficients are tested.

Figure 9.2 shows the impact of the new parameter $X_{a,d}$ on the pressure shape. The vertical lines show when the inlet closes (IC), the exhaust closes (EC), the top dead centre is reached (TDC), the exhaust opens (EO), and when the inlet opens (IO). The figure focuses on the Seiliger process, therefore not the entire 360 degree cycle is shown and the moment of IC and IO is not visible in this figure. When $X_{a,d}$ increases the initial pressure rise increases, creating a higher maximum pressure. Furthermore, p_2 seems to decrease when $X_{a,d}$ increases, the compression exponent is constant and not changed, however, the initial pressure p_1 changes. The change in initial pressure is caused by the higher exhaust pressure, as shown in figure 9.3, which impacts the inlet receiver pressure via the turbocharger.

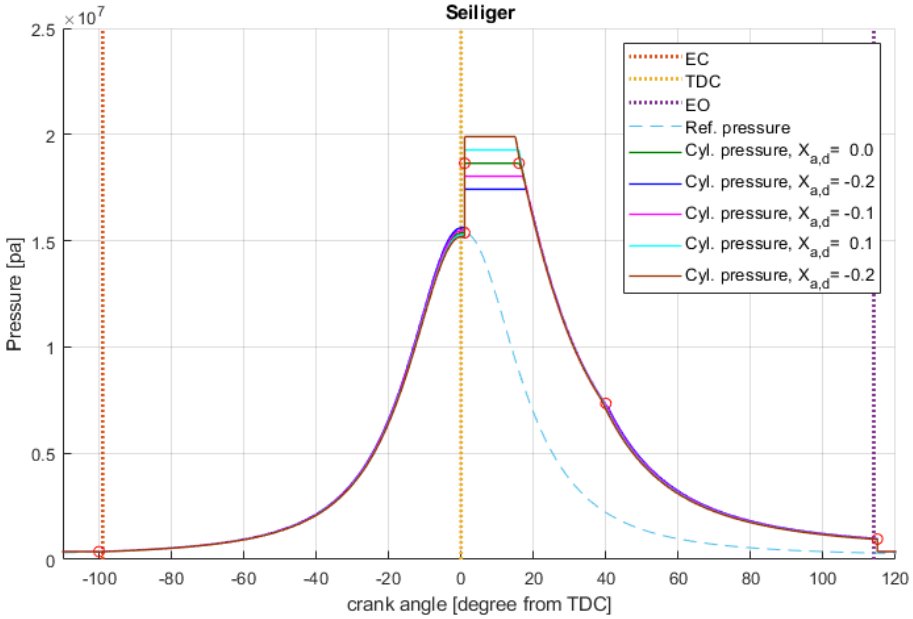

Figure 9.2: Pressure as function of the crank angle.

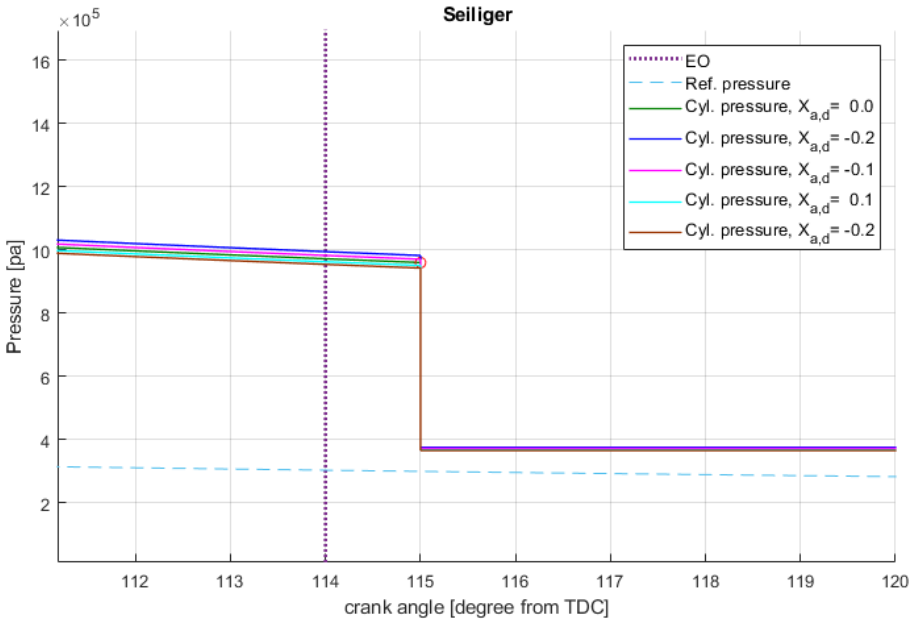

Figure 9.3: Pressure as function of the crank angle closeup on p_6.

The next figure shows the impact of parameter $X_{b,d}$, as expected an increase in this parameter increases the length of trajectory 3-4. However, more changes happen to the combustion shape, a low value of $X_{b,d}$ causes a higher maximum pressure. However, the initial pressure rise does not increase, the pressures p_1 and p_2 increase, again because of the higher outlet receiver pressure.

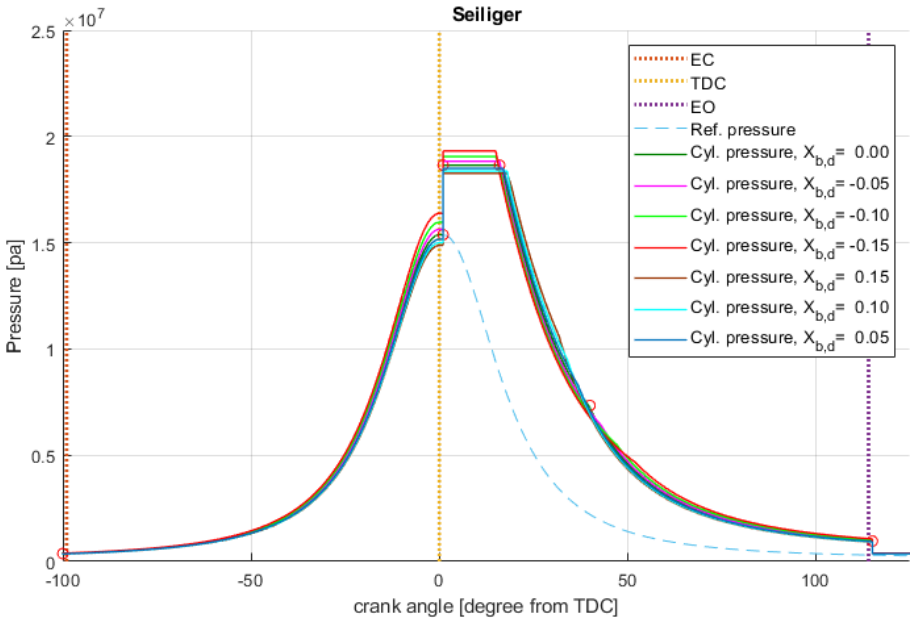

Figure 9.4: Pressure as function of the crank angle.

The model does not have a parameter c that can be changed, all the leftover energy is assumed to be released in the final combustion stage of the Seiliger process, so is parameters $X_{a,d}$, and $X_{b,d}$, are low, a high value for c and thus stage 4-5 is expected. Figure 9.5 shows the results. A big difference in the pressure p_2 is seen, it seems like the pressure in stage 4-5 is relatively high with high values for $X_{a,d}$, and $X_{b,d}$ since the pink line is the highest line in this stage. However, when we zoom in as shown in figure 9.6, we can see that stage 4-5 gets shorter with high values for $X_{a,d}$ and $X_{b,d}$. High values for $X_{a,d}$ and $X_{b,d}$ decrease the amount of energy released in stage 4-5.

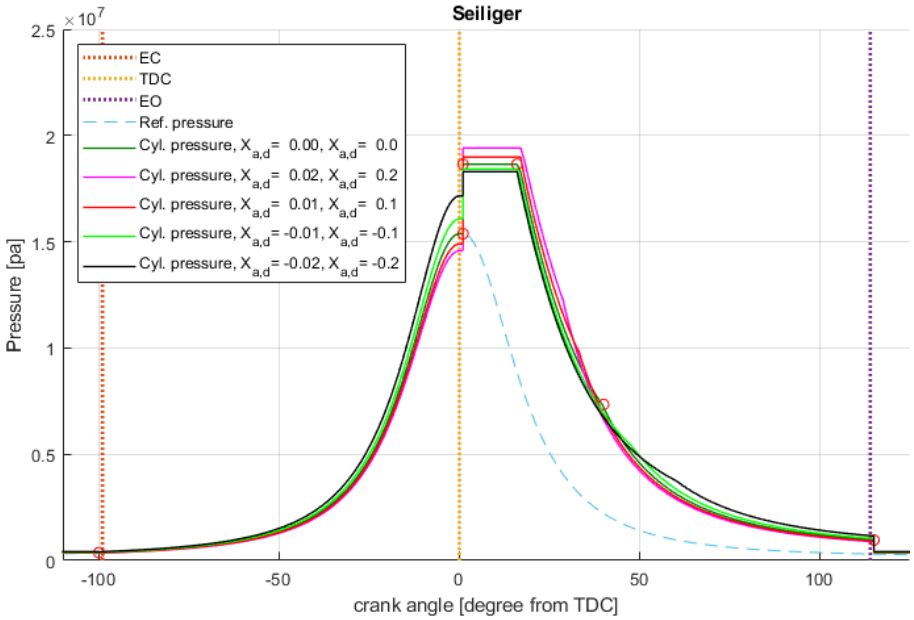

Figure 9.5: Pressure as function of the crank angle.

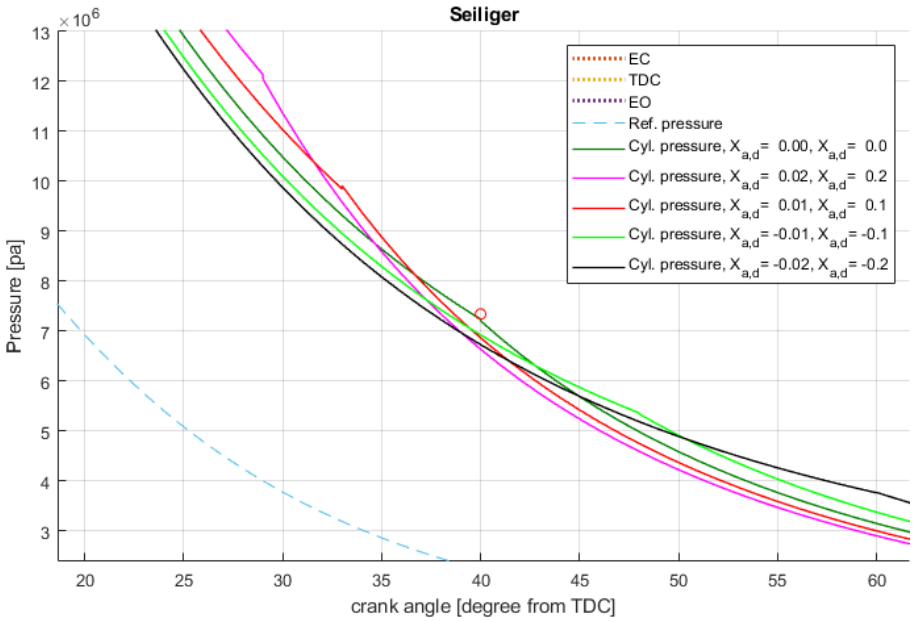

Figure 9.6: Pressure as function of the crank angle.

As expected varying the compression exponent n_{comp} results in a bigger pressure increase over stage 1-2. The compression exponent is constant a constant value of 1.3208 which is calculated from the inlet pressure and maximum pressure measured during test with an engine.

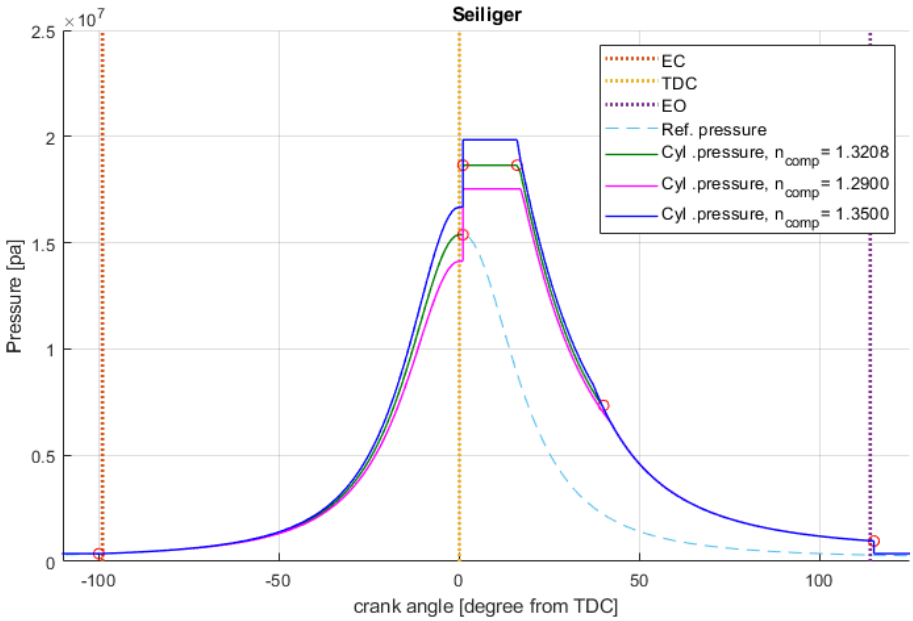

Figure 9.7: Pressure as function of the crank angle.

Figure 9.8 shows the impact of the expansion coefficient, normally the coefficient has a constant value of 1.33 which is determined using measurements with an engine. Although the changes in the last trajectory seem small in figure 9.9, the impact of the compression coefficient is quite big, because its has an direct impact on the exhaust receiver pressure, which as stated before impacts the inlet receiver pressure via the turbo charger. Therefore, a big variation in maximum pressure is seen in

figure 9.8.

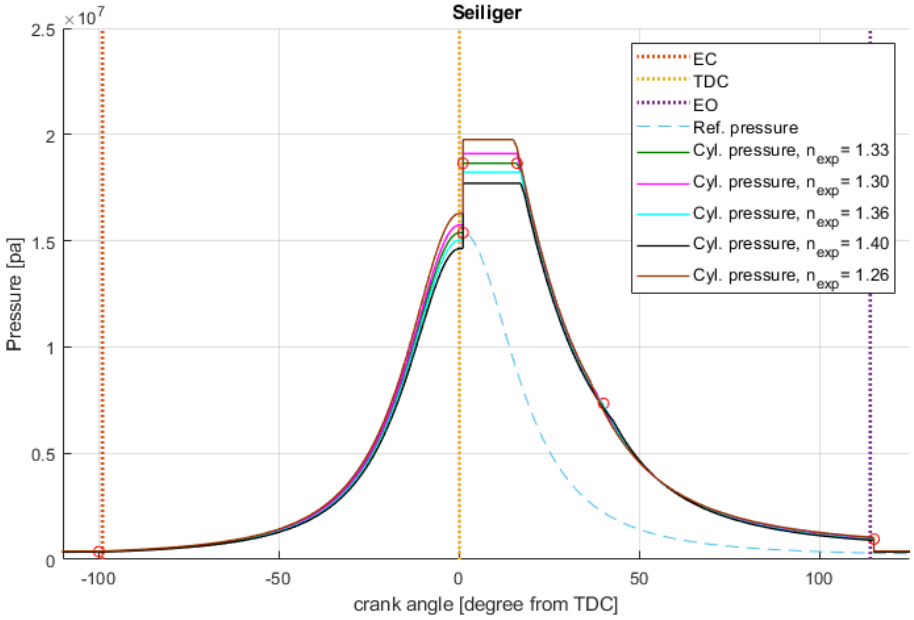

Figure 9.8: Pressure as function of the crank angle.

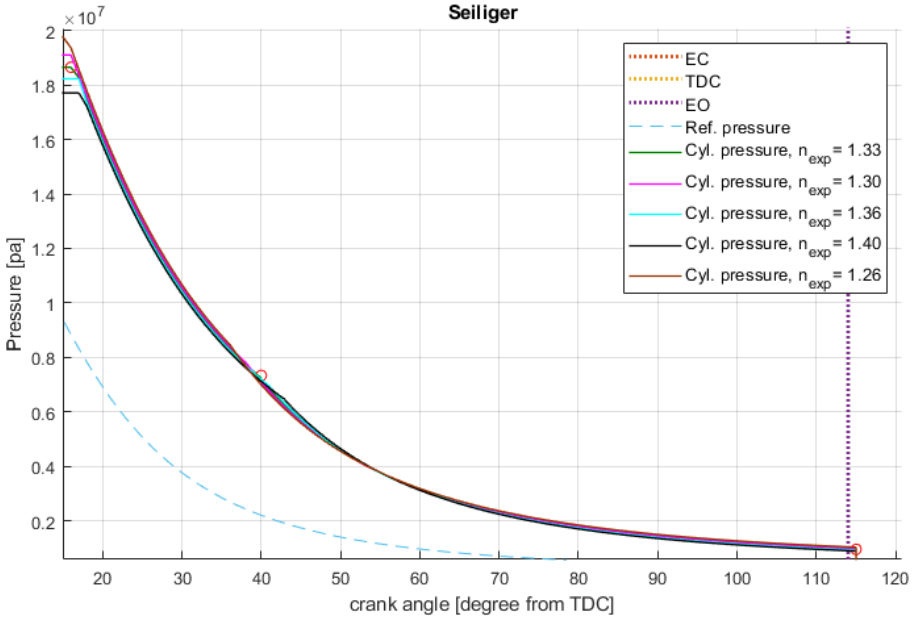

Figure 9.9: Pressure as function of the crank angle.

The values of $X_{a,d}$ and $X_{b,d}$ decrease when less ammonia is used, until they are zero for 100% diesel operation. However, n_{exp} and n_{comp} do not change with the use of ammonia. For the compression this is not a problem. The experiments from Reiter have shown a slight decrease in the compression due to the ammonia gasses present in the cylinder in stage 1-2, because the model simulates an engine with direct ammonia injection this behaviour is not expected. However, during expansion different gasses are present in the cylinder, the model already has two different options build in to determine the expansion coefficient. The method from Stapersma and the method from E.J. Boone, figure 9.10 shows the effect of these methods.

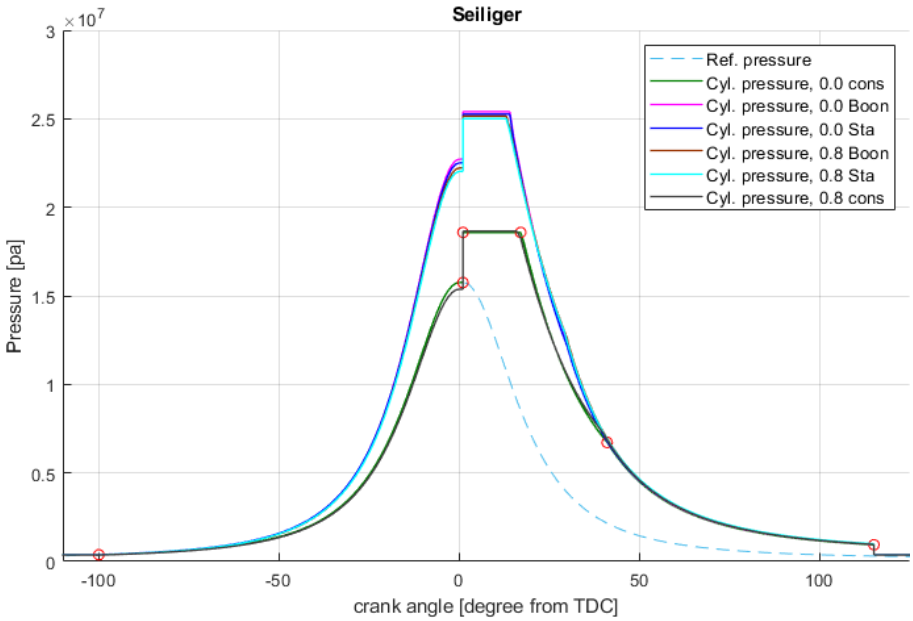

Figure 9.10: Pressure as function of the crank angle.

Figures 9.11a and 9.11b show the expansion and compression coefficient for all three methods, during the simulation run the ammonia energy share ratio is raised from 0% to 80%. The first figures show that there is no impact on the compression coefficient for all three methods, this is expected because the inlet pressure is higher that the outlet pressure so no negative scavenging takes place. Which means no exhaust gasses are present during compression.

The expansion coefficient changes for both methods when ammonia is used, this is expected because the methods are dependent on kappa, the ratio between n_p and n_v. However, the method of E.J. Boone is the only one which gives a value also representative for the 100% diesel operation during the expansion. Therefore, the method from E.J. Boone is used to calculate the expansion coefficient, the compression coefficient is not changed.

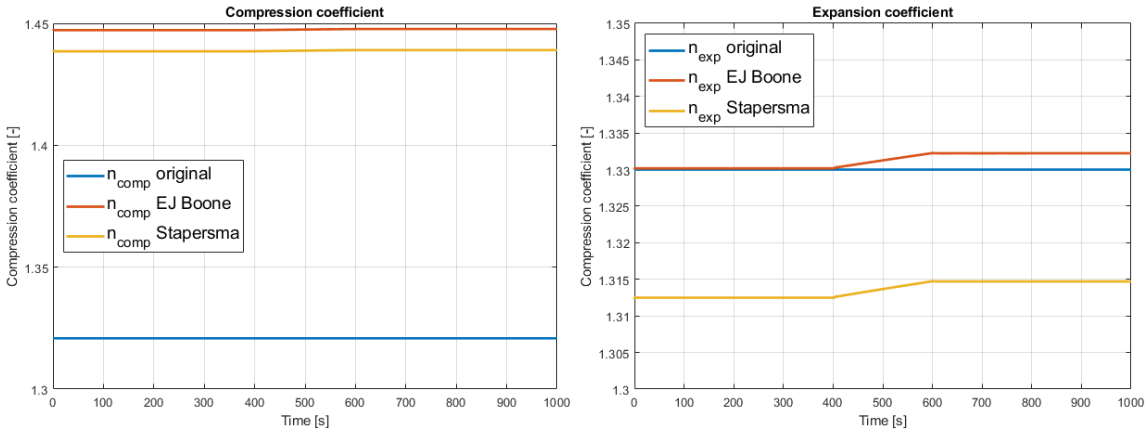

(a) Compression coefficient (b) Expansion coefficient

Figure 9.11: Impact of compression and expansion coefficient on cylinder pressure.

9.5 Chosen values and final combustion shape

Now the impact of the parameters available are known and the effects of ammonia on the combustion shape is discussed the proper parameters can be chosen to study the effect of ammonia on the engine characteristics.

The compression coefficient is not altered since ammonia is injected only in the last stage of this trajectory and should barley impact it. The initial pressure rise should be lower, to do so a negative value of $X_{a,d} = -0.02$ is chosen. A positive value of $X_{b,d} = 0.05$ is chosen, this moves the right hand half of the combustion shape to the right, creating higher pressure is the later stages. The results are shown in figure 9.12. The figure shows a decrease in maximum pressure, which matches the measurements from Reiter and was pointed out as a important parameter by Yu Ding. Furthermore, higher pressures are shown in stage 4-5, which also matches the characteristics measured by Reiter. The Seiliger figure does not match the combustion shape from Reiter exactly, this is not the goal, a very different type of engine is used so matching the curve would not make sense, however, the impact of ammonia on the original characteristic is captured in the new combustion shape, and the new shape can be used to see the impact of ammonia on the engine performance.

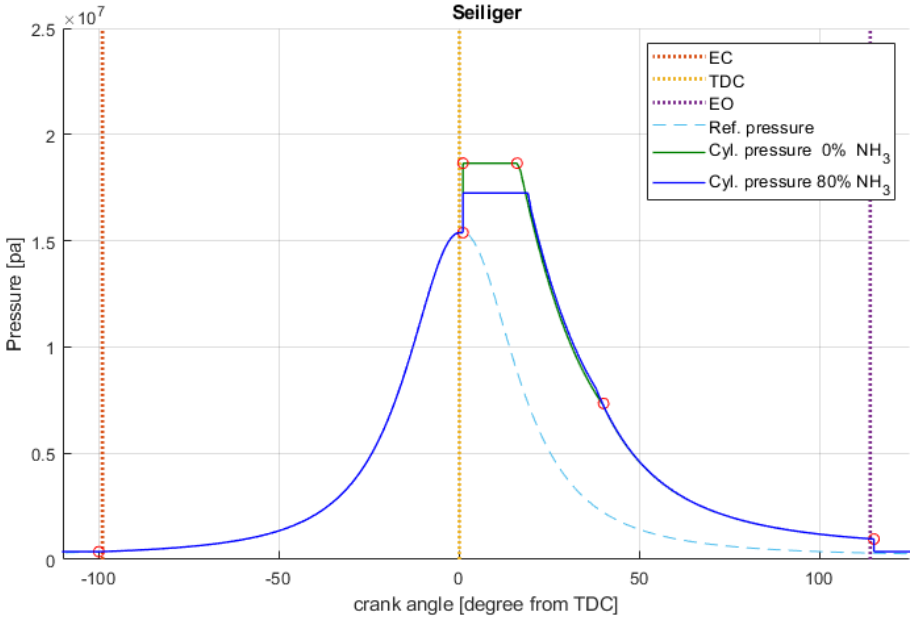

Figure 9.12: Pressure as function of the crank angle.

Chapter 10

Performance analysis

10.1 Introduction

In this chapter the new model is verified and compared to the original model to analyse the impact of ammonia on the engine performance. The models efficiency and fuel consumption are compared, the power density, cylinder temperatures and pressures are analysed and it is verified if the turbocharger still matches the engine when ammonia is used.

10.2 Model verification

There are no suitable measurements publicly available to validate the model. However, it can be verified if the changes to the model are implemented correctly. The verification of the model will be done by comparing the original model with the diesel-ammonia model to see if the diesel-ammonia model behaves as expected.

First the efficiencies and Seiliger parameters of the original model are compared to the the diesel-ammonia model with a 0% ammonia energy ratio, these values should be the same.

Figure 10.1 shows the different engine efficiencies as function of the engine power, the simulation has been set up with a propeller load and the fuel rack has been decreased from 100% to 40%. The continuous lines are from the new model v10 and the dashed lines are from the original TU Delft engine B model. Since both models represent the same engine under the same conditions the efficiencies should be equal. The figure shows that there are only very small differences between the efficiencies of the original model and model v10. These differences could be explained by rounding errors in the numerical differential blocks of the adapted model.

Figure 10.2 shows the mass fraction air in all six Seiliger points for both models as function of engine power. During the simulation a propeller load is used, the fuel

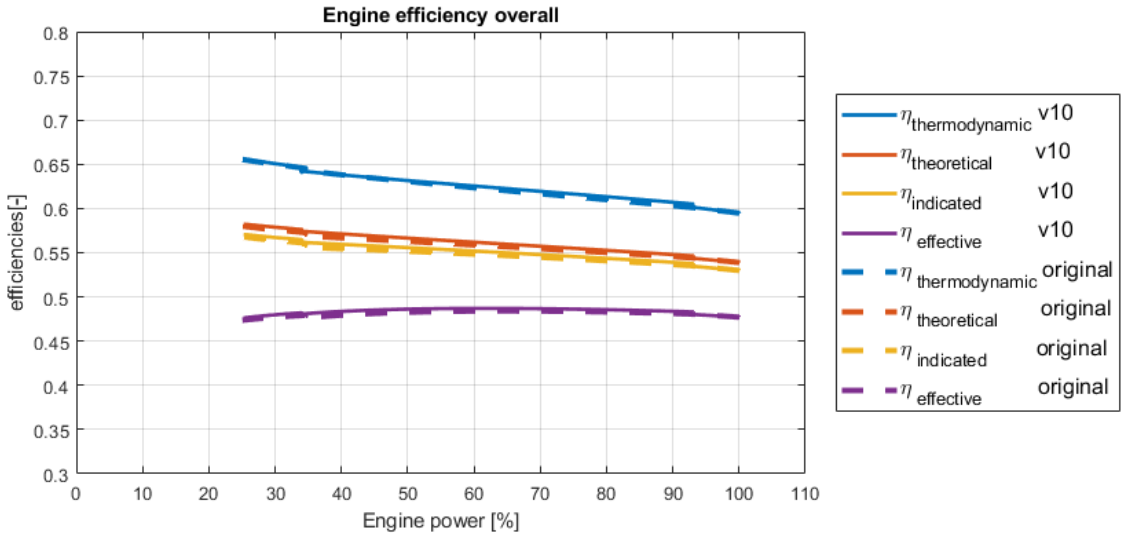

Figure 10.1: Comparison efficiencies original model and model v10.

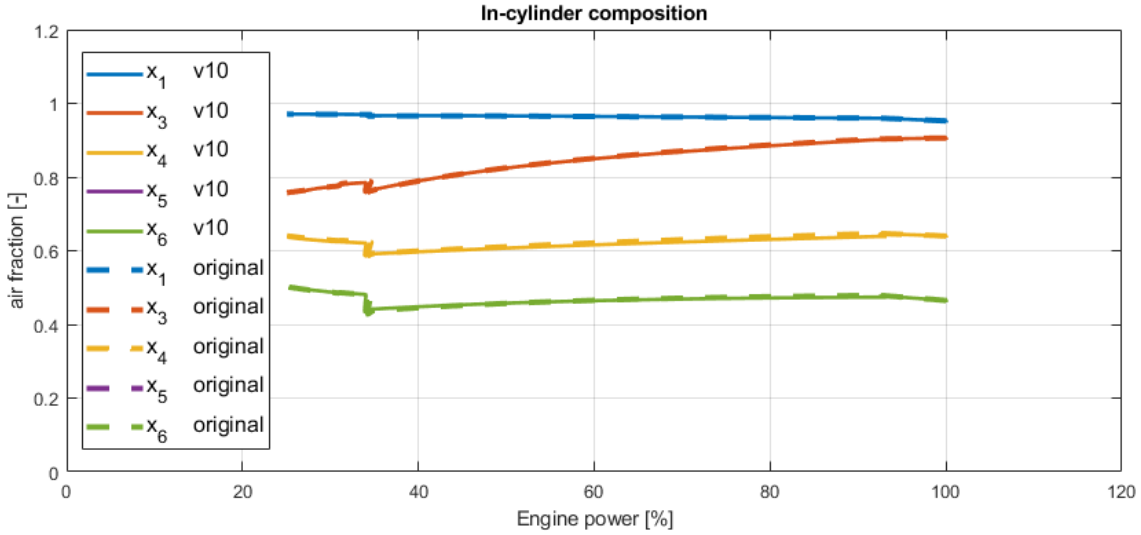

Figure 10.2: Comparison gas composition original model and model v10.

rack is decreased from 100% to 40% and model v10 used a 0% ammonia energy share ratio. The lines from the original model and model v10 overlap, which confirms that the changes to the gas exchange model have not caused any unexpected problems.

Secondly the impact of the ammonia energy ratio on the diesel ammonia engine is verified. In this section it is checked if the changes to the model behave as intended.

Figure 10.3 shows the mass fractions stoichiometric gas as function of the ammonia energy share ratio. A nominal engine load is used and the engine is run at nominal speed. The figure shows that the model changes behave as expected, when the ammonia energy share ratio increases, the mass fraction stoichiometric gas produced by diesel in the outlet receiver decreases, and the mass fraction of stoichiometric gas produced by ammonia in the outlet receiver increases. Noticeably the overall mass fraction stoichiometric gas in the outlet receiver decreases, in other words there is more air in outlet receiver. This can be explained by the increased overall engine

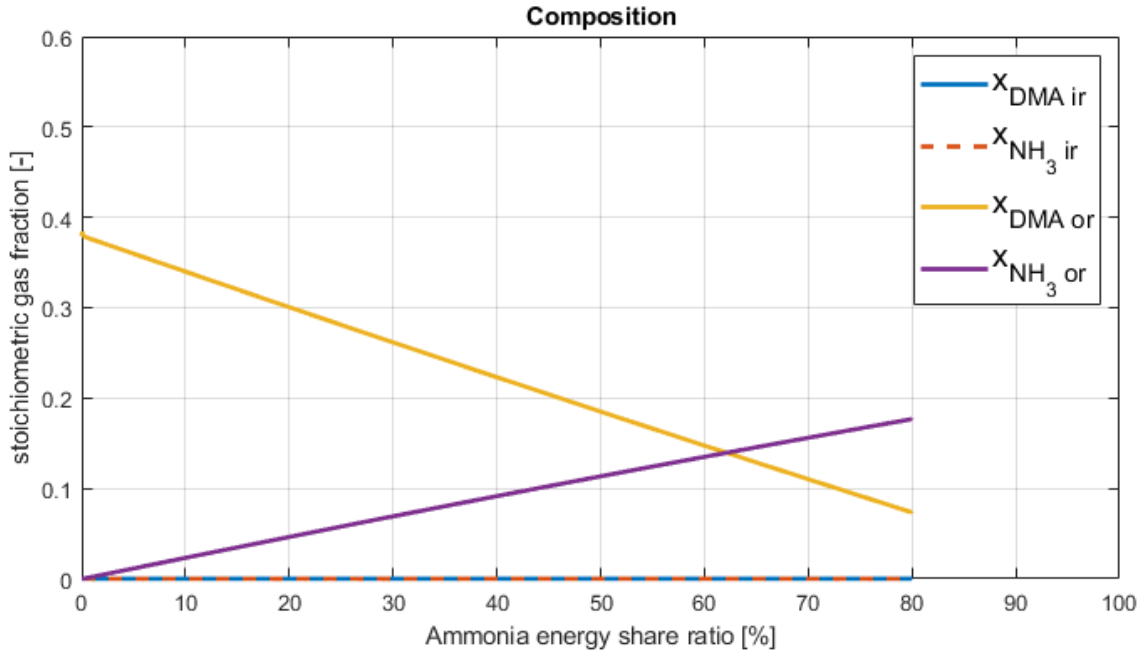

Figure 10.3: Mass fraction stoichiometric gas as function of the ammonia energy ratio

efficiency, because of the increased efficiency less fuel is required to achieve the same power output, so less exhaust gasses are produced. The increased efficiency will be discussed in section 10.3.1. Furthermore, the decrease in the overall stoichiometric gas fraction in the outlet receiver can be explained by the smaller stoichiometric air-fuel ratio of ammonia. The stoichiometric air-fuel ratios of ammonia and diesel are 6.05 and 14.67 respectively, which means that ammonia consumes less air when burned, this also contributes to the increased air fraction.

Figure 10.3 also shows that there are no exhaust gasses present in the inlet receiver, which means that no negative scavenging takes place. This is important because the changes to the gas exchange model discussed in section 8.11 have introduced a new limitation to the model: the gas mixture in the inlet receiver should consist of 100% air. This figure confirms that the model complies to this condition.

Figure 10.4 shows the temperatures after the combustion, stoichiometric ammonia gas has a higher specific heat, therefore, if the thermodynamic properties are implemented correctly into the model, the temperature should drop when more stoichiometric ammonia gas is present. The figure shows that the temperatures T_6 and T_7 after the combustion decrease when the ammonia energy share ratio increases.

To conclude, the changes to the gas mixture part of the model behave as they are intended and the newly introduced limitation is not exceeded.

Figure 10.5 shows the Seiliger combustion parameters as function of the ammonia energy share ratio at nominal engine speed and engine load. The figure shows that when ammonia is used, parameter a, which determines the initial pressure rise indeed decreases, and that parameter b, which determines the diffusive combustion phase increases. The ammonia dependent terms added to the fit functions X_a and

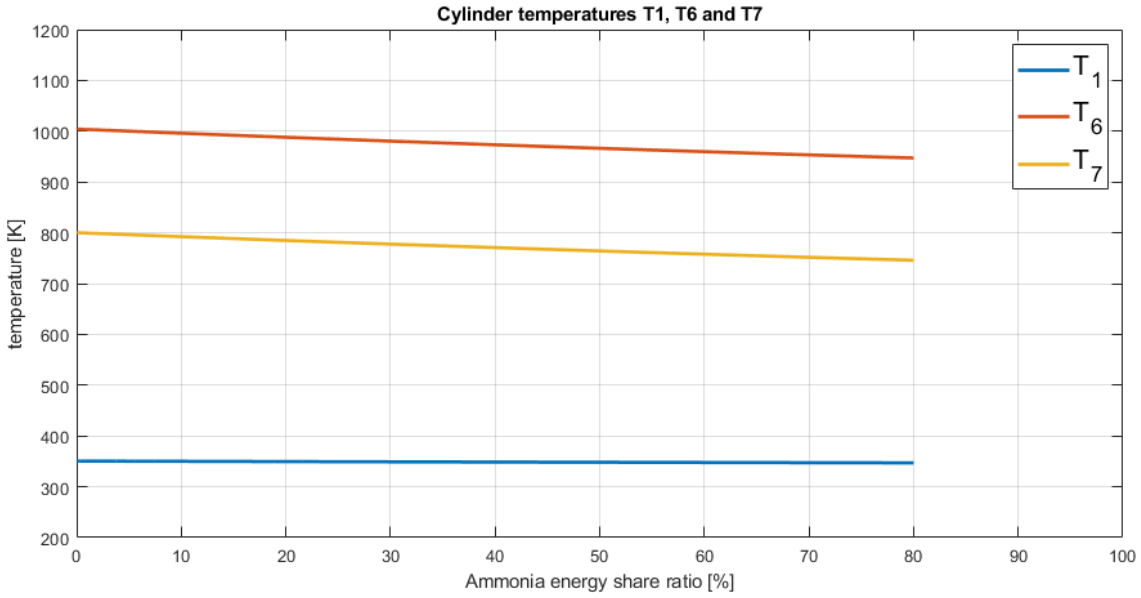

Figure 10.4: Cylinder temperatures high

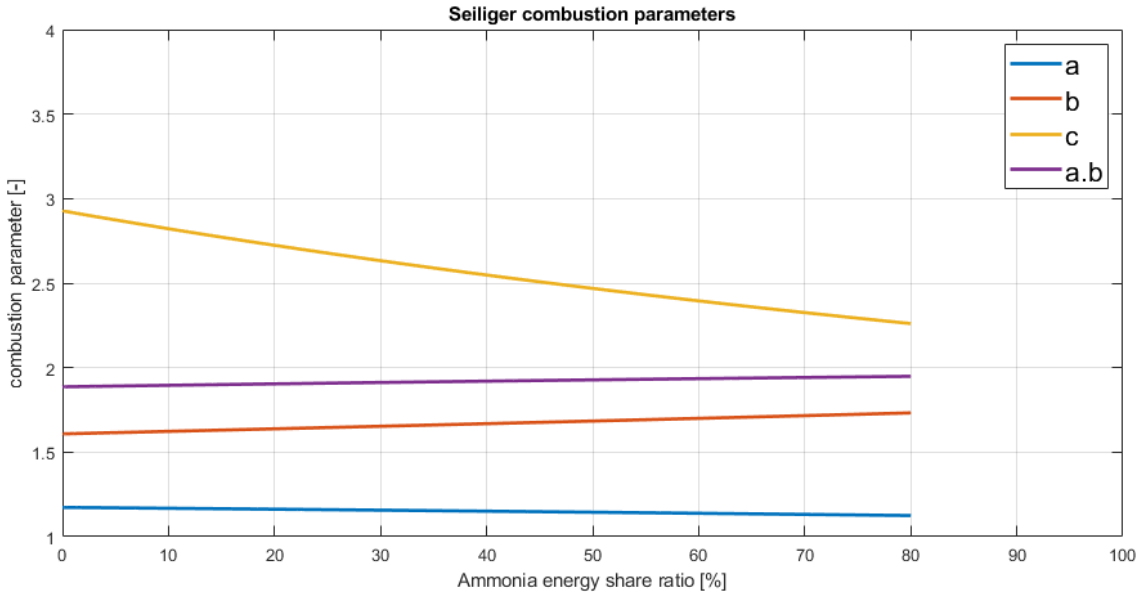

Figure 10.5: Combustion parameters

X_b seem to work as intended. However, figure 10.5 also shows that the combustion parameter c decreases. This is an unexpected effect and causes the late combustion phase to be shorter. Furthermore, it decreases the overall combustion duration.

The shorter late combustion phase and shorter combustion duration are unexpected results. The lower combustion rate of ammonia would more likely increase both the overall combustion duration and the late combustion phase [25]. In the model the Seiliger parameter c is dependent on the Seiliger parameters a and b. Parameters a and b determine how much heat is released in the first two combustion stages, the residual heat after the first two combustion stages determines Seiliger parameter c. Figure 10.5 shows that a $\cdot$ b increases, causing c to be decreased.

The decrease in Seiliger parameter c and in the late combustion phase is caused by how the model determines the value for parameter c and is not caused by a physical effect. Even more so, the decreased late combustion phase and the overall combustion duration is counter intuitive and most likely not a good representation of the reality. It is important that during the performance analysis of the diesel-ammonia engine no conclusions are based upon effects caused by the decreased Seiliger parameter c.

10.3 Results

In this section the engine performance of a diesel only engine will be compared to a diesel-ammonia engine. The goal of the engine is to produce mechanical power, the performance parameters are quantities that relate the useful output power to the required input and the unwanted consequences. The engine performance is divided in three parameters to indicate its performance: efficiency and fuel economy, power density and pollutant emissions [56]. Furthermore, the operational limits of the engine are further investigated to make sure they are not exceeded during diesel-ammonia operation.

10.3.1 Engine efficiency and fuel consumption

Diesel engines transform fuel heat energy into mechanical work, the chain of efficiencies as defined in the model is shown below. The overall efficiencies are η_i and η_e, their definitions are shown in formulas 10.1 and 10.2

$$Q_f \xrightarrow{\eta_{comb}} Q_{comb} \xrightarrow{\eta_q} Q_i \xrightarrow{\eta_{th}} W_i \xrightarrow{\eta_m} W_e$$

$$\eta_i = \frac{W_i}{Q_f} \tag{10.1}$$

$$\eta_e = \frac{W_e}{Q_f} \tag{10.2}$$

	$\eta_{combustion}$	$\eta_{heatinput}$	$\eta_{thermodynamic}$	$\eta_{indicated}$	$\eta_{mechanical}$	$\eta_{effective}$
00% NH_3	1.000	0.983	0.595	0.530	0.900	0.477
80% NH_3	1.000	0.986	0.638	0.565	0.905	0.512

Table 10.1: Engine efficiencies with and without ammonia at nominal engine speed and power.

Table 10.1 shows the engine efficiencies at nominal engine speed and load for both diesel only and 80% ammonia energy operation. The table shows that the overall efficiency, which is the effective efficiency, increases in the 80% ammonia energy operation. The cause of these changes will be discussed in the following sub-sections.

Combustion efficiency

The combustion efficiency defined as the heat released during combustion divided by the heat put into the cycle. This efficiency specifies the losses due to incomplete combustion. A low combustion efficiency does not only decrease the overall efficiency but also increases the hydrocarbon and ammonia emissions due to unburned fuel in the exhaust gasses. The combustion efficiency at nominal load is for both operational modes 100%, this was expected because, as discussed in chapter 8 paragraph 8.8 the combustion efficiency was not changed in the new model. However, due to the bad combustive properties of ammonia, it is questionable if complete combustion is achieved. It remains to be seen how realistic the assumption of complete combustion is.

Heat input efficiency

The heat input efficiency η_q increases when 80% ammonia is used, which means that less heat is lost during combustion. The heat generated by the combustion is dissipated via the cylinder walls into the cooling pockets around the cylinder. The amount of heat lost is dependent on the cylinder wall area, the temperature in the cylinder, the time for heat dissipation to take place and the heat transfer coefficient. The time for heat to be dissipated is reduced because the Seiliger parameter c is decreased and therefore, the overall combustion duration is also decreased. This decrease in combustion duration is not expected in reality, and therefore the increase in heat input efficiency due to a shorter combustion duration is uncertain.

However, the lower temperatures caused by ammonia could also increase heat input efficiency, since a lower temperature difference reduces the heat loss. The Woschni model is used to determine the heat input efficiency. This model determines the heat via the Seiliger parameters and the temperatures, T_1 and T_2, this results in a temperature reduction of 15.6 K. However, the model does not consider the impact of the bigger specific heat and injected mass of ammonia, which could decrease the temperature even further and compensate for the possible longer combustion duration.

Thermodynamic efficiency

Most of the efficiency gain seems to be caused by the thermodynamic efficiency, which shows the biggest increase from 59.5% to 63.6%. The thermodynamic efficiency is completely dependent by the shape of the cycle in the thermodynamic diagram [71], therefore, these changes in efficiency are mostly caused by the change in Seiliger parameters.

Figure 10.6 shows that when the Seiliger parameter c is decreased, the theoretical efficiency of the engine increases. The figure also shows that a decrease of parameter a decreases the efficiency and a increase in parameter b also decreases the efficiency. Since parameter a is decreased and parameter b is increased in diesel-ammonia operation both these parameters decrease the efficiency. Therefore, Seiliger parameter c must be the cause of the increase in thermodynamic efficiency. In section 10.2 it is concluded that the decrease in Seiliger parameter c, and in the late combustion is an effect caused by the model and not likely to happen in reality. Therefore, the increase in thermodynamic efficiency is caused by an unrealistic model effect.

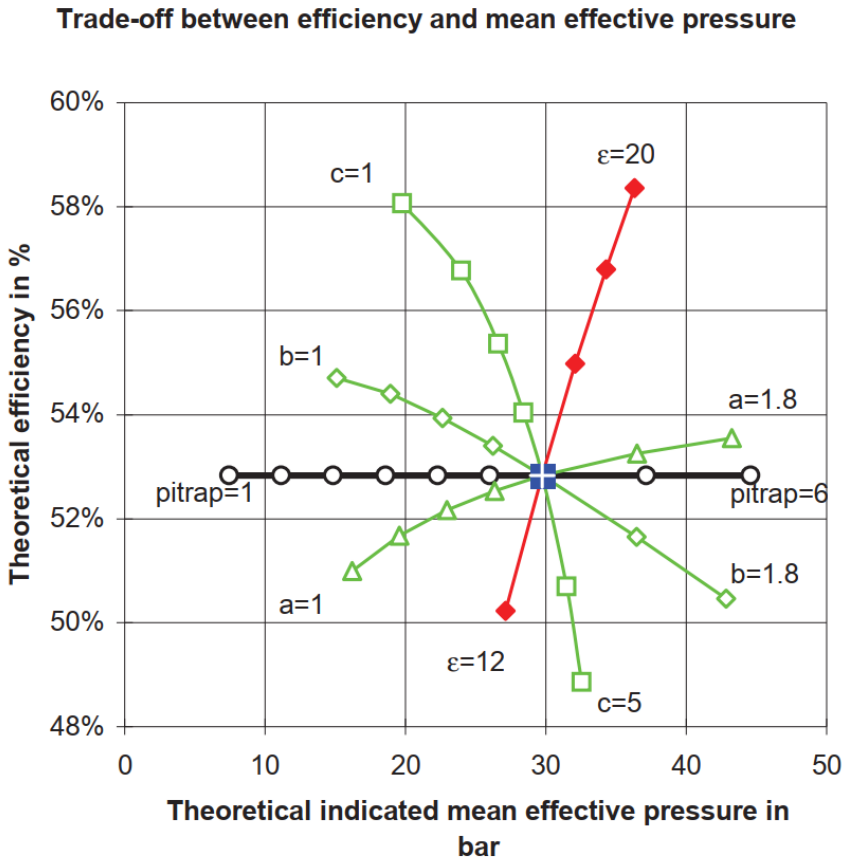

Figure 10.6: Effect of influence factors on efficiency and mean effective pressure [56]

Indicated efficiency

The indicated efficiency is defined as the indicated work divided by the heat input, the difference between the indicated efficiency and the effective efficiency is the mechanical efficiency. The indicated efficiency is greatly increased and contributes the biggest part to the effective efficiency increase. The increase in indicated efficiency is caused by the increase in thermodynamic efficiency.

Mechanical efficiency

The mechanical efficiency plays a smaller role in the increase in effective efficiency but does play a part in it. When 80% ammonia is used the mechanical efficiency increases due to lower mechanical losses. These losses are determined using the Chen & Flyn model, which determines the engine friction as a function of the maximum engine pressure and the engine speed. The engine speed remains constant, but ammonia lowers the maximum engine pressure, which decreases the friction in the engine.

Effective efficiency

The effective efficiency of the engine is defined as the work output divided by the heat input, this efficiency shows the overall efficiency of the engine. Naturally this value is the lowest of all efficiencies since all losses are considered. The effective efficiency clearly shows that ammonia increases the effective efficiency of the engine. This result is opposite of the results measured with smaller 4-stroke engines. However, the increase in effective efficiency is mostly caused by the increase in thermodynamic efficiency, and the increase in thermodynamic efficiency is caused by the lower value for the Seiliger parameter c. Therefore, the increase in effective efficiency is caused by a model effect and unlikely to happen in reality.

Fuel consumption

The fuel consumption of the engine is an important factor, the fuel cost are often a major part of the operational cost of a ship, and the sfc, together with the fuel tank size and the ship resistance determine the range of the vessel. Table 10.2 shows the sfc of the engine in model v10 and the original model for 0% ammonia mode and 80% ammonia mode at nominal load and speed of the engine. The specific fuel consumption is dependent on the engine efficiency and of course on the LHV of the fuel. Due to the relatively lower LHV of ammonia the sfc is about two times higher as diesel fuel.

The table also shows that the sfc of the original model is equal to the sfc of model v10 in 100% diesel mode, which suggests again that there are no modelling mistakes

in model v10. Furthermore, the table shows that the sfc of ammonia is zero in the 100% diesel mode as it should be, confirming that model v10 behaves as expected.

Furthermore, the table shows that both the original model and model v10 in 100% diesel mode have a sfc of 176.4 g/kWh and that with a 80% ammonia energy share ratio the sfc of ammonia is 302.4 g/kWh and the sfc of diesel is 32.9 g/kWh, which results in a total of 335.3 g/kWh. As was expected because of the LHV of ammonia, the sfc nearly doubles in diesel-ammonia operation.

	sfc diesel [g/kWh]	sfc ammonia [g/kWh]
original	176.4	0.0
v10 00% NH_3	176.4	0.0
v10 80% NH_3	32.9	302.4

Table 10.2: Comparison of the specific fuel consumption for both models.

10.3.2 Power density

The increased air excess ratio shown in figure 10.10 and the increased effective engine efficiency, discussed in section 10.3.1 indicate that the engine, running on ammonia, could provide more power. This would increase the power density of the engine. Figure 10.7 shows the Break Mean Effective Pressure (BMEP) and Indicated Mean Effective Pressure (IMEP) as function of the ammonia energy share ratio, this simulation is run with a propeller load at a constant fuel energy input. The Mean Effective Pressure (MEP) is seen as a measure of power density, a greater value means the engine is more power dense. The increase in MEP in figure 10.7 is caused by the increase in effective energy.

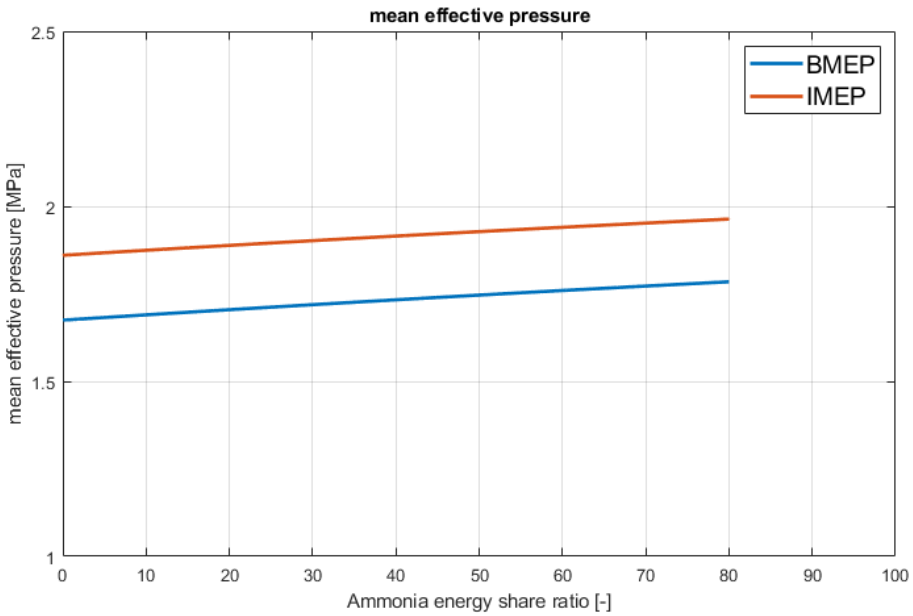

Figure 10.7: Ammonia energy ratio dependent mean effective pressure.

It should be noted, that only the power density of the engine is considered, and that a decrease in power density of the entire power plant can be expected due to the additional systems required for the safe storage and supply of the ammonia fuel, but that is out of the scope of this thesis. Furthermore, as discussed in section 10.3.1 the increase in effective efficiency is caused by a model effect, and it is unlikely that diesel-ammonia operation will increase the overall engine efficiency. Therefore, the focus is on the air excess ratio and the mechanical limits of the engine and not on the effective engine efficiency.

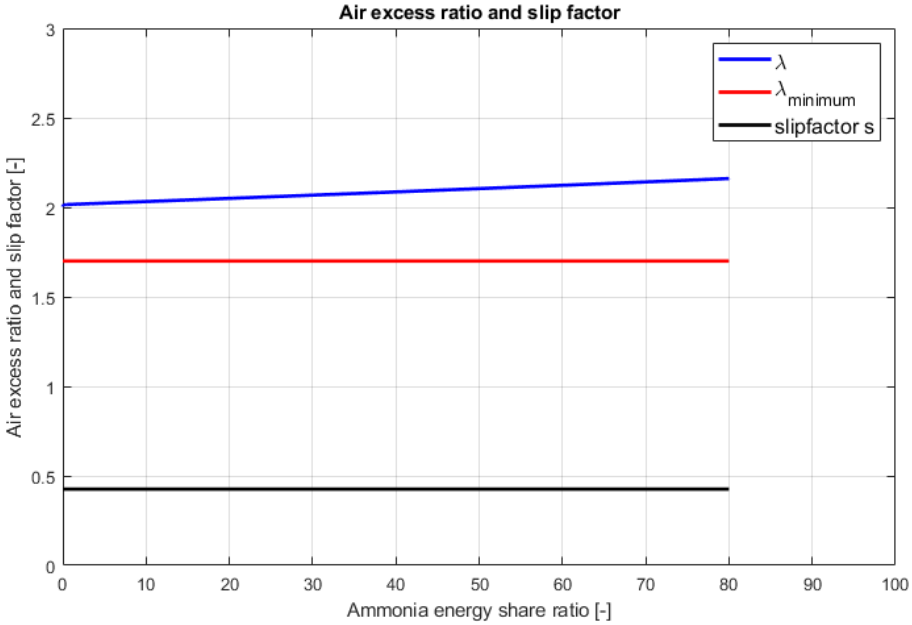

Figure 10.8: Air excess ratio as function of the ammonia energy share ratio at nominal engine speed and power.

First the engine is run with an increasing ammonia energy share ratio at 100% energy input with a propeller load. Figure 10.8 shows the air excess ratio as function of the ammonia energy share ratio. The figure shows that the air excess ratio increases with the ammonia energy share ratio. This is caused by the stoichiometric air-fuel ratio of ammonia, which is more than twice as low as the stoichiometric air-fuel ratio of diesel.

To see if the power density of the engine can actually be increased when ammonia is used, the engine model is run with an increasing generator load at nominal engine speed. Figure 10.9 shows the air excess ratio in diesel only operation and in the 80% ammonia energy share ratio operation. The air excess ratio in the 80% ammonia energy operational mode remains greater than the air excess ratio of the diesel only operational mode.

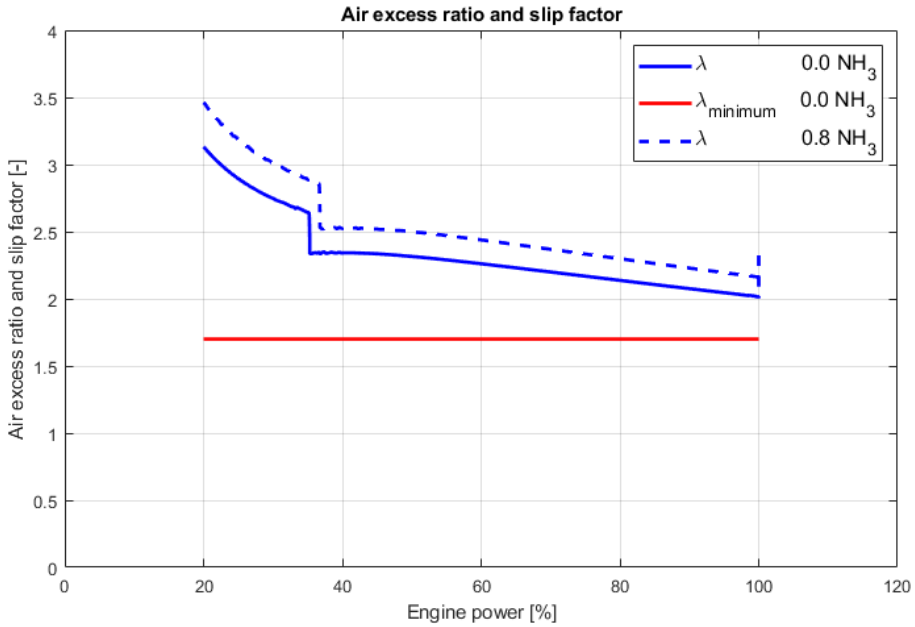

Figure 10.9: Comparison of the air excess ratio at nominal engine speed

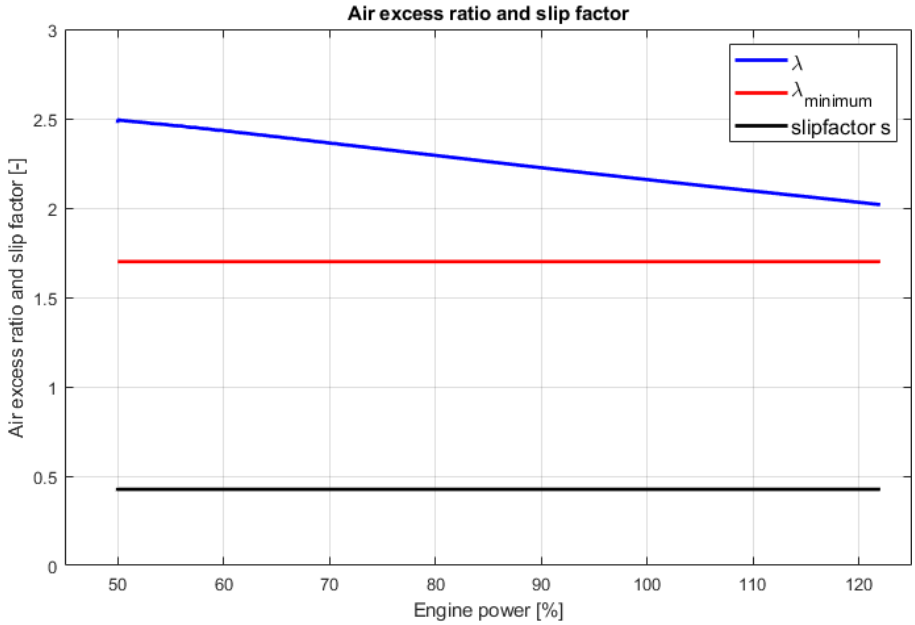

Figure 10.10: Air excess ratio at nominal engine speed and increased power

Ammonia is known for its bad combustibility, so the minimal air excess ratio required to achieve an acceptable combustion efficiency will probably be higher in ammonia-diesel operation. Therefore, it is expected that more heat can be punt into the cylinder in ammonia-diesel operation, but that this is limited by the combustion efficiency.

Figure 10.11 shows the BMEP, the increase in engine power output increases the BMEP and therefore the power density of the engine.

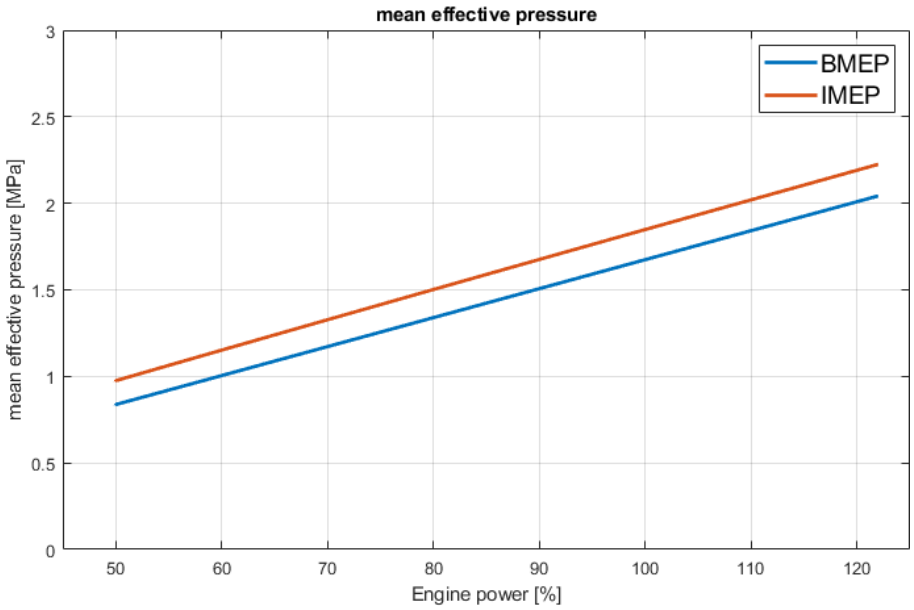

Figure 10.11: BMEP and IMEP at nominal engine speed and increased power

However, the air excess ratio is not the only limiting factor for the power density of the engine. The maximum cylinder temperature and pressure should also not be exceeded. Figures 10.12 and 10.13 show the maximum cylinder pressure and temperature in ammonia-diesel operation. The maximum pressure and temperature in diesel only operation are 186.9 bar and 1810 K respectively, these values are not exceeded when the fuel energy into the engine is increased to 122% of the nominal value. The decrease in maximum temperatures in ammonia-diesel operation can be explained by the higher specific heat of ammonia, and the lower maximum pressure can be explained by the shift from premixed combustion to diffusive combustion. However, the initial pressure rise becomes zero at 120% engine power. This effect is caused by how the model determines the Seiliger parameter a, it is not expected that the initial pressure rise completely disappears. Therefore, the very low maximum pressure, which is dependent on parameter a, decreases more than is expected in reality and could be a limiting factor in the power density of the engine.

Furthermore, the engine has some mechanical limits, going over the nominal engine power will most likely exceed the maximum engine speed and the maximum engine torque. This could damage engine components such as the pistons, piston rods, crankshaft and bearings. Therefore, it is unlikely that the power density of an engine will increased when an existing engine is re-fitted to run on diesel-ammonia. But when a new diesel-engine is developed those components can be designed to withstand the additional forces.

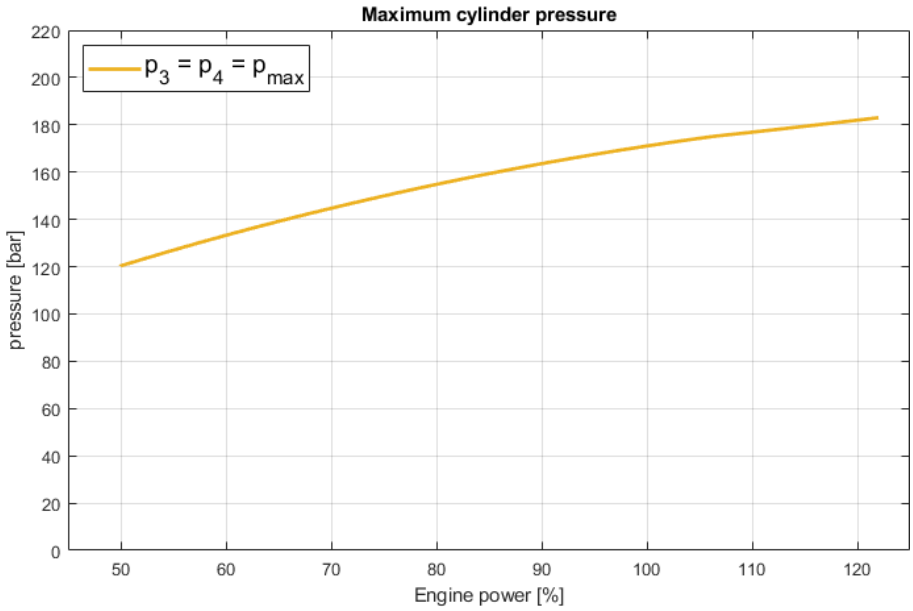

Figure 10.12: Maximum cylinder pressure engine speed and increased power

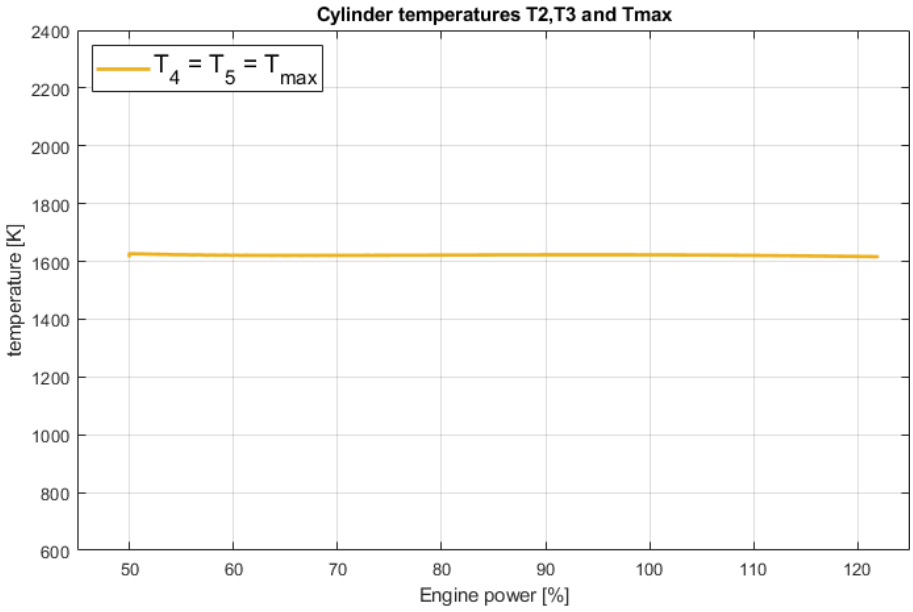

Figure 10.13: Maximum cylinder temperature at nominal engine speed and increased power

To conclude, the lower stoichiometric air-fuel ratio of ammonia could increase the power density of the engine. However, the worse combustion characteristics of ammonia could require a higher air excess ratio to achieve an acceptable combustion efficiency. Furthermore, the maximum temperatures and pressures are lower during ammonia operation, but the model exaggerates the decrease in maximum pressure, therefore, the maximum power output could be increased but probably not as much as the model suggests. Lastly, when the engine power is increased beyond the nominal power engine components could be damaged because they are not designed to withstand such loads.

10.3.3 Emissions

The emissions of internal combustion engines are an important performance parameter, the negative effects of the emissions are becoming more clear and stricter rules regarding the emissions have been introduced. This is why the emissions are discussed in this section although the model itself does not model how much emissions the engine releases.

Although the emissions are not modelled, some conclusions can be drawn. First the fuel related emissions are discussed. Some of the emissions can directly be associated with the fuel consumption, the CO_2 and SO_x emissions are directly dependent on the diesel fuel consumption. CO_2 is a direct result of the combustion reaction of diesel fuel with oxygen, and the SO_x emissions are caused by the sulphur in the diesel fuel [59].

It should be noted that the diesel fuel consumption is also dependent on the ammonia energy ratio, and that the diesel fuel bound emissions decrease when the ammonia energy ratio increases. However, the maximum achievable ammonia energy ratio is uncertain. Therefore, it is uncertain how much the emissions will decrease.

Although an ammonia energy share ratio of 80% is used in most of the simulations due to the available experiments also using this value higher ammonia energy share ratios could be possible. The engine manufacturer MAN does not make any statements about how much pilot fuel is required to ignite ammonia, however, they predict that the CO_2 emissions decrease with 95% [40]. Since the CO_2 emissions are directly linked to the mass fraction diesel fuel this means they also expect 95% ammonia mass fraction, which is an ammonia energy ratio of 89%. Experiments with smaller four-stroke engines were able to achieve combustion up to an ammonia energy share ratio of 80% [47] [48]. However, due to poor combustion efficiency is was recommended to operate the engine between a 40-60% ammonia energy ratio.

With an ammonia energy ratio of 80%, which is on the safe side of what is possible, the sfc for diesel fuel is 32.9 g/kWh, it should be considered that this sfc is a result of the ammonia energy share ratio and the increased overall efficiency, which was deemed a model effect. However, this specific fuel consumption will cause decrease in SO_x and CO_2 emissions. The sfc of diesel is reduced to 18.7% of the nominal value, which means that both the power specific emission ratio (pse) for both SO_x and CO_2 are reduced with 17.8%. This decrease in emissions is mostly caused by using 80% ammonia energy, but also by the increased effective efficiency.

It is difficult to make any predictions for the other emissions, who are dependent on the combustion process. However, two emissions stand out in diesel-ammonia operation: the newly introduced ammonia emissions and the NO_x emissions.

As already mentioned in section 8.8 the combustion efficiency remains unchanged, but it is likely that the combustion efficiency decreases during diesel-ammonia operation. This means that unburned fuel will be expelled into the exhaust. This unburned fuel will normally be categorised under the Hydro Carbon (HC) emissions, however, in diesel-ammonia operation part of these emissions caused by incomplete

combustion will be ammonia, and ammonia is a toxic gas. Therefore, it is highly likely that additional equipment has to be installed to scrub the ammonia emissions from the exhaust gasses to reduce the ammonia emissions to an acceptable level[40].

Lastly the NO_x emissions, which are caused by the reaction between oxygen and nitrogen in high temperature areas. Since the model uses a mean value method, the hot spots in the cylinder, where these emissions are created, cannot be simulated. However, research suggests that the higher specific heat of ammonia causes the overall temperature to decrease, which decreases the NO_x emissions [47]. With higher ammonia energy share ratios the NO_x emissions increase because ammonia itself contains nitrogen [47]. It is expected that scrubbers are necessary to reduce the NO_x emissions to an acceptable level [40].

To conclude, the CO_2 and SO_x emissions are directly dependent on how much diesel fuels is consumed, the increased effective efficiency plays a small role in the reduction of these emissions, but most of the reduction is caused by ammonia replacing the diesel fuel. The maximum ammonia mass fraction achievable in two-stroke engines is uncertain, but some manufactures suggest a reduction up to 95% is possible. Running the engine in diesel-ammonia mode will most likely increase the ammonia and NO_X emissions, additional equipment is required to reduce these emissions.

10.3.4 Operational limits

The operation of an engine is limited to the physical capabilities of the engine. For example there is an engine speed limit, which, when, exceeded, could cause damage because the components of the engine are not made to handle the force introduced by the increased maximum speed. The limits investigated in this section are the maximum engine pressure, maximum engine temperature, and the operational limits of the turbocharger system.

Thermal limit

Thermal overload can be defined as a condition under which design threshold values such as the maximum surface temperature of combustion chamber components are exceeded [42]. The exact maximum temperatures of the separate components of the MAN S35ME engine are not known. However, big increases in the maximum cylinder temperatures could indicate that engine components are thermally overloaded.

Figure 10.14 shows that there is a slight increase in the maximum temperature, but the temperature after the initial pressure rise is decreased, and the temperature T_2 barley changes. The maximum temperature is increased from 1613 K to 1622 K, this change in temperature is very small and is most likely within the thermal limits of the engine.

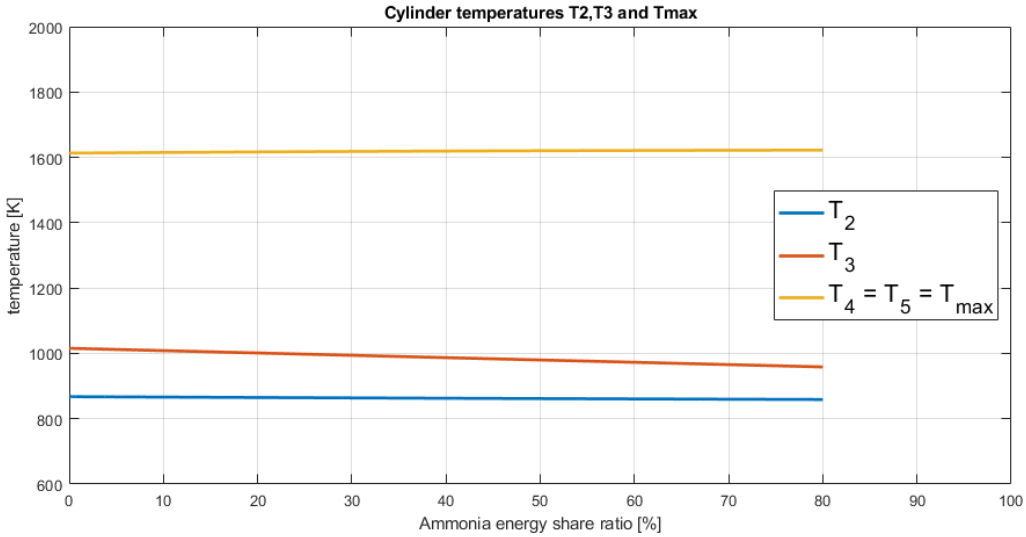

Figure 10.14: Cylinder temperatures high

However, an increase in maximum temperature with ammonia was not expected, ammonia and stoichiometric ammonia gas both have a higher heat capacity, which means they absorb more heat before their temperature increases, resulting in lower temperatures. Experiments with small four-stroke engines also showed that the use of diesel-ammonia resulted in lower combustion temperatures [48]. The increase in maximum combustion temperature can be explained with formula 10.3, this formula shows the relation between the temperature at the start of the cycle and the maximum temperature.

$$T_{max} = a \cdot b \cdot r_c^{n_c - 1} \cdot T_1 \tag{10.3}$$

The initial temperature T_1 does not change, and the compression and compression coefficient r_c and n_c do not change, because ammonia is not yet present in the cylinder at the start of compression. Therefore, the increase in maximum temperature is caused by the Seiliger parameters $a \cdot b$, these parameters have been changed to decrease the premixed combustion and to increase the diffusive combustion. The increase in the maximum temperature is not a physical effect but a modelling effect caused by these changes, and based upon the properties of ammonia and experiments [48] not a realistic result.

Maximum cylinder pressure

The engine components are designed to withstand a certain force, the maximum cylinder pressure gives a good representation of the maximum force on these components. When the cylinder pressure is increased the mechanical limits of the engine could be exceeded. Therefore, a big increase in the maximum cylinder pressure during combustion could indicate that the mechanical limits of the engine are exceeded.

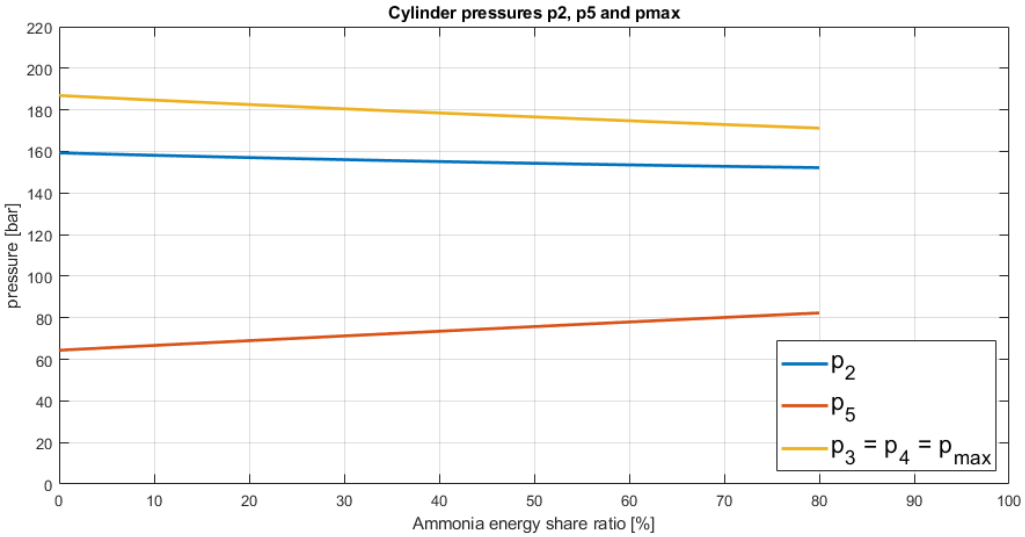

Figure 10.15: Combustion pressure

Figure 10.15 shows the maximum cylinder pressure as function of the ammonia energy share ratio. The measurements are done at nominal engine speed and power. As expected due to the changes made to Seiliger parameters a the maximum cylinder pressure decreases when the ammonia energy share ratio increases. Since the maximum cylinder pressure decreases, it is expected that the engine operates within its mechanical limits.

Turbo charging

The turbine of the turbocharger requires a pressure, a temperature and a mass flow to operate properly, the turbocharger is selected based on these properties of the engine [57]. As seen in previous sections the exhaust temperature, pressure and flow change due to the use of ammonia, therefore it should be checked if the current turbo charger is still a proper match for the engine with ammonia.

First it has to be checked if the turbine produces enough power to propel the compressor and create the required charge pressure [57]. Figure 10.16 shows the pressures in the inlet receiver and the outlet receiver, the dotted lines represent the scenario with 80% ammonia. The figure clearly shows a drop in pressure over the entire range. The jump in the pressures, around 35% engine power is caused by the auxiliary blower turning on, this blower is automatically activated when the inlet receiver pressure becomes too low.

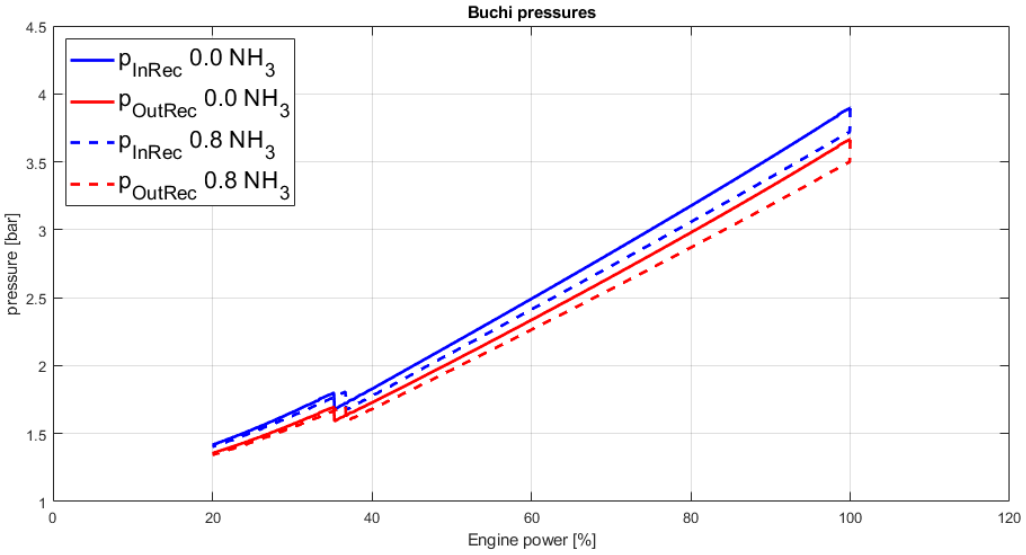

Figure 10.16: Pressure in the inlet receiver and outlet receiver with and without ammonia

Figure 10.17 shows the temperature in the compressor, inlet receiver, outlet receiver, and turbine, the compressor and inlet receiver temperatures barely change because it is mostly dependent on the ambient conditions, who remain constant. However, the other temperatures drop with the use of ammonia. The drop in cylinder temperatures is already discussed, which might be caused by the different thermodynamic behaviour of stoichiometric gasses. The stoichiometric ammonia gasses have a higher gas constant, meaning that more energy is required to increase the temperature of the gas, which could explain the lower temperatures. Furthermore, the efficiency increases when ammonia is used, the turbine is driven by the leftover energy in the exhaust gasses, the increase in efficiency means a decrease in energy in the exhaust gasses. Therefore, less energy is available to drive the turbine.

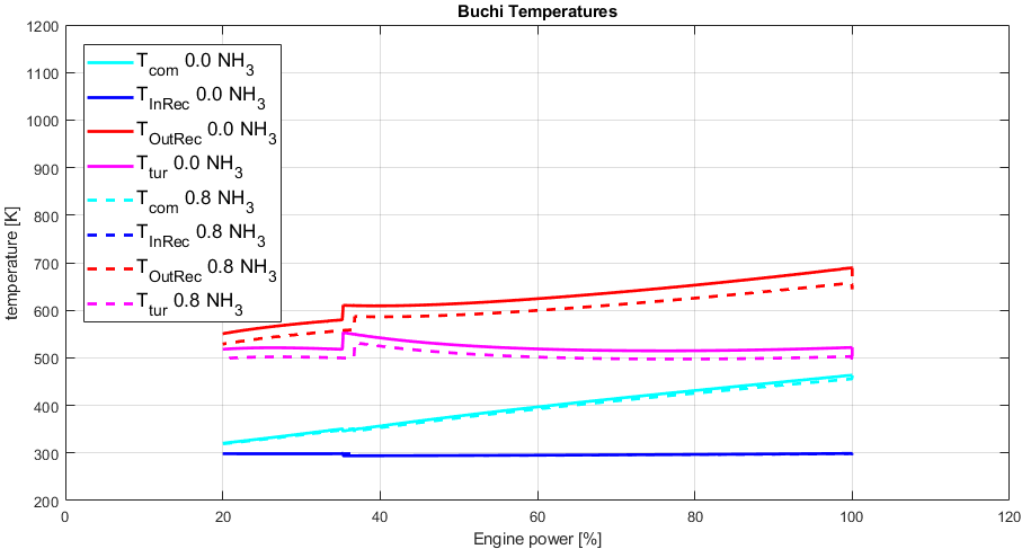

Figure 10.17: Temperature in the inlet receiver, outlet receiver, turbine and compressor with and without ammonia

The turbine receives less energy which causes the inlet receiver and outlet receiver pressures to drop, it is important to check if the decrease in pressure stops the engine from running properly. A good indicator to see if the engine is supplied with enough energy is the air excess ratio. Figure 10.18 shows the air excess ratio, which shows an overall increase in available air in the cylinder. However, this is not caused by more air in the cylinder, since ammonia requires relatively less air to be burned. If the lower heating values of both fuels are divided by the corresponding stoichiometric air fuel ratio the amount of energy per kg air can be calculated. For diesel this is 2915 kJ/kg air and for ammonia 3074 kJ/kg, so to produce the same amount of heat, less air is required when ammonia is used. Furthermore, the engine efficiency increases, so less fuel has to be injected to produce the same amount of power. This explains the increase in the air excess ratio, when the same amount of air is present and the same amount of power is produces the air excess ratio is automatically higher with ammonia.

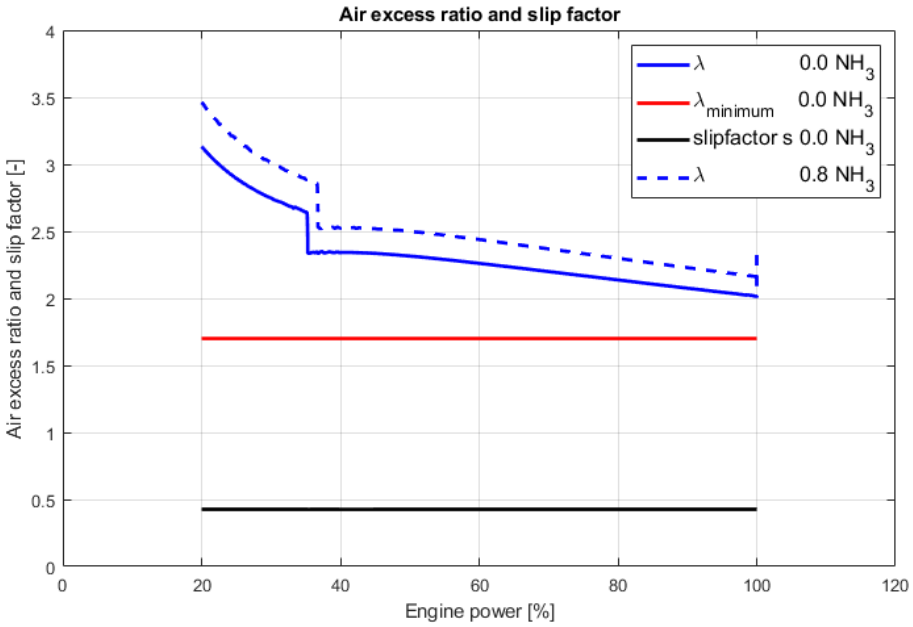

Figure 10.18: The air excess ratio with and without ammonia

The drop in inlet and outlet pressure decreases the air flow into the cylinder as shown in figure 10.19, which impacts the scavenging. Figure 10.20 shows a slight decrease in the scavenging efficiency and the air purity when ammonia is used as a fuel. However, these changes are well within the operational limits of the engine.

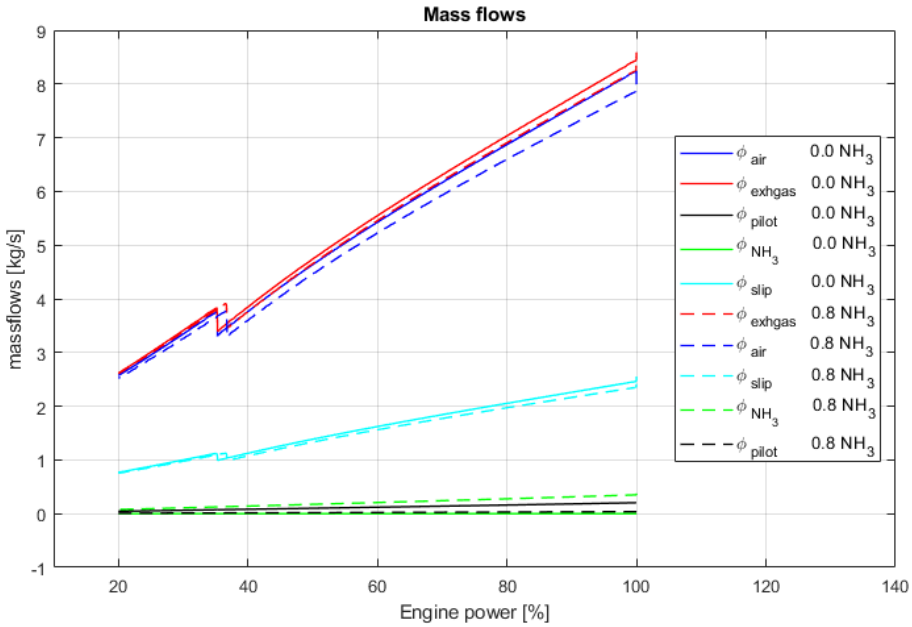

Figure 10.19: Mass flow with and without ammonia

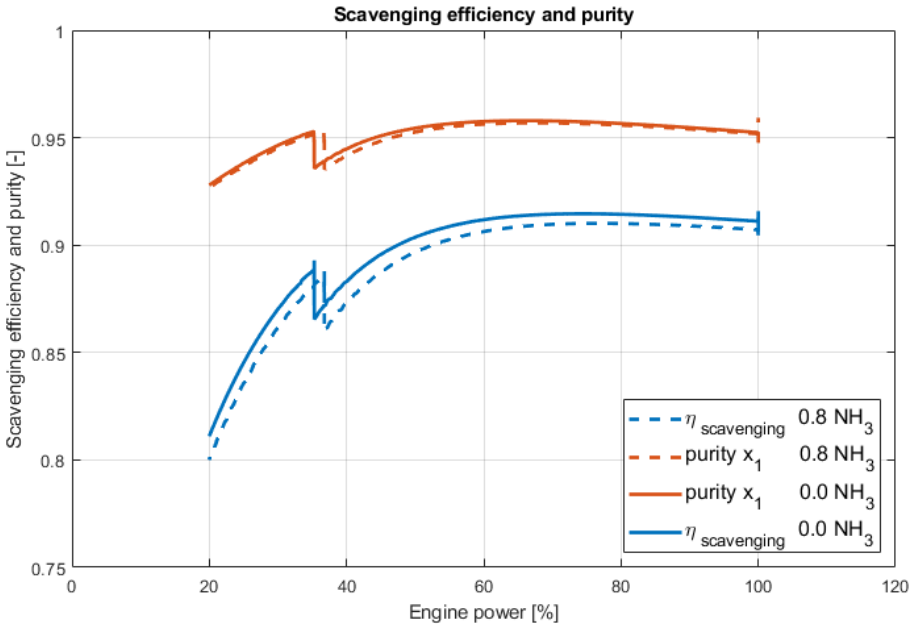

Figure 10.20: Scavenging with and without ammonia

The flow between the turbine and the engine also has to be in balance. The model does not allow for mass to disappear, so the flow through the compressor, cylinder and turbine is always matched. However, it should be checked if the flows are within the operational limits of the compressor and turbine. The limiting factor in the compressor is the surge line. When the lines of constant speed are followed from right to left, there comes a point where the pressure ratio starts to decrease instead of increase with decreasing mass flow. From this point there are two solutions for the mass flow given a pressure ratio. This leads to unstable behaviour and should always be avoided [57]. The surge line of the compressor is indicated with a black line in figure 10.21. The compressor trajectories are almost the same in both the

diesel only and the 80% ammonia case. The 100% diesel case has overall a slightly higher flow for the same pressure ratio. This is well within the operational limit of the compressor and nowhere near the surge line. Furthermore, when ammonia is used the pressure ratio and mass flow drop, for the nominal load the operational point follows the curve to a lower point as indicated with the blue line. This moves the working point to a slightly more efficient operational point.

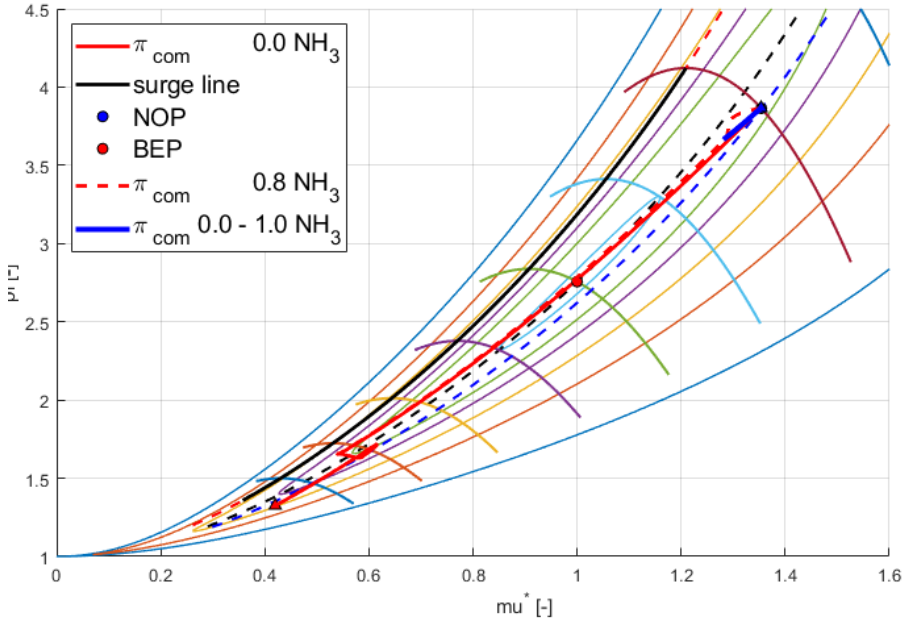

Figure 10.21: The compressor map

The engine manufacturer MAN has announced that they will have the first ammonia engine available by 2024 and refits of their existing engines by 2025, which makes it extra interesting to see if the same turbocharger can be used on a engine operating with ammonia [11]. When the turbo charging system does not have to be changed a lot of cost can be spared during the refit, making the conversion to ammonia diesel duel fuel more attractive for ship owners.

10.4 Discussion

Most changes in the efficiencies discussed in section 10.3.1, and the changes in temperatures and pressures in section 10.3.4, are a direct result of the changes made to the combustion shape in chapter 6. These changes are based on tests with different engines that are smaller and run on higher speeds. The lower speed of the engine in the TU Delft engine B model will allow more time for the fuel to be injected and ignited, this could mean that the shift from rapid combustion to diffusive combustion due to the lower flame speed of ammonia is smaller than anticipated. It is expected that the results from the test with smaller engines give a good indication of the direction in which certain values go, but that the magnitude of these values can be quite different. Therefore, it is important to realise an increase in efficiencies and a decrease in maximum pressure is expected due to more diffusive combustion, but the magnitude of these changes is uncertain.

Furthermore, the decrease in overall combustion time and in the late combustion phase is caused by how the model determines the value for parameter c and is not caused by a physical effect. The decreased late combustion phase and the overall combustion duration is counter intuitive and not expected to happen in reality.

Lastly, the combustion efficiency of the engine is still dependent on the air excess ratio and has not been changed because large marine reciprocating engines running on an ammonia-diesel mixture do not yet exist. Therefore, representative data is missing. The combustion efficiency remains 100% at nominal engine speed and load. The engine manufacturer MAN expect no or a limited reduction in efficiency [40]. It remains to be seen how realistic this assumption is.

10.5 Conclusion

In diesel-only operation the new model behaves the same as the original model, which confirms that the changes made to the model do not cause any problems. Furthermore, in diesel-ammonia operation, the gas exchange model behaves as expected and the newly introduces limitations of the new model are not exceeded.

However, the ammonia energy share ratio dependent changes to the Seiliger parameters behave in an unexpected way. When the ammonia energy ratio is increased, Seiliger parameter c decreases, which also decreases the overall combustion duration and the late combustion phase. This effect is caused by how the model determines the Seiliger parameter c and is opposite of what is expected to happen in reality.

The model predicts an increase in both the thermodynamic and mechanical efficiency, the lower peak pressure will decrease the load on the mechanical components of the engine and therefore increase the mechanical efficiency. The smaller late combustion phase increases the thermodynamic efficiency of the engine model. In reality the increase in thermodynamic efficiency is unlikely, the increase in the model is caused by the unexpected decrease in Seiliger parameter c. The effective efficiency impacts the specific fuel consumption, however, the LHV of ammonia has the biggest impact on the overall sfc. Therefore, as expected, the overall specific fuel consumption almost doubles with an ammonia energy share ratio of 80%.

Due to the lower stoichiometric air-fuel ratio of ammonia the power density of the engine could be increased. However, the relatively bad combustive properties of ammonia could require a higher air excess ratio to achieve an acceptable combustion efficiency, reducing this effect. Additionally, the lower pressure and temperatures in diesel-ammonia operation reduce the mechanical and thermal load on the engine, allowing more fuel to be injected without exceeding the maximum temperatures and pressures reached during diesel-only operation. However, it should be considered that the model most likely exaggerates the decrease in maximum cylinder pressure. Lastly, it should be considered that when the power output of the engine is increased, the maximum load of the engine components could be exceeded and they could fail.

The CO_2 and SO_x emissions are directly dependent on how much diesel fuel is consumed, the increased effective efficiency plays a small role in the reduction of these emissions, but most of the reduction is caused by ammonia replacing the diesel fuel. It is uncertain what the maximum achievable ammonia mass fraction in two-stroke engines is. Some manufactures suggest a reduction up to 95% is possible. Running the engine in diesel-ammonia mode will most likely increase the ammonia and NO_X emissions, additional equipment is required to reduce these emissions to acceptable levels.

A bigger part of the fuel is burned during the diffusive combustion phase, this causes a drop in the maximum cylinder pressure. The pressure p_2 at the start of the combustion also decreases slightly, the temperature T_2 barely changes, it is important that these values are high enough to ignite the ammonia diesel mixture in the cylinder. The maximum temperature seems to go up very slightly, while the other temperatures are lower. The change in maximum temperature and pressure will most likely not exceed the mechanical limitations of the engine.

With an ammonia energy share ratio of 80% the maximum temperature is slightly increased. This is caused by the Seiliger parameters $a \cdot b$, these parameters have been changed to decrease the premixed combustion and to increase the diffusive combustion. The increase in the maximum temperature is not a physical effect but a modelling effect caused by these changes, and based upon the properties of ammonia and experiments [48] not a realistic result. It is expected that the temperature during diesel-ammonia operation is within the thermal limits of the engine.

Due to the shift from pre-mixed combustion to diffusive combustion the maximum cylinder pressure decreases when the ammonia energy share ratio increases. Since the maximum cylinder pressure decreases it is expected that the engine operates within its mechanical limits.

The turbo charger operates at a sightly lower pressure ratio providing the engine with a lower inlet receiver pressure. However, the engine is still provided with enough air to allow for complete combustion. Furthermore, the original turbo charger system seems to operate within its operational limits when ammonia is used, the surge line of the compressor is not exceeded which means that the compressor operates in its stable region.

Chapter 11

Conclusion and recommendations

11.1 Conclusion

The goal of this research is to characterise diesel-ammonia combustion based on the available literature, and to implement this characterisation into a time-domain mean value two-stroke engine model. This model will be used to indicate the technical feasibility of diesel-ammonia as a marine fuel.

The main research question of this project is: How does the performance of the main engine of a deep-sea cargo vessel fuelled with diesel-ammonia compare to one fuelled by diesel only? To answer the main research question, the sub questions have to be answered, which are addressed separately below.

How to model the behaviour of a dual fuel diesel-ammonia engine on a deep-sea cargo vessel?

To run the model in a dual fuel mode a second fuel supply line is added and a new variable is introduced: the ammonia energy share ratio. This new variable indicates how much of the injected fuel energy is provided by ammonia. The maximum fuel flow is scaled to the same amount of energy flow into the engine as with diesel fuel.

The Seiliger stages have kept their original definitions. However, the injected energy into the combustion stages is now dependent on both the ammonia and diesel fuel flow.

The original formulas for the Seiliger parameters are used, however, they had to be slightly adapted to accommodate two fuels. To make the combustion shape of the model dependent on the ammonia energy share ratio two new terms are added to the formula for X_a and X_b.

Based upon literature research values are chosen for the new ammonia energy share ratio dependent parameters to replicate the impact of ammonia on the combustion

shape. The main changes are a decrease in maximum pressure and a shift of energy release to the diffusive combustion phase.

The function to calculate the ignition delay is multiplied with an new function, which is dependent on the ammonia energy ratio and increases the ignition delay when the ammonia energy share ratio is increased. The new function is based on measurements with a small four-stroke engine. The increase in ignition delay is very likely, however the magnitude of this increase is uncertain.

The combustion efficiency of the engine is still dependent on the air excess ratio and was not changed because no representative data is available. The combustion efficiency remains 100% at nominal engine speed and load.

The gas mixture in the engine was defined by the air mass fraction, this has been changed to the stoichiometric diesel gas fraction and the stoichiometric ammonia gas fraction. The same assumption as before has been used, no other reactions take place besides the combustion of the fuels itself.

The properties of the stoichiometric ammonia gas are defined in the model and the model blocks used for calculating the thermodynamic properties of the gas mixture are updated to use the new definition of the gas mixture. Furthermore the gas exchange model has been altered to consider the new definition for the gas mixture. This change introduces a limitation to the gas exchange model since it no longer supports negative savaging.

How do the specific fuel consumption and efficiency of a diesel only engine compare to a diesel-ammonia engine?

The model predicts an increase in both the thermodynamic and mechanical efficiency, the lower peak pressure will decrease the load on the mechanical components of the engine and therefore increase the mechanical efficiency. The smaller late combustion phase increases the thermodynamic efficiency of the engine model. In reality the increase in thermodynamic efficiency is unlikely, the increase in the model is caused by the unexpected decrease in Seiliger parameter c. The effective efficiency impacts the specific fuel consumption, however, the LHV of ammonia has the biggest impact on the overall sfc. Therefore, as expected, the overall specific fuel consumption almost doubles with an ammonia energy share ratio of 80%.

How does the power density of a diesel only engine compare to a diesel-ammonia engine?

The lower stoichiometric air-fuel ratio of ammonia could increase the power density of the engine. However, the worse combustion characteristics of ammonia could require a higher air excess ratio to achieve an acceptable combustion efficiency. Furthermore, the maximum temperatures and pressures are lower during ammonia operation, but the model exaggerates the decrease in maximum pressure. There-

fore, the maximum power output could be increased, but probably not as much as the model suggests. Lastly, when the engine power is increased beyond the nominal power engine components could be damaged because they are not designed to withstand such loads.

How do the emissions of a diesel only engine compare to a diesel-ammonia engine?

The CO_2 and SO_x emissions are directly dependent on how much diesel fuels is consumed, the increased effective efficiency plays a small role in the reduction of these emissions, but most of the reduction is caused by ammonia replacing the diesel fuel. The maximum achievable ammonia mass fraction in two-stroke engines is uncertain. However, some manufacturers suggest a reduction up to 95% is possible. Running the engine in diesel-ammonia mode will most likely increase the ammonia and NO_X emissions, additional equipment is required to reduce these emissions.

What impact does diesel-ammonia operation have on the operational limits of a diesel only engine?

Diesel-ammonia operation increases the maximum cylinder temperature. This is caused by the Seiliger parameters $a \cdot b$, these parameters have been changed to decrease the premixed combustion and to increase the diffusive combustion. The increase in the maximum temperature is not a physical effect but a modelling effect caused by these changes, and based upon the properties of ammonia and experiments [48] not a realistic result.

The maximum cylinder pressure is decreased because the pre-mixed combustion is reduced in diesel-ammonia operation. It is expected that the temperature and pressure during diesel-ammonia operation is within the mechanical limits of the engine.

The turbo charger operates at slightly lower power due to the higher thermodynamic efficiency. However, the turbo charger still manages to supply the engine with enough air to operate at sufficient pressures and air excess ratios. The compressor operates within the stable region with and without the use of ammonia as fuel, therefore no different turbocharger is necessary. This is an important result, as for other alternative fuels it is highly likely that different turbochargers would be necessary.

11.2 Recommendations

Multiple additions to the model can be recommended to improve the application possibilities and accuracy of the model.

The combustion shape in the new model has been altered to suit the combustion characteristics of ammonia combustion. However, these changes are based on tests with relatively small four-stroke engines. To improve the understanding of the ammonia diesel combustion process in big two-stroke marine engines it would be interesting to look further into the impact of the scaling in both engine speed and size, and to further explore the impact of the difference between a two-stroke and four-stroke cycle.

The combustion efficiency remains unchanged in the new model, while tests with relatively small four-stroke engines show a significant decrease in the combustion efficiency. However, marine engine manufacturers which have started the development of two-stroke marine engine fuelled by ammonia predict that the decrease in combustion efficiency will be very small. To better predict the overall efficiency, the ammonia emissions and the possible increase in power density of a two-stroke marine engine fuelled by ammonia, the impact of ammonia on the combustion efficiency in large two-stroke marine engines should be further investigated, and the model should be adapted to reflect the results of this research.

Furthermore, the combustion model could be improved and even validated when measurements with actual ammonia fuelled two-stroke marine engine are available. It would be interesting to see if the approach of this thesis has delivered a good prediction of the performance of two-stroke ammonia diesel marine engines.

Load response is seen as an important engine performance parameter, the impact of ammonia on the load response has not been analysed in this study. How fast an engine can increase its power output is dependent on how fast fuel can be burned in the cylinder. The combustion of the fuel in diesel engines is mostly limited by the air supply to the engine. Therefore, the load response is limited by the air supply to the engine in diesel engines. However, due to the low flame speed of ammonia it could very well be that the load response of the engine is limited by the combustion speed of ammonia and not by the air supply to the engine. The TU Delft engine B model does not consider the flame speed of the fuel and therefore is incapable of predicting the impact of the combustion speed of ammonia on the load response of the engine. It is recommended to further investigate the impact of ammonia and its lower combustion speed on the load response of the engine with experiments or another model.

Lastly, the regulations regarding NO_x emissions are becoming more strict and therefore it becomes increasingly more important to predict the NO_x emissions of a vessel, to see if it is within the allowed limits of the regulations. Although ammonia as a fuel greatly decreases the CO_2 emissions, there are concerns regarding the NO_x emissions of ammonia powered engines, because of the nitrogen in ammonia. Further investigation into the effects of ammonia on the NO_x emission of two-stroke marine engines and the implementation of a model predicting these emissions is recommended.

Bibliography

[1] G Abbaszadehmosayebi and Lionel Ganippa. "Determination of specific heat ratio and error analysis for engine heat release calculations". In: *Applied Energy* 122 (June 2014), pp. 143–150. ISSN: 03062619. DOI: 10.1016/j.apenergy.2014.01.028. URL: http://dx.doi.org/10.1016/j.apenergy.2014.01.028%20https://linkinghub.elsevier.com/retrieve/pii/S0306261914000476.

[2] M. Altosole and Massimo Figari. "Effective simple methods for numerical modelling of marine engines in ship propulsion control systems design". In: *Journal of Naval Architecture and Marine Engineering* 8.2 (2011), pp. 129–147. ISSN: 1813-8535. DOI: 10.3329/jname.v8i2.7366.

[3] Hiromitsu Ando, Jun Takemura, and Eiichi Koujina. "A knock anticipating strategy basing on the real-time combustion mode analysis". In: *SAE Technical Papers* 98.1989 (1989), pp. 481–493. ISSN: 26883627. DOI: 10.4271/890882.

[4] Jonas Asprion, Oscar Chinellato, and Lino Guzzella. "A fast and accurate physics-based model for the NOx emissions of Diesel engines". In: *Applied Energy* 103.x (2013), pp. 221–233. ISSN: 03062619. DOI: 10.1016/j.apenergy.2012.09.038. URL: http://dx.doi.org/10.1016/j.apenergy.2012.09.038.

[5] P Baan. "Modulair simulatiemodel van een dieselmotor van een dieselmotor Modulair simulatiemodel". In: ().

[6] Francesco Baldi, Gerasimos Theotokatos, and Karin Andersson. "Development of a combined mean value-zero dimensional model and application for a large marine four-stroke Diesel engine simulation". In: *Applied Energy* 154 (2015), pp. 402–415. ISSN: 03062619. DOI: 10.1016/j.apenergy.2015.05.024. URL: http://dx.doi.org/10.1016/j.apenergy.2015.05.024.

[7] Mirko Baratta et al. "Combustion chamber design for a high-performance natural gas engine: CFD modeling and experimental investigation". In: *Energy Conversion and Management* 192.January (2019), pp. 221–231. ISSN: 01968904. DOI: 10.1016/j.enconman.2019.04.030. URL: https://doi.org/10.1016/j.enconman.2019.04.030.

[8] Alois Betz and Gerhard Woschni. "Umsetzungsgrad und Brennverlauf aufgeladener Dieselmotoren im instationären Betrieb". In: *MTZ Motortechnische Zeitschrift* (1986), pp. 263–267.

[9] Shubham Biyani and Gangadhar Jagdale. "Effect of Ammonia Injection on Performance Characteristics of a Spark-ignition Engine". In: *International Journal of Trend in Research and Development* 3.2 (2016), pp. 2394–9333. ISSN: 03062619. DOI: 10.1016/j.apenergy.2013.11.067.

[10] Trevor Brown. *Green ammonia pilot plants now running, in Oxford and Fukushima*. 2018. URL: https://ammoniaindustry.com/green-ammonia-pilot-plants-now-running-in-oxford-and-fukushima/.

[11] Trevor Brown. *Picking bunker winners: the mono-fuel / dual-fuel duel*. 2020. URL: https://www.ammoniaenergy.org/articles/picking-bunker-winners-monofuel-dual-fuel-duel/.

[12] Mehmet Salih Cellek and Ali Pınarbaşı. "Investigations on performance and emission characteristics of an industrial low swirl burner while burning natural gas, methane, hydrogen-enriched natural gas and hydrogen as fuels". In: *International Journal of Hydrogen Energy* 43.2 (2018), pp. 1194–1207. ISSN: 03603199. DOI: 10.1016/j.ijhydene.2017.05.107.

[13] Walter Cornelius, L. William Huellmantel, and Harry R. Mitchell. "Ammonia as an engine fuel". In: *SAE Technical Papers* 74.1966 (1965), pp. 300–326. ISSN: 26883627. DOI: 10.4271/650052.

[14] C Dijkstra. *Description of Simulink mean value diesel engine model "0EI"I*. Tech. rep. December. TU Delft, 2004. DOI: DMS04/10.

[15] Pavlos Dimitriou and Rahat Javaid. "A review of ammonia as a compression ignition engine fuel". In: *International Journal of Hydrogen Energy* 45.11 (Feb. 2020), pp. 7098–7118. ISSN: 03603199. DOI: 10.1016/j.ijhydene.2019.12.209. URL: https://doi.org/10.1016/j.ijhydene.2019.12.209%20https://linkinghub.elsevier.com/retrieve/pii/S0360319920300124.

[16] Yu Ding. *Characterising Combustion in Diesel Engines*. 2011. ISBN: 9789065622891.

[17] Yu Ding, Congbiao Sui, and Jincheng Li. "An experimental investigation into combustion fitting in a direct injection marine diesel engine". In: *Applied Sciences (Switzerland)* 8.12 (2018). ISSN: 20763417. DOI: 10.3390/app8122489.

[18] Catherine Duynslaegher. "Experimental and numerical study of ammonia combustion". PhD thesis. Universite catholique de Louvain, 2011. URL: https://uclouvain.academia.edu/CatherineDuynslaegher.

[19] Engineering Toolbox. *Fuels - Higher and Lower Calorific Values*. 2003. URL: https://www.engineeringtoolbox.com/fuels-higher-calorific-values-d_169.html.

[20] R. D. Geertsma et al. "Pitch control for ships with diesel mechanical and hybrid propulsion: Modelling, validation and performance quantification". In: *Applied Energy* 206.April (2017), pp. 1609–1631. ISSN: 03062619. DOI: 10.1016/j.apenergy.2017.09.103. URL: https://doi.org/10.1016/j.apenergy.2017.09.103.

[21] Ioana Georgescu et al. "Characterisation of Large Gas and Dual-fuel Engines". In: *MTZ industrial* 6.3 (2016), pp. 64–71. ISSN: 2194-8682. DOI: 10.1007/s40353-016-0029-z.

[22] J.I I. Ghojel. "Review of the development and applications of the Wiebe function: A tribute to the contribution of Ivan Wiebe to engine research". In: *International Journal of Engine Research* 11.4 (2010), pp. 297–312. ISSN: 14680874. DOI: 10.1243/14680874JER06510. URL: https://doi-org.tudelft.idm.oclc.org/10.1243%2F14680874JER06510.

[23] James T. Gray et al. “Ammonia fuel - Engine compatibility and combustion”. In: *SAE Technical Papers* 75.1967 (1966), pp. 785–807. ISSN: 26883627. DOI: 10.4271/660156.

[24] P. G. Grimes. “Energy Depot Fuel Production and Utilization”. In: *SAE Technical Papers*. Vol. 74. Feb. 1965, pp. 281–299. DOI: 10.4271/650051. URL: https://www.sae.org/content/650051/.

[25] Christopher W. Gross and Song-Charng Kong. “Performance characteristics of a compression-ignition engine using direct-injection ammonia–DME mixtures”. In: *Fuel* 103 (Jan. 2013), pp. 1069–1079. ISSN: 00162361. DOI: 10.1016/j.fuel.2012.08.026. URL: http://dx.doi.org/10.1016/j.fuel.2012.08.026%20https://linkinghub.elsevier.com/retrieve/pii/S001623611200662X.

[26] Lino Guzzella and Christopher H. Onder. *Introduction to Modeling and Control of Internal Combustion Engine Systems*. seccond. Berlin, Heidelberg: Springer Berlin Heidelberg, 2010. ISBN: 978-3-642-10774-0. DOI: 10.1007/978-3-642-10775-7. URL: http://link.springer.com/10.1007/978-3-642-10775-7.

[27] H. O. Hardenberg and F. W. Hase. “An empirical formula for computing the pressure rise delay of a fuel from its cetane number and from the relevant parameters of direct-injection diesel engines”. In: *SAE Technical Papers*. 1979. DOI: 10.4271/790493. URL: https://www-jstor-org.tudelft.idm.oclc.org/stable/44658184?seq=3#metadata_info_tab_contents.

[28] John B. Heywood. *Internal combustion engine fundamentals*. Vol. 26. 02. 1988, pp. 26–0943. ISBN: 007028637X. DOI: 10.5860/choice.26-0943.

[29] IMO. *Air Pollution*. URL: http://www.imo.org/en/OurWork/Environment/PollutionPrevention/AirPollution/Pages/Air-Pollution.aspx.

[30] Insitute for Sustainable Process Technology. *Power to Ammonia*. Tech. rep. Amersfoort: Insitute for Sustainable Process Technology, 2017, p. 51. URL: http://www.ispt.eu/media/ISPT-P2A-Final-Report.pdf.

[31] Ghazi A Karim. “Combustion in gas fueled compression: Ignition engines of the dual fuel type”. In: *Journal of Engineering for Gas Turbines and Power* 125.3 (2003), pp. 827–836. ISSN: 07424795. DOI: 10.1115/1.1581894.

[32] Ghazi A. Karim. “A review of combustion processes in the dual fuel engine-The gas diesel engine”. In: *Progress in Energy and Combustion Science* 6.3 (1980), pp. 277–285. ISSN: 03601285. DOI: 10.1016/0360-1285(80)90019-2.

[33] M Kom. *Onderzoek naar verloop van de Seiliger parameters met behulp van een multizone model van het cilinderproces in een dieselmotor*. Delft, 2020.

[34] Charles F. Kutscher. *Principles of Sustainable Energy Systems, Third Edition*. CRC Press, Aug. 2018. ISBN: 9780429485589. DOI: 10.1201/b21404. URL: https://www.taylorfrancis.com/books/9780429485589.

[35] D B Lata and Ashok Misra. “Theoretical and experimental investigations on the performance of dual fuel diesel engine with hydrogen and LPG as secondary fuels”. In: *International Journal of Hydrogen Energy* 35.21 (2010), pp. 11918–11931. ISSN: 03603199. DOI: 10.1016/j.ijhydene.2010.08.039. URL: http://dx.doi.org/10.1016/j.ijhydene.2010.08.039.

[36] D.B. Lata and Ashok Misra. "Analysis of ignition delay period of a dual fuel diesel engine with hydrogen and LPG as secondary fuels". In: *International Journal of Hydrogen Energy* 36.5 (Mar. 2011), pp. 3746–3756. ISSN: 03603199. DOI: 10.1016/j.ijhydene.2010.12.075. URL: https://linkinghub.elsevier.com/retrieve/pii/S0360319910024171.

[37] Donggeum Lee. "Simulation Study of the New Combustion Strategy of Pre-combustion-assisted Compression Ignition for Internal Combustion Engine Fueled by Pure Ammonia". PhD thesis. Seoul National University, 2018.

[38] Xin Chen Ling, Feng Wu, and Dong Wei Yao. "A reduced combustion kinetic model for the methanol-gasoline blended fuels on SI engines". In: *Science China Technological Sciences* 59.1 (2016), pp. 81–92. ISSN: 1862281X. DOI: 10.1007/s11431-015-5954-5.

[39] Jinlong Liu and Cosmin E. Dumitrescu. "Single and double Wiebe function combustion model for a heavy-duty diesel engine retrofitted to natural-gas spark-ignition". In: *Applied Energy* 248.January (Aug. 2019), pp. 95–103. ISSN: 03062619. DOI: 10.1016/j.apenergy.2019.04.098. URL: https://doi.org/10.1016/j.apenergy.2019.04.098%20https://linkinghub.elsevier.com/retrieve/pii/S0306261919307652.

[40] MAN Energy Solutions. "Engineering the future two-stroke green-ammonia engine". In: (2019), pp. 1–20. URL: https://marine.man-es.com/docs/librariesprovider6/test/engineering-the-future-two-stroke-green-ammonia-engine.pdf?sfvrsn=7f4dca2_4.

[41] Michele Martelli. *Marine Propulsion Simulation*. Ed. by Elisa Capello and Mary Boyd. Berlin: De Gruyter Open Ltd, 2014. ISBN: 9783110401493.

[42] Sangram Kishore Nanda et al. "Fundamental analysis of thermal overload in diesel engines: Hypothesis and validation". In: *Energies* 10.3 (2017). ISSN: 19961073. DOI: 10.3390/en10030329.

[43] Mohammadreza Nazemi, Sajanlal R. Panikkanvalappil, and Mostafa A. El-Sayed. "Enhancing the rate of electrochemical nitrogen reduction reaction for ammonia synthesis under ambient conditions using hollow gold nanocages". In: *Nano Energy* 49.March (July 2018), pp. 316–323. ISSN: 22112855. DOI: 10.1016/j.nanoen.2018.04.039. URL: https://doi.org/10.1016/j.nanoen.2018.04.039%20https://linkinghub.elsevier.com/retrieve/pii/S2211285518302684.

[44] Thomas J. Pearsall and Charles G. Garabedian. "Combustion of Anhydrous Ammonia in Diesel Engines". In: *SAE Technical Papers*. Vol. 76. Feb. 1967, pp. 3213–3221. DOI: 10.4271/670947. URL: https://www.sae.org/content/670947/.

[45] Maxime Pochet et al. "Ammonia-Hydrogen Blends in Homogeneous-Charge Compression-Ignition Engine". In: *SAE Technical Papers*. Vol. 2017-Septe. September. Sept. 2017. ISBN: 2017240087. DOI: 10.4271/2017-24-0087. URL: https://www.sae.org/content/2017-24-0087/.

[46] G. Prakash, A Ramesh, and Anwar Basha Shaik. "An Approach for Estimation of Ignition Delay in a Dual Fuel Engine". In: *SAE Technical Papers*. Vol. 108. Mar. 1999, pp. 399–405. DOI: 10.4271/1999-01-0232. URL: https://www.sae.org/content/1999-01-0232/.

[47] Aaron J. Reiter and Song Charng Kong. "Demonstration of compression-ignition engine combustion using ammonia in reducing greenhouse gas emissions". In: *Energy and Fuels* 22.5 (2008), pp. 2963–2971. ISSN: 08870624. DOI: 10.1021/ef800140f.

[48] Aaron J. Reiter and Song-Charng Kong. "Combustion and emissions characteristics of compression-ignition engine using dual ammonia-diesel fuel". In: *Fuel* 90.1 (Jan. 2011), pp. 87–97. ISSN: 00162361. DOI: 10.1016/j.fuel.2010.07.055. URL: http://dx.doi.org/10.1016/j.fuel.2010.07.055%20https://linkinghub.elsevier.com/retrieve/pii/S001623611000414X.

[49] Myung-Il Roh and Kyu-Yeul Lee. *Computational Ship Design*. Singapore: Springer Singapore, 2018, pp. 1–353. ISBN: 978-981-10-4884-5. DOI: 10.1007/978-981-10-4885-2. URL: http://link.springer.com/10.1007/978-981-10-4885-2.

[50] A. B. Rosenthal. "Energy Depot - A Concept for Reducing the Military Supply Burden". In: *SAE Technical Papers*. Vol. 74. 1966. Feb. 1965, pp. 316–326. DOI: 10.4271/650050. URL: https://www.sae.org/content/650050/.

[51] Harsh Sapra et al. "Hydrogen-natural gas combustion in a marine lean-burn SI engine: A comparitive analysis of Seiliger and double Wiebe function-based zero–dimensional modelling". In: *Energy Conversion and Management* 207.January (Mar. 2020), p. 112494. ISSN: 01968904. DOI: 10.1016/j.enconman.2020.112494. URL: https://doi.org/10.1016/j.enconman.2020.112494%20https://linkinghub.elsevier.com/retrieve/pii/S0196890420300303.

[52] P.J.M. Schulten. "Quasi Stationair Model Vor Het Cilinderproces Van Een Dieselmotor". PhD thesis. Technical University Delft, 1998.

[53] M. Shahabuddin et al. "Ignition delay, combustion and emission characteristics of diesel engine fueled with biodiesel". In: *Renewable and Sustainable Energy Reviews* 21 (May 2013), pp. 623–632. ISSN: 13640321. DOI: 10.1016/j.rser.2013.01.019. URL: http://dx.doi.org/10.1016/j.rser.2013.01.019%20https://linkinghub.elsevier.com/retrieve/pii/S1364032113000506.

[54] S. Singh et al. "Development of a flame propagation model for dual-fuel partially premixed compression ignition engines". In: *International Journal of Engine Research* 7.1 (2006), pp. 65–75. ISSN: 14680874. DOI: 10.1243/146808705X7464.

[55] Pal Skogtjarn. "Modelling of the Exhaust Gas Temperature for Diesel Engines". PhD thesis. Linköpings universitet, 2002. URL: http://citeseerx.ist.psu.edu/viewdoc/summary?doi=10.1.1.7.597.

[56] D Stapersma. *Diesel Engines Volume 1 Performance Analysis*. Delft, 2010.

[57] D Stapersma. *Diesel Engines Volume 2 Turbo charging*. Delft, 2010.

[58] D Stapersma. *Diesel Engines Volume 3 Combustion*. Delft, 2010.

[59] D Stapersma. *Diesel Engines Volume 4 Emissions and Heat transfer*. Delft, 2010.

[60] E. S. Starkman, G. E. James, and H. K. Newhall. "Ammonia as a diesel engine fuel: Theory and application". In: *SAE Technical Papers* 76 (1967), pp. 3193–3212. ISSN: 26883627. DOI: 10.4271/670946.

[61] Congbiao Sui et al. "Energy effectiveness of ocean-going cargo ship under various operating conditions". In: (2019). DOI: 10.1016/j.oceaneng.2019.106473. URL: https://doi.org/10.1016/j.oceaneng.2019.106473.

[62] Congbiao Sui et al. "Fuel Consumption and Emissions of Ocean-Going Cargo Ship with Hybrid Propulsion and Different Fuels over Voyage". In: *Journal of Marine Science and Engineering* 8.8 (2020), p. 588. ISSN: 20771312. DOI: 10.3390/jmse8080588.

[63] Congbiao Sui et al. "Mean value modelling of diesel engine combustion based on parameterized finite stage cylinder process". In: *Ocean Engineering* 136.May (2017), pp. 218–232. ISSN: 00298018. DOI: 10.1016/j.oceaneng.2017.03.029.

[64] Michalis Syrimis, Kei Shigahara, and Dennis N. Assanis. "Correlation between knock intensity and heat transfer under light and heavy knocking conditions in a spark ignition engine". In: *SAE Technical Papers* 105.1996 (1996), pp. 592–605. ISSN: 26883627. DOI: 10.4271/960495.

[65] Kun Lin Tay et al. "Effects of Injection Timing and Pilot Fuel on the Combustion of a Kerosene-diesel/Ammonia Dual Fuel Engine: A Numerical Study". In: *Energy Procedia* 105 (2017), pp. 4621–4626. ISSN: 18766102. DOI: 10.1016/j.egypro.2017.03.1002. URL: http://dx.doi.org/10.1016/j.egypro.2017.03.1002.

[66] Gerasimos P Theotokatos. "Ship Propulsion Plant Transient Response Investigation using a Mean Value Engine Model". In: *INTERNATIONAL JOURNAL OF ENERGY* 2.4 (2008). URL: http://citeseerx.ist.psu.edu/viewdoc/download?doi=10.1.1.1031.944&rep=rep1&type=pdf.

[67] Niels de Vries. *Safe and effective application of ammonia as a marine fuel*. Tech. rep. TU Delft, 2019. URL: http://resolver.tudelft.nl/uuid:be8cbe0a-28ec-4bd9-8ad0-648de04649b8%20https://repository.tudelft.nl/.

[68] A Vrijdag, D. Stapersma, and T. van Terwisga. "Control of propeller cavitation in operational conditions". In: *Journal of Marine Engineering and Technology* 9.1 (2010), pp. 15–26. ISSN: 20568487. DOI: 10.1080/20464177.2010.11020228. URL: https://doi-org.tudelft.idm.oclc.org/10.1080/20464177.2010.11020228.

[69] I Wilkinson. *Green Ammonia*. 2017.

[70] World Health Organization. *Climate change and human health*. 2003. URL: http://www.who.int/globalchange/climate/summary/en/print.html.

[71] Hans Klein Woud and Douwe Stapersma. *Design of Propulsion and Electric Power Generation Systems*. London, 2002. ISBN: 1902536479.

[72] Melih Yıldız and Bilge Albayrak Çeper. "Zero-dimensional single zone engine modeling of an SI engine fuelled with methane and methane-hydrogen blend using single and double Wiebe Function: A comparative study". In: *International Journal of Hydrogen Energy* 42.40 (2017), pp. 25756–25765. ISSN: 03603199. DOI: 10.1016/j.ijhydene.2017.07.016. URL: https://doi.org/10.1016/j.ijhydene.2017.07.016.

[73] Liang Yu et al. "The effect of ammonia addition on the low-temperature autoignition of n-heptane: An experimental and modeling study". In: *Combustion and Flame* 217 (July 2020), pp. 4–11. ISSN: 00102180. DOI: 10.1016/j.combustflame.2020.03.019. URL: https://doi.org/10.1016/j.combustflame.2020.03.019%20https://linkinghub.elsevier.com/retrieve/pii/S0010218020301206.

[74] Javad Zareei, Abbas Rohani, and Wan Mohd Faizal Wan Mahmood. "Simulation of a hydrogen/natural gas engine and modelling of engine operating parameters". In: *International Journal of Hydrogen Energy* 43.25 (2018), pp. 11639–11651. ISSN: 03603199. DOI: 10.1016/j.ijhydene.2018.02.047. URL: https://doi.org/10.1016/j.ijhydene.2018.02.047.

[75] Kesong Zhang et al. "Numerical simulation of diesel combustion based on n-heptane and toluene". In: *Propulsion and Power Research* 8.2 (2019), pp. 121–127. ISSN: 2212540X. DOI: 10.1016/j.jppr.2019.01.009. URL: http://dx.doi.org/10.1016/j.jppr.2019.01.009.